PHARMACOKINETIC AND PHARMACODYNAMIC MODELING OF INSULIN FOLLOWING DIFFERENT ROUTES OF ADMINISTRATION IN HEALTHY AND DIABETIC SUBJECTS

By

ELIZABETH POTOCKA

A DISSERTATION PRESENTED TO THE GRADUATE SCHOOL
OF THE UNIVERSITY OF FLORIDA IN PARTIAL FULFILLMENT
OF THE REQUIREMENTS FOR THE DEGREE OF
DOCTOR OF PHILOSOPHY

UNIVERSITY OF FLORIDA

2009

To my Dad

ACKNOWLEDGMENTS

I would like to thank Dr. Hartmut Derendorf for his encouragement to take the giant leap into the return to graduate school, his guidance and advice, as well as his supervision and encouragement during this project. I would also like to thank Dr. Robert Baughman for not only giving me the opportunity to finish my degree, but to experience so many new sides of drug development and to grow to a great extent as a pharmaceutical scientist. His encouragement and support both at work and during my research were invaluable. I would also like to acknowledge and thank the other members of my committee, Dr. Mark Atkinson, Dr. Gunther Hochhaus and Dr. Veronika Butterweck, for their advice and support with this project.

I would like to thank MannKind Corporation for providing me with such exciting data, as well as the means and time to complete my research. My years with MannKind gave me not only the chance to finish my degree, but also an amazing opportunity to broaden my knowledge of the drug development process, including the exciting and unforgettable experience of contributing as an author to the Technosphere® Insulin NDA. I express my deepest gratitude for the support, advice and friendship to all my colleagues, especially Jim Cassidy. I'd also like to thank Mella Diaz and Pam Haworth for their efforts in running one of my key research studies. Finally, I'd like to extend my thanks to Dr. Klaus Rave and the rest of the Profil staff, for conducting most of the studies that I have used in my research. Their excellent standards made it that much easier to see the relationships in my modeling work.

I would also like to thank my friends in Gainesville, especially Viki Keener and Oliver Grundmann. Their help and advice made many challenges easier, and their friendship is one of the greatest gifts I leave with. My special thanks go out to Viki, not only for the wonderful friendship, but also opening her home to me on countless occasions. I'd also like to thank

Ichiban Sushi for its existence, and for making my years, as well as the subsequent trips to Gainesville, that much brighter.

Most importantly, my thanks go to my family. I wanted to thank my parents for instilling in me the drive to see my goals and aspirations through, and for encouraging me during my years working on this degree, and all the other years of my life. Finally, I wanted to thank my husband, whose patience and support knows no end, and whose encouragement and faith in me were so often the only things that got me to the finish line.

TABLE OF CONTENTS

page

LIST OF TABLES

LIST OF FIGURES

Abstract of Dissertation Presented to the Graduate School
of the University of Florida in Partial Fulfillment of the
Requirements for the Degree of Doctor of Philosophy

PHARMACOKINETIC AND PHARMACODYNAMIC MODELING OF INSULIN FOLLOWING DIFFERENT ROUTES OF ADMINISTRATION IN HEALTHY AND DIABETIC SUBJECTS

By

Elizabeth Potocka

August 2009

Chair: Hartmut Derendorf
Major: Pharmaceutical Sciences

Diabetes is one of the largest public health concerns worldwide, with the prevalence of type 1 and type 2 diabetes projected to more than double by the year 2030. Insulin therapy is used routinely in diabetic patients to manage their response to glucose, however, available insulin products do not match the healthy body's insulin concentration-time profile very well. As a result, insulin treatment often results in poor glucose control and associated adverse events. With a number of new insulins in development, an understanding of the insulin pharmacokinetic (PK) profile and its relationship to the resulting effect is an important element to the design of improved insulin therapy.

It was the purpose of this research to: 1) characterize insulin PK, 2) determine the effect that demographic variables have on insulin exposure, and 3) to characterize the relationship of insulin pharmacokinetics and pharmacodynamics (PK/PD). To this end, insulin administered via different routes was modeled using a population approach, revealing the two compartment characteristics of insulin pharmacokinetics, with the differences in the shapes of the insulin concentration-time profiles attributable to differences in absorption of the various formulations and routes of administration.

For all insulins included in this analysis, age was the only covariate that was found to affect insulin PK regardless of route of administration, with an increase in the central volume of distribution with increasing age. The rate of inhaled insulin absorption from the lung was found to decrease with increasing age, and increasing BMI was associated with a decrease in insulin absorption rate following subcutaneous administration.

Analysis of the effect of pharmacokinetically diverse insulins, as determined by the glucose infusion rate (GIR) in glucose clamp studies, found that the relationship between insulin PK and PD was well described by an E_{max} model, once the hysteresis was collapsed using an effect compartment. The model was expanded to include data from subjects with type 2 diabetes, revealing similar pharmacodynamic parameter estimates for both populations, with an approximately three-fold increase in insulin EC_{50} in the type 2 diabetic population compared to healthy subjects. This difference was attributed to the decreased insulin sensitivity that is associated with this disease state.

The relationships described by the models presented in this dissertation can be readily applied to the development of novel insulins, potentially resulting in improved insulin therapy.

CHAPTER 1
INTRODUCTION

Diabetes Mellitus

Diabetes mellitus has reached epidemic proportions in the United States and, more recently, worldwide. The morbidity and mortality associated with diabetes is anticipated to account for a substantial proportion of health care expenditures, and according to the American Diabetes Association (ADA), the prevalence of diabetes will continue to grow. The number of people in the U.S. with diagnosed diabetes reached 17.5 million with the national cost of diabetes exceeding $174 billion in 2007 [1]. This estimate includes $116 billion in medical expenditures attributed to diabetes, as well as $58 billion in reduced national productivity. According to the ADA, approximately $1 out of every 10 health care dollars spent in the U.S. is attributed to diabetes [1]. Looking beyond American borders, the incidence of diabetes is increasing not only in developed nations, but at an alarmingly high rate worldwide. The prevalence of type 1 and type 2 diabetes is projected to more than double, from 177 million cases in the year 2000 to 366 million in the year 2030. In fact, by the year 2030, India is projected to have the highest prevalence of diabetes, with an estimated 79 million cases [2].

Diabetes mellitus is a chronic metabolic disorder characterized by hyperglycemia caused by defective insulin secretion, resistance to insulin action, or a combination of both. Long-term diabetes-related complications involve microvascular (such as retinopathy, nephropathy, and neuropathy) and macrovascular (eg, stroke, coronary heart disease) complications as well as alterations of lipid and protein metabolism [3]. The primary clinical parameter to assess patient glycemic control is glycosylated hemoglobin (HbA1c), a form of hemoglobin used primarily to identify the average plasma glucose concentration over prolonged periods of time. Landmark studies such as the Diabetes Control and Complications Trial (DCCT) and the United Kingdom

Prospective Diabetes Study (UKPDS) have clearly demonstrated the benefit of better glycemic control in subjects with both type 1 and type 2 diabetes [4], as exhibited in the reduction of HbA1c and relative risk of complications (Figure 1-1).

Most cases of diabetes mellitus fall into the two broad etiologic categories of type 1 or type 2 diabetes mellitus. Type 1 diabetes is characterized by loss of the insulin-producing β-cells of the islets of Langerhans in the pancreas, leading to a deficiency of insulin. The majority of type 1 diabetes is immune-mediated, where β-cell loss results from a T-cell mediated autoimmune attack [5]. Type 2 diabetes mellitus is characterized differently, due to insulin resistance or reduced insulin sensitivity combined with relatively reduced, and sometimes an absolute, lack of insulin secretion.

There are numerous theories as to the exact cause and mechanism in type 2 diabetes. It is believed that there are both genetic and environmental components that affect the risk of developing the disease. There is a high prevalence for developing type 2 diabetes in siblings and offspring of affected individuals, and certain ethnic groups, such as Hispanics, African Americans and Polynesian Islanders have a higher incidence of type 2 diabetes. Both findings suggest a genetic link, but the genetic mechanisms are not known. Obesity is also known to predispose individuals to developing type 2 diabetes [6], and other factors include age, family history, lifestyle choices and environmental exposures.

Insulin

Insulin is a peptide hormone composed of 51 amino acid residues with a molecular weight of 5808 Da. It is produced in the β-cells of the islets of Langerhans in the pancreas, and exerts its actions on global metabolism, including glucose disposal and utilization by the body, fat metabolism and protein synthesis. Insulin is synthesized as a single chain precursor, in which

the A and B chains are connected by C-peptide. C-peptide is secreted in equimolar amounts with insulin, and is often used as a measure of acute insulin secretion [6].

Carbohydrate Metabolism

The human body aims to maintain blood glucose concentrations within the narrow range of 80-115 mg/dL, and insulin's primary role is to maintain homeostasis by keeping glucose levels within this range. Glucose is the principal stimulus to insulin secretion and, most commonly, the source of this glucose is dietary. Immediately following a meal, glucose absorbed into the blood is detected by the β-cells causing a rapid secretion of insulin. In turn, this causes a rapid uptake, storage and use of glucose by almost all tissues of the body.

Insulin is secreted into the portal circulation for immediate presentation to the liver, which is exposed to the highest insulin concentrations, and which may be a target of the oscillatory nature of insulin secretion [7]. As insulin is secreted, it also directly affects the pancreatic α-cells and inhibits the production of glucagon, a counterregulatory hormone to insulin, which promotes hepatic conversion of stored glycogen into glucose. This hormone is also regulated by blood glucose and free fatty acid levels [8].

One of the most important effects of insulin is that which it exerts on the liver. Insulin simultaneously shuts down hepatic glucose production and, at the same time, stimulates glucose uptake by the liver. Insulin enhances liver glucose absorption by increasing the activity of glucokinase. By stimulating glycogen synthase, insulin also causes most of the glucose absorbed after a meal to be stored almost immediately in the liver in the form of glycogen. The liver serves as the largest storage unit of glycogen, which is converted into glucose and released back into the circulation to be used as an energy source during times of fasting (glycogenolysis).

Elevated insulin concentrations inactivate liver phosphorylase, the principal enzyme responsible for the conversion of glycogen to glucose and hence, inhibit glycogenolysis. At

higher concentrations, insulin also inhibits gluconeogenesis [9], a metabolic pathway that results in the generation of glucose from non-carbohydrate carbon substrates such as lactate, glycerol, and glucogenic amino acids, and is the source of blood glucose after an extended period of fasting, when glycogen stores have been depleted. The inhibition of gluconeogenesis is more complex than glycogenolysis. Insulin decreases quantities and activities of enzymes required for gluconeogenesis, but also, its effect on fat metabolism limits the required precursors for this metabolic pathway. It has been hypothesized that the disruption of this signaling and the increased presence of free fatty acids (FFAs) in the bloodstream are an important factor in the pathophysiology of type 2 diabetes, with a direct impact on insulin sensitivity [10-12].

In the muscle, insulin induces the redistribution of the GLUT4 transporter from intracellular storage sites to the plasma membrane. Once at the cell surface, GLUT4 facilitates the passive diffusion of circulating glucose down its concentration gradient into muscle cells, causing rapid transport of glucose into the cells. The abundance of glucose causes the cells to use glucose preferentially over fatty acids for energy, and glucose not used for energy in the post-prandial period is converted in the muscle cells to glycogen and stored for later use.

Fat Metabolism

In the presence of insulin, the increase in glucose utilization by the body's tissues automatically decreases the utilization of fat as an energy source and promotes FFA synthesis by the liver. Insulin directly lowers FFA presence in the bloodstream by 1) facilitating the storage of FFAs in adipose tissue and 2) inhibiting the release of FFAs from the adipose tissue back into the bloodstream.

In the long run, insulin's effect on fat metabolism is equally important to its effect on glucose. When insulin presence is diminished, all aspects of fat breakdown and use for energy are enhanced, and FFAs become the main energy substrate used by essentially all body tissues,

with the exception of the brain. This, in turn, leads to an increase in lipid concentration, in particular cholesterol, in the bloodstream and the development of atherosclerosis in diabetic subjects. Furthermore, the use of fat for energy causes the formation of excessive amounts of acetonic acid, which leads to ketosis and acidosis, coma and even death in subjects with severe diabetes.

Protein Metabolism and Growth

During the hours after a meal, not only carbohydrates and fats, but also proteins are stored in the tissues, and insulin stimulates transport of many amino acids into cells. It also increases the translation of mRNA, and increases the rate of transcription of selected DNA genetic sequences, thus increasing protein synthesis and functioning as a growth promoter in certain cases [6]. Finally, insulin inhibits the catabolism of proteins, in particular, in the muscle cells. When insulin is not available, virtually all protein storage comes to a halt; protein catabolism increases, protein synthesis stops and large quantities of amino acids appear in the plasma, to be used for energy directly or as substrates for gluconeogenesis. The resulting protein wasting is a serious effect of severe diabetes, leading to extreme weakness as well as many altered organ functions.

Normal Physiologic Insulin Secretion as a Component of Carbohydrate Metabolism

Normal physiologic insulin secretion consists of 2 components: a steady low insulin release to maintain basal glucose levels within a narrow range in between meals, and prandial-related rapid insulin surges, secreted in response to meals in order to control and limit postprandial glucose (PPG) excursions [13]. Insulin response can further be characterized by qualitative and dynamic features, consisting of an initial quick spike in insulin secretion (what has been termed the “early”or “first” phase) which occurs and reaches a peak quickly, followed

by a more gradual insulin peak (the "late phase") which corresponds qualitatively and quantitatively to the elevated presence of glucose in the bloodstream [6].

The biphasic nature of insulin secretion has been observed under experimental conditions during both an intravenous glucose tolerance test (IVGTT) [14-16] and under hyperglycemic clamp conditions [17]. This is demonstrated in Figure 1-2, where the initial insulin spike subsequent to glucose infusion (termed the "first" phase) is then followed by a steady response to the elevated presence of glucose in the bloodstream during the clamp procedure.

Physiological models attempting to explain the above phenomenon includes the storage-limited model developed by Grodsky *et al* [18] on the basis of experimental data of insulin secretion obtained *in vitro* from the isolated perfused pancreas. This model assumes that the β-cell contains two distinct pools of insulin granules: a small (2%), labile pool accessible for immediate release and a larger (98%), stable pool that feeds slowly into the labile pool. The signal-limited model was developed by Cerasi *et al* [19]. These investigators abandoned the pool model in favor of the idea that biphasic insulin release is the result of the dynamic interaction between stimulatory and inhibitory events initiated by glucose, each of them having its own kinetics and dose dependence.

A clear-cut first-phase insulin response can be elicited *in vivo* resorting only to stimuli that rapidly elevate blood glucose concentration. However, such stimuli do not occur naturally following a meal, and when glucose concentration increases gradually, the insulin response measured in the peripheral blood does not bear a clear sign of a biphasic shape. In healthy individuals, insulin concentrations are clearly elevated over the first 60 minutes following a meal (Figure 1-3) but the first-phase becomes blunted in response to the continuous appearance of glucose. In fact, a distinction has been made in describing these early insulin responses, terming

the insulin response to a square wave glucose profile as "first phase," and the blunted response to a meal-like glucose profile as "early phase."

Although no clear first phase spike is distinguishable following a meal, it has been suggested that the same β-cell dynamic properties that are able to generate a biphasic secretion in response to a brisk, intravenous glucose challenge are still operating in response to the gradual entry of glucose from the gut, and that the difference between first and early phase is driven by glucose appearance rate [17]. Regardless of the mechanism driving the initial surge of insulin following a meal, its presence is believed to be a critical factor in maintaining glucose homeostasis in the healthy individual through the prompt inhibition of endogenous glucose production [17, 20-22]. Work by Cherrington *et al* [9] has demonstrated that because insulin exerts its effect directly on the liver, it has a significant effect on hepatic glucose output within minutes and, hence, the early insulin response is believed to be aimed at quickly shifting glucose metabolism from the fasting to the prandial state.

Insulin Secretion in the Type 2 Diabetic

A characteristic finding in the early stages of type 2 diabetes is the loss of first phase insulin secretion in response to intravenous glucose [23-25]. It has been hypothesized that in the early stages of the disease this alteration in the insulin secretion pattern is responsible for the loss of glycemic control, despite an increased insulin production overall. Although the exact mechanism of this relationship has not been completely elucidated, a number of theories have been proposed [25-27], all of which suggest the lack of effect on hepatic glucose output, the hypothesized target of the early insulin response. In a hyperglycemic clamp study, Luzi *et al* demonstrated the almost complete and prolonged suppression of hepatic glucose production (HGP) when the first phase insulin release was simulated, while no difference was observed in peripheral tissue glucose uptake [25]. It has been further suggested that when the first-phase

insulin response is lacking, the insulin-to-glucagon ratio is rapidly altered in favor of glucagon, thus leading to increased hepatic glucose production and hyperglycemia; restoration of the first-phase insulin profile in plasma, even in the absence of the second phase, curbs the glucagon-mediated rise in plasma glucose concentration [28]. Finally, it is clear from clinical studies that subjects with diabetes are unable to match the magnitude of the early response compared to healthy subjects. This is presumably due to alterations in insulin secretion patterns, in particular, the loss of the early phase response.

The difference in insulin response to a meal was demonstrated by Polonsky, who studied healthy and type 2 diabetic subjects matched for age, sex and degree of obesity [13]. In response to the same meal, the overall insulin exposure was not significantly different between groups over the time period studied, but the magnitude of the insulin response was clearly higher in the healthy subjects immediately following the meal (Figure 1-4). The overall glucose levels were approximately 2-3 fold greater in the group with diabetes [13]. In a similar study, Luzio studied subjects with type 2 diabetes [27]. Following a meal, insulin and glucose concentrations were measured. The subjects were then studied again, but an intravenous insulin infusion was administered following the meal, significantly increasing the insulin concentrations and simulating an early phase insulin response (Figure 1-5). Blood glucose concentrations were shown to be significantly reduced when the additional insulin was infused, even though the total insulin exposure was only increased over the first hour of the study. This work demonstrated the importance of the insulin's early phase in glycemic control, as well as clearly linked the hyperglycemia observed in type 2 diabetes to its absence.

Insulin Therapy

Insulin is the mainstay of diabetes management, and is used routinely in both type 1 and type 2 diabetic subjects to manage the body's insulin needs in response to glucose. Preparations

of insulin are classified according to their duration of action into short, intermediate and long acting.

Diabetic subjects with complete or almost complete loss of β-cell function, such as type 1 diabetic subjects or subjects with advanced type 2 diabetes, require insulin replacement for both the basal insulin release and the meal-related insulin surges which are a part of a healthy insulin response. A variety of long acting insulins are commercially available, and are combined with prandial insulins, which are administered at the time of a meal [6].

Short acting insulins, on the other hand, are used for control of prandial glucose in subjects on complete insulin replacement therapy, or subjects requiring only prandial insulin, such as type 2 diabetic subjects with some remaining β-cell function. Prandial insulins attempt to reproduce the physiologic secretion of the pancreatic β-cells as closely as possible. Since the shape of the exposure curve in a healthy individual is wholly dependent on glucodynamic changes and blood glucose concentrations, and is a direct response to the needs of the body, it is impossible to truly mimic endogenous insulin response. However, certain characteristics, such as a quick peak insulin concentration and an overall exposure that does not outlast glucose absorption, would characterize a desirable insulin pharmacokinetic profile. Unfortunately, commercially available insulin products, administered primarily by the subcutaneous route, do not match this profile very well [29].

Subcutaneously administered insulin exhibits a slow and variable absorption profile in contrast to the healthy endogenous postprandial insulin response, which is characterized by an insulin spike and elevated insulin concentrations which match the post-prandially elevated glucose concentrations. Due to this pharmacokinetic difference, exogenous insulin fails to match the early insulin response in three ways: 1) the initial low insulin levels do not match the quick

surge of the early insulin response, 2) slow exogenous insulin absorption does not provide adequate glucose control early following meal ingestion, and 3) exogenous insulin is associated with a slower decline in blood levels compared to endogenous insulin, and exposure oftentimes outlasts the timeframe of glucose absorption following a meal. The first two differences result in elevated post prandial glucose concentrations (PPG) [30, 31]. Control of PPG is critical, since elevated PPG is an earlier and frequent abnormality in type 2 diabetes and is a stronger predictor of cardiovascular disease than elevation of fasting blood glucose (FBG) [32]. Furthermore, as HbA1c levels decrease, PPG contributes proportionately more and more to the glycation of hemoglobin [33]. The difference in exogenous and endogenous insulin duration of insulin exposure is driven by the slow release characteristics of subcutaneous insulin, and results in action profiles which outlast elevated post-prandial blood glucose. This mismatch in peak delivery and a duration of action that outlasts glucose absorption following a meal can result in postprandial hypoglycemia [34, 35]. Hypoglycemia poses an immediate danger to subjects, as it can lead to coma or even death, but more often is associated with a need to "feed the insulin" and the resulting insulin therapy-associated weight gain. Perhaps more importantly, the inability of exogenous insulin to control PPG results in the lack of long-term glycemic control, elevated HbA1c levels, and an elevated risk of diabetic complications.

Finally, there is evidence that better insulin therapy may be associated with more than providing insulin presence in the bloodstream to "cover" the glucose absorbed from the meal. Pharmacokinetic properties related less to the extent of exposure, and rather to its absorption rate and peak most likely play an important role in optimizing the pharmacodynamic response. Although the relationship of different insulin pharmacokinetics and their respective pharmacodynamics has not been clearly elucidated, it is clear that the relationship exists, and that

an insulin which more closely resembles healthy endogenous insulin secretion characteristics would result in better pharmacodynamics and improved glycemic control.

Types of Prandial Insulins

The first insulins to be commercially available were purified proteins from non-human sources, most prominently, forms of porcine insulin. Although still used in other countries, these insulins have been replaced by recombinant human insulin (RHI) in the United States. Administered primarily by the subcutaneous route, RHI is produced by genetic engineering techniques using recombinant DNA technology [6].

When in solution, both animal source and RHI associates into stable hexamers in the presence of zinc, and commercially available insulins make use of this characteristic to provide stability and to extend the product shelf-life [36]. However, this feature is also a drawback, as the increased molecular weight and steric size of hexamers delay absorption from the subcutaneous injection site, as the molecule has to first dissociate into dimers and monomers before it is absorbed [37]. Because of the length of time required for dissociation into the readily absorbed monomer, the absorption profile of subcutaneous RHI is slow, with peak concentrations detected approximately 1.5 to 2.5 hours post-dose, and a peak insulin effect 1.5 to 3.5 hours post-dose [38]. The absorption step is so slow in fact, that it drives drug clearance, giving subcutaneous RHI a long presence in the bloodstream and a 7-8 hour duration of action [38].

The development of rapid acting insulin analogs (RAA) was an attempt to address the pharmacokinetic and pharmacodynamic shortcomings of subcutaneously administered RHI. RAA's are insulin molecules containing subtle alterations in amino acid sequence which still bind to the insulin receptor, but have more favorable ADME (absorption, distribution,

metabolism, and excretion) characteristics. Like regular insulin, RAAs exist as a hexamer in commercially available formulations, but unlike RHI, they dissociate into monomers almost instantaneously following injection, resulting in a much quicker absorption [6]. Eli Lilly & Co. marketed the first insulin analogue, lispro (Humalog ®), engineered through recombinant DNA technology so that the penultimate lysine and proline residues on the C-terminal end of the B-chain were reversed [39]. The side chains of single amino acids at the C-terminal end of the B-chain play a particular role in the self-association of the insulin molecules [40, 41], and when these amino acids are reversed, the binding forces between the two insulin molecules of a dimer are reduced so that the dimerization constant is 300 times less than that of human insulin [36]. Lispro can be stabilized as a hexamer in the presence of phenol and zinc; however, the rapid uptake of phenol after injection causes the molecules to quickly dissociate into monomers, which are rapidly absorbed.

Although the rapid acting analogues exhibit an earlier peak (t_{max} of ~50 minutes) and a more rapid clearance compared to subcutaneous RHI, onset of action is still relatively slow compared with prandial glucose absorption (peak effect at 60-90 minutes post-dose), and the duration of action still exceeds the timing of the return to normal blood glucose levels following a meal (4-6 hours post-dose) [42]. Hence, even the RAA insulins do not mimic endogenous insulin release closely enough, and result in substantial post-meal blood glucose excursions and continued incidence of hypoglycemic events [39].

Inhaled insulins showed promise and were under development by a number of pharmaceutical companies from the late 1990s until the present. Until now, only one inhaled insulin has been approved and marketed. Exubera® (Pfizer) was approved in 2006 by the Food and Drug Administration (FDA), and was available commercially until 2007, when Pfizer

withdrew it from the market [43]. The failure of Exubera has been attributed to many factors, ranging from lack of a successful marketing strategy, to pricepoint and cost versus benefit considerations, to a cumbersome inhalation device. Whatever the reasons for the lack of Exubera's commercial success, its withdrawal from the market resulted in a rather abrupt end to the development of other similar products with, most prominently, Eli Lilly (AIR® Inhaled Insulin) and Novo Nordisk (AERx® insulin Diabetes Management System) terminating their prandial inhaled insulin development programs within weeks of the Pfizer announcement [43].

Exubera's pharmacokinetic (PK) and pharmacodynamic (PD) profile was similar to that of the subcutaneously administered RAAs, with an insulin peak of about 49 minutes post-dose, an associated peak in activity ranging at approximately 2 hours following dosing, and a duration of action of 6 hours [44]. This similarity to the RAAs meant that Exubera only offered the convenience of an inhaled formulation that did not require injection as the only benefit over the existing therapy. The PK and PD properties of the other inhaled insulins were similar to that of Exubera [45].

One inhaled insulin still in development is Technosphere® Insulin (TI). TI is a novel inhaled insulin whose unique delivery characteristics result in rapid absorption followed by rapid systemic clearance. Following TI administration, insulin C_{max} occurs approximately 14 minutes post-dose. Due to its rapid clearance, insulin concentrations return to baseline levels much more quickly compared to subcutaneously administered insulin, with little residual effect by three hours post-dose. Data from glucose clamp studies suggest a much faster onset (within minutes post-dose) and shorter duration of glucodynamic effect (return to baseline by 180 minutes post-dose) when compared to subcutaneous insulins [46].

Clinical Pharmacology Studies Involving Insulin

The clinical administration of insulin necessitates counteracting insulin activity so as to keep the study subject safe. Studies designed to explore the glucodynamic effect of insulin are generally of two types: 1) insulin action is countered by administering the insulin with a meal; or, 2) insulin action is countered by an infusion of glucose. This latter study design, commonly referred to as a glucose clamp study, provides the most direct measurement of insulin action. These studies can be subdivided into a few different types, dependent on the research purpose and/or study conditions.

Glucose Clamp Studies

Glucose clamp studies are commonly used to study diabetes and insulins [9, 17, 35, 39]. The glucose clamp procedure has been a great research tool to define several biochemical and feedback mechanisms associated with diabetes, including determination of insulin sensitivity [47], the effects of exercise [48], and counterregulatory and glucagon responses [49]. More recently, the glucose clamp procedure has been used to temporally represent insulin activity. These time–activity profiles are available for numerous insulins and insulin analogs in healthy volunteers and subjects with diabetes [50-53].

During a glucose clamp study, subjects are administered insulin, while at the same time they receive a varying infusion of glucose to counteract insulin's action and keep the subject in a constant glycemic state. This methodology allows for the safe dosing of insulin while eliminating the need for a meal to control blood glucose and prevent hypoglycemia. It also allows for a direct way of measuring insulin effects by determining the amount of glucose required to maintain blood glucose levels within a defined range.

The subject receives a constant rate insulin infusion to suppress the secretion of insulin from the pancreas only during the run-in period, or during the entire study procedure.

Suppressing endogenous insulin secretion is important for distinguishing between the effects of the administered insulin and insulin secreted by the pancreas in response to the administered glucose. With endogenous insulin suppressed and the rate of insulin infusion known, the glucose infusion rate can be used as a measure of the pharmacodynamic response to the test insulin treatment. The rate of glucose administration is termed the glucose infusion rate or GIR [36].

The clinical setting of these studies makes it easy to obtain numerous blood samples for insulin concentration determination and assessment of insulin pharmacokinetics. It also allows for a direct measurement of blood glucose levels as well as the GIR, both of which have been used as markers of insulin pharmacodynamics. An example of two GIR-time profiles from two different dose strengths of an insulin preparation is presented in Figure 1-6, and the relative potency can be readily observed.

Data Analysis of the Glucose Infusion Rate

GIR data has been analyzed in a similar fashion to a noncompartmental analysis of pharmacokinetic data. The total amount of glucose administered is directly related to the overall effect of the insulin administered, and the GIR at any time point is an indicator of the effect of insulin at that time point. Thus, the maximum GIR (GIR_{max}) is indicative of the maximum effect, GIR t_{max} is indicative of its timing, while the area under the glucose infusion time curve (GIR AUC) is indicative of the overall extent of the insulin effect. Insulins with greater overall activity have relatively higher GIR AUCs, while insulins with a quicker onset of activity have a shorter GIR t_{max} [36].

The relative ease of these calculations and intuitive nature of the GIR-derived parameter interpretation means that extensive use of the data has been made in order to compare insulin activity. These pharmacodynamic parameters have been used to asses the onset, duration and

extent of insulin activity, and remain the methodology of choice when direct pharmacological effect of insulins is compared [36].

Insulin Pharmacokinetics and Pharmacodynamics

Insulin Pharmacokinetics

Insulin has been used as a therapeutic agent for more than 80 years, and insulin pharmacokinetics have been extensively studied since a specific radioimmunoassay became available in 1960 [54]. Although early work suggested a one compartment pharmacokinetic model following intravenous insulin administration, advances in analytical technology have made it possible to observe insulin concentrations in the elimination phase. The multiple compartment disposition of intravenous insulin was demonstrated in studies utilizing radiolabels over 30 years ago, and more recently, using unlabeled intravenous insulin and a more sensitive RIA, by Hooper *et al* [55].

Insulin has been extensively studied following the various routes of administration, with most pharmacokinetic profiles from subcutaneously administered formulations, as this has been the dominant route of administration since insulin therapy was instituted. Unlike intravenously administered insulin, other routes of administration have been described, for the most part, using a one compartment model [56-61]. Because the α-phase following intravenous dosing lasts about an hour [55], the slow absorption of subcutaneously administered insulin obscures the second compartment. Furthermore, because the α-half-life following intravenous dosing is quick (approximately 5-6 minutes) [55], absorption dominates the pharmacokinetics in a phenomenon commonly termed “flip-flop” kinetics [62], where the terminal phase reflects the slowest step in the sequential/parallel processes of drug absorption, distribution and elimination (ie, the terminal phase reflects absorption not elimination, hence a “flip-flop” of kinetic processes) [62]. As a result of this, the differences in insulin profiles, especially the terminal phase, observed among

the various non-iv routes of administration reflect the differences in absorption, not elimination. This is well described by assessing the clearance of insulin lispro and RHI, two products with differing PK profiles after subcutaneous dosing, but whose clearance, when administered intravenously, is almost identical, indicating that the differences observed in the terminal phase reflect differences in absorption [37].

Insulin Clearance

All insulin-sensitive cells remove and degrade the hormone. Once an insulin molecule has docked onto the receptor and effected its action, it may be degraded by the cell. Degradation normally involves endocytosis of the insulin-receptor complex followed by the action of insulin degrading enzyme (IDE), which is relatively ubiquitous, and present in all insulin-sensitive tissue. Most evidence supports IDE as the primary degradative mechanism, but other systems (lysosomes and other enzymes) undoubtedly contribute to insulin metabolism [63]. Since most insulin clearance involves the coupling of insulin and its receptor as a first step, insulin clearance is ultimately dependent on the number of insulin receptors, as well as an individual's insulin sensitivity.

The liver is the primary site of insulin clearance and approximately 50% of portal insulin is removed during first pass transit [64]. Hepatic uptake is not static, however, and varies with both physiological and pathophysiological factors [63]. The kidney is another major site of insulin clearance from the systemic circulation [65], removing approximately 50% of peripheral insulin by two mechanisms: glomerular filtration and proximal tubular reabsorption and degradation [63]. Insulin not cleared by liver and kidney is ultimately removed by other tissues, such as muscle and adipose tissue.

Although docking at the insulin receptor is a first step toward insulin clearance, removal of insulin from the circulation does not imply immediate degradation and inactivation of the

hormone. A significant amount of receptor-bound insulin is released from the cell and is returned to the circulation intact or partially degraded [66]. A model developed by Hovorka *et al.* [67] estimates that the mean residence time of endogenously secreted insulin is 71 minutes. Of these, 62 minutes is spent bound to the liver receptor, 6 minutes is spent bound to peripheral receptors, and 3 minutes is spent in blood or interstitial fluid. With this model, 80% of the total insulin in the body was bound to liver receptors. Other tissues also transiently bind and can release insulin back into the circulation [63].

Insulin Pharmacodynamics

As with many therapeutic agents, insulin effect is consistent with an E_{max} model, which is non-proportional in nature [68]. Theoretically, the E_{max} model is based on receptor theory, and is described by a version of the Hill equation:

$$Effect = \frac{E_{\max} \cdot C}{EC_{50} + C} \qquad (1\text{-}1)$$

where E_{max} is the maximum effect, C is drug concentration and EC_{50} is the concentration that causes 50% of the effect.

In practice, this equation describes a relationship in which, as drug concentrations increase, the effect reaches an asymptote. This is the maximum effect (E_{max}) the drug can exert, regardless of how far the concentration is increased. This phenomenon has been observed when multiple doses of insulin are administered, and although the relationship remains linear for dose and insulin exposure, a doubling of the dose results in less than doubling of the effect [69].

Hysteresis in Insulin PD

Because insulin exerts its activity in the periphery (tissue), and measurements for insulin exposure are taken from the central compartment (blood), there is a disconnect, or shift, between the rise and fall for insulin concentration in the central compartment, and the effect that it exerts

peripherally (most often a measure of glucose utilization). The shift in the PK and PD changes is dependent on the time required to complete the cascade of events composing the cellular mediation of insulin action. Hence, insulin's activity cannot be directly related to its presence in the bloodstream, as its pharmacodynamics exhibits a counter-clockwise hysteresis [59]. The hysteresis shape varies following insulins with different pharmacokinetic properties, and is most pronounced following intravenous insulin administration.

To overcome this complication in determining a relationship between insulin concentration and its effect, a number of techniques have been used to collapse the hysteresis in the PK/PD model development. The effect-compartment link model, first proposed by Sheiner et al in 1979 [70], has successfully been used in a number of models. This model assumes the presence of a hypothetical effect compartment (biophase) and proposes that a drug must enter this compartment from the pharmacokinetic (central) to the peripheral compartment before its pharmacological response is exerted. This model has been criticized by some for the lack of parameters which can readily be translated to describe the physiology and pharmacology of the system [71]. More recently, indirect pharmacodynamic response models have been proposed to describe the insulin pharmacodynamic response. Both inhibitory [72] and stimulatory [56, 57, 72] models have been used to successfully describe insulin action. Such models described insulin effect on the glucose-insulin homeostasis more mechanistically than the biophase models, but tend to require different parameter estimates for different dose groups [71] which severely restricts any predictive usefulness of the models.

Insulin Pharmacokinetic and Pharmacodynamic Modeling

Models of Insulin PK/PD

Models describing the pharmacokinetic-pharmacodynamic relationship of insulin have been developed for many purposes. These models range in complexity from a simple description

of the concentration-effect relationship of a single insulin formulation, which tend to be empirically or mechanistically based, to the physiologically based (PB) models which attempt to describe the physiological situation as closely as possible for organs, organ systems or even the body as a whole, to the development of an artificial pancreas which incorporates a model that completely describes the closed loop system of insulin and glucose.

Most of the PB models comprise multiple compartments with complicated blood glucose bioprocesses in order to take into account the counter-regulatory feedback system between insulin and glucose and account for the indirect relationship between the two [67, 73, 74]. Complex models derived from IVGTT and OGTT [75] using radiolabelled glucose have been used to describe the interrelationship of insulin and glucose, as well as the effect of both glucose and insulin on hepatic glucose production and tissue disposal.

It is the purpose of the work presented here to explore the insulin concentration-effect relationship as determined from glucose clamp data, so as to compare the acute insulin effect between different formulations; thus, the more empirical models will be discussed, with examples offered, and the more physiologically-based pharmacodynamic models will not be presented.

Empirical Models and Mechanistic Models

Effect compartment models

The simplest models exploring the relationship between insulin concentration and its effect have been based on an E_{max} relationship between insulin and either the GIR (glucose clamp studies) or blood glucose. As described earlier, under euglycemic glucose clamp conditions, the GIR reflects glucose utilization, and is a measure of total insulin activity. If the contributions of endogenous insulin are suppressed, the GIR reflects test insulin action, and a number of analyses have been preformed using the GIR as the pharmacodynamic endpoint. The

effect compartment is a hypothetical compartment in the model, which makes it possible to account for the delay between insulin dynamics in the central compartment and its action [68]. The model is presented in Figure 1-7.

Independent work by Hooper, Tornoe and Woodworth [55, 59, 60] utilized a sequential PK/PD approach, and the hypothetical effect compartment to take into account the delay in insulin action and effectively collapse the hysteresis observed in their analyses. The work by Hooper *et al* was based on intravenously administered insulin and, as a result, enables modeling the two compartment pharmacokinetics of insulin [55]. The PD was expressed as a simple gamma-linear model and sigmoidal E_{max} model with the effect site concentration, described by:

$$GIR = \frac{E_{\max} \cdot C_e^{\gamma}}{EC_{50}^{\gamma} + C_e^{\gamma}} \tag{1-2}$$

where E_{max} is the maximum effect, C_e is drug concentration at the effect site, γ is the shape factor, or Hill coefficient, whose addition increases the versatility of the model to describe the concentration-effect relationship, and EC_{50} is the concentration that causes 50% of the effect.

Both Tornoe and Woodworth developed pharmacodynamic models which incorporate the same sigmoidal E_{max} model to compare subcutaneously administered RHI with other insulins. The model proposed by Tornoe *et al* estimates the PD parameters individually for Novo Rapid (Novo Nordisk, Bagsvaerd, Denmark) and RHI individually. The model estimates a very similar EC_{50} and γ for both insulins, which suggests similar potency for both NovoRapid and RHI [59]. On the other hand, Woodworth *et al*, found that the individually estimated parameters for RHI and NPH (Neutral Protamine Hagedorn) insulin differ substantially in EC_{50} and γ [60] using the same model. Although the fits for both insulins are reasonable, the predictive usefulness of their model was lost since the model parameters were estimated for each formulation independently, and cannot be extrapolated to insulins with different pharmacokinetic properties.

Indirect effect models

Because the effect compartment-based models lack physiological meaning, investigators began using indirect effect models, viewing them as more mechanistic and less empirical. Studies in animals make it possible to explore the relationship between the time course of insulin in the blood stream and blood glucose concentrations without necessitating either food intake or glucose infusion. This allows for the study of the system without the introduction of exogenous glucose, as well as allows blood glucose to be the pharmacodynamic endpoint.

Interesting work by Lin *et al* compares the use of the effect compartment versus two indirect response models; the stimulatory (increase in glucose utilization by the tissues) and inhibitory (decrease in hepatic glucose production) [72]. Unlike the models previously described, the animals (minipigs) were not infused with glucose during the study and blood glucose was used as the pharmacodynamic endpoint. The PK/PD model was sequential, with two compartment characteristics for the insulin-time curve. The inhibitory and stimulatory models are presented in Figure 1-8. The two models are described by the following equations:

Inhibition model: $$\frac{dR}{dt} = k_{in}\left(1 - \frac{Cp}{IC50 + Cp}\right) - k_{out} \cdot R \quad (1\text{-}3)$$

Stimulation model: $$\frac{dR}{dt} = k_{in} - k_{out}\left(1 + \frac{S_{\max} Cp}{SC50 + Cp}\right) \cdot R \quad (1\text{-}4)$$

where Cp is the plasma insulin concentration, k_{in} is the rate of glucose production, k_{out} is the first order glucose utilization constant, IC50 is the insulin concentration that inhibits the maximal production of glucose by 50%, R is the hypoglycemic effect of insulin on blood glucose, S_{max} is the maximum utilization of blood glucose contributed by insulin and SC50 is the insulin concentration that stimulates the maximal utilization of blood glucose by 50%.

The authors found that based on the resultant correlation coefficient, weighted residuals sum of squares and Akaike information criterion were improved when the indirect models were used as compared to the fit obtained from the effect compartment model. Interestingly, others have noted that the use of the indirect model is better suited for data where counterregulatory mechanisms do not contribute to the system, such as during a glucose clamp procedure [61, 76]. The study conditions most certainly invoked counterregulatory feedback, and this may explain the better fit obtained with the indirect response model.

Gopalakrishnan *et al* also utilized an indirect model, assuming insulin-induced stimulation of glucose uptake [56]. The data was taken from a study in rats, where the animals were administered either subcutaneous or spray-instilled insulin, with no additional glucose provided post-dose. The PK and PD components of the analysis were performed in a sequential manner, and the same PD model was successfully applied to both routes of administration. These results are not surprising because there appeared to be little difference in the pharmacokinetics of the insulins studied. Although the fit was good, the model was never challenged as it was never applied to external data, and, in particular, to insulins with different pharmacokinetics properties than those used to develop the model.

Subsequently, this model was expanded by Landersdorfer *et al* and applied to human glucose clamp data from healthy volunteers and subjects with T1DM) [77]. In this analysis, the model included an effect compartment to account for the delay in insulin action and a stimulatory effect on glucose disposal, making it possible to use blood glucose as the dependent variable. The model is presented in Figure 1-9. The following equations describe the model:

$$\frac{dCe}{dt} = k_{e0} \cdot (Cp(Is - Is^0) - Ce(Is - Is^0)) \quad (1\text{-}5)$$

$$\frac{dG}{dt} = k_{in} - k_{out}\left(1 + \frac{S_{\max} \cdot (Is - Is^0)}{SC50 + (Is - Is^0)}\right) \cdot G_{ss} = 0 \quad (1\text{-}6)$$

where k_{in} is the zero order rate constant for glucose input (GIR), k_{out} is the rate of glucose utilization, Is is the insulin concentration, Is^0 is the baseline insulin concentration, SC50 is the insulin concentration at half-maximal effect, S_{max} is the maximal effect, G is glucose concentration and k_{e0} is the first order rate constant between the central and effect compartments.

All data were modeled simultaneously. No significant differences were detected between the inhaled and sc insulins, however, the insulin and GIR profiles were similar, so no differences were expected. As with the work of Gopalakrishnan *et al,* the model was not challenged with different pharmacokinetic insulin profiles. However, parameters are estimated for both healthy subjects and subjects with type 1 diabetes, who showed signs of insulin resistance by higher EC50 and lower Ce estimates.

Relationship between GIR and blood glucose

Interesting work by Woodworth e*t al* presents a model which attempts to link a PD model developed using GIR data to glucose concentrations [61]. Glucose clamp procedures are used extensively to study insulin effect and compare the glucodynamic activity of different formulations, however, there is little information on whether GIR accurately represents blood glucose dynamics following insulin administration. Woodworth *et al* combined data from a glucose clamp study and a study where subjects were dosed with insulin without being clamped, and developed a simple inhibitory E_{max} model to relate the two:

$$BG = \frac{(BG_{base} - BG_0) \cdot GIR^{\lambda}}{GIR^{\lambda} + GIR_{50}^{\lambda}} \quad (1\text{-}7)$$

where BG is blood glucose at time t from the non-clamp study, GIR is the glucose infusion rate from the clamp procedure at the same time t, GIR_{50} is the GIR that relates to a 50% maximum

reduction in BG, BG_{base} is the blood glucose measured at baseline, BG_0 is the maximum tolerable reduction in BG, and γ is the sigmoidicity factor.

The E_{max} model was chosen since both the GIR and blood glucose concentrations were expected to produce a maximum response. Since these responses may correlate to different insulin amounts, the relationship cannot be assumed to be linear, but an E_{max} model can collapse to a linear relationship if one does not exist. Unfortunately no parameter estimates, or their associated error terms, were provided. However, the model appears predictive when applied to external data, when visually comparing simulated glucose concentrations overlaid with observed values. The authors conclude that the model is more predictive if counterregulatory responses can be avoided.

Hypothesis and Objectives

The goal of this specific research is the development of a PK/PD model for insulins with different pharmacokinetic properties, and the characterization and bridging of the pharmacokinetic and pharmacodynamic properties of a rapidly absorbed inhaled insulin, a subcutaneous insulin and insulin administered intravenously, using a population approach in healthy and type 2 diabetic subjects. The main hypothesis to be tested is that insulin effect is dependent upon the dynamic features of insulin pharmacokinetics, enabling the insulin pharmacokinetic profile to be used to predict insulin effect. Furthermore, a secondary hypothesis is that insulin effect is altered to some degree in type 2 diabetic subjects, whose sensitivity to insulin has been compromised by the disease state.

It is proposed that the development of a PK/PD model will make it possible to:

1. Mathematically express the relationship between insulin PK and PD
2. Link the pharmacokinetic properties of different insulins with their effect
3. Directly compare pharmacokinetically different insulins

4. Account for the effect of different demographic covariates on insulin pharmacokinetics

5. Elucidate the difference in response to insulin action in healthy volunteers and subjects with type 2 diabetes

6. Perform model-based simulation and predictions of insulin activity under different conditions.

The development of a successful insulin PK/PD model will aid in understanding the relationship of insulin PK and its effect—knowledge critical to designing improved insulin therapy.

The following specific aims are used to further explore the hypothesis:

Specific Aim 1: Develop a population pharmacokinetic (PK) model for intravenous, subcutaneous and inhaled insulin in healthy subjects following a range of doses.

A population pharmacokinetic model will be developed for single doses of insulin administered via three different routes of administration (inhaled, subcutaneous, and intravenous) to healthy subjects. This population based model will estimate insulin pharmacokinetic parameters, including relative and absolute bioavailability of inhaled and subcutaneous insulin, as well as identify and incorporate any possible demographic covariate effects on insulin pharmacokinetics in healthy volunteers.

Specific Aim 2: Develop a population pharmacodynamic (PD) model for intravenous, subcutaneous and inhaled insulin in healthy subjects following a range of doses

A population pharmacodynamic model relating serum insulin concentrations and insulin effect will be elucidated using glucose clamp data from healthy volunteers. Predicted insulin concentrations from Aim #1 will be used as the independent variable in this sequential PK/PD model. The effect variable in the model will be the glucose infusion rate (GIR), a measurement of insulin effect on glucose disposal. A pharmacodynamic model will be developed to describe the temporal dissociation between the pharmacokinetics and pharmacodynamics of insulin. The

model will attempt to describe the shift in hysteresis with respect to the different pharmacokinetic profiles of the three routes of administration, and then to describe the relationship between insulin concentration at the effect site and the response.

Specific Aim 3: Develop a population pharmacokinetic model for subcutaneously administered regular human insulin, insulin lispro, and inhaled insulin in healthy, Type 1 and Type 2 diabetic subjects.

A population pharmacokinetic model will be developed for RHI and insulin lispro administered via different routes (inhalation and subcutaneous) to healthy and type 2 diabetic subjects. This population model will estimate insulin pharmacokinetic parameters, relative bioavailability of inhaled and subcutaneously administered regular human insulin and a rapid acting analog, as well as determine demographic, route of delivery-specific and disease state-specific covariate effects on insulin pharmacokinetics.

Specific Aim 4: Develop a population pharmacodynamic model for inhaled insulin in healthy and Type 2 diabetic subjects.

A PK/PD model relating serum insulin concentrations and insulin effect will be developed, using glucose clamp data from healthy and Type 2 diabetic subjects. Differences in pharmacodynamic parameter estimates will be compared across both groups to establish the effect of the disease state on insulin effect, as described by the GIR.

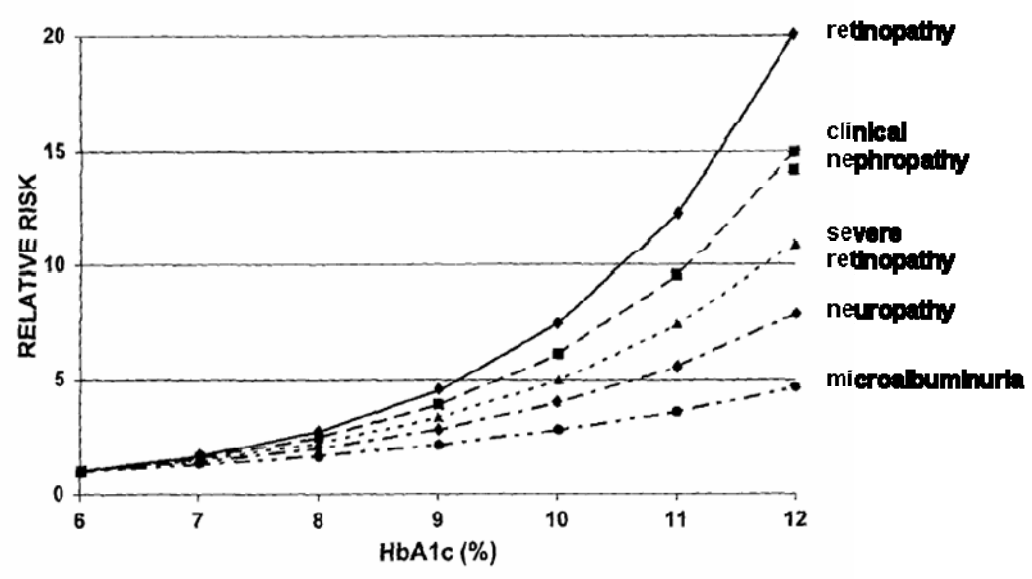

Figure 1-1 Relative risks for the development of various complications as a function of mean HbA1c during follow up in the DCCT [Source: Skyler, J, Diabetes, 1995. 44(8): p. 968-83]

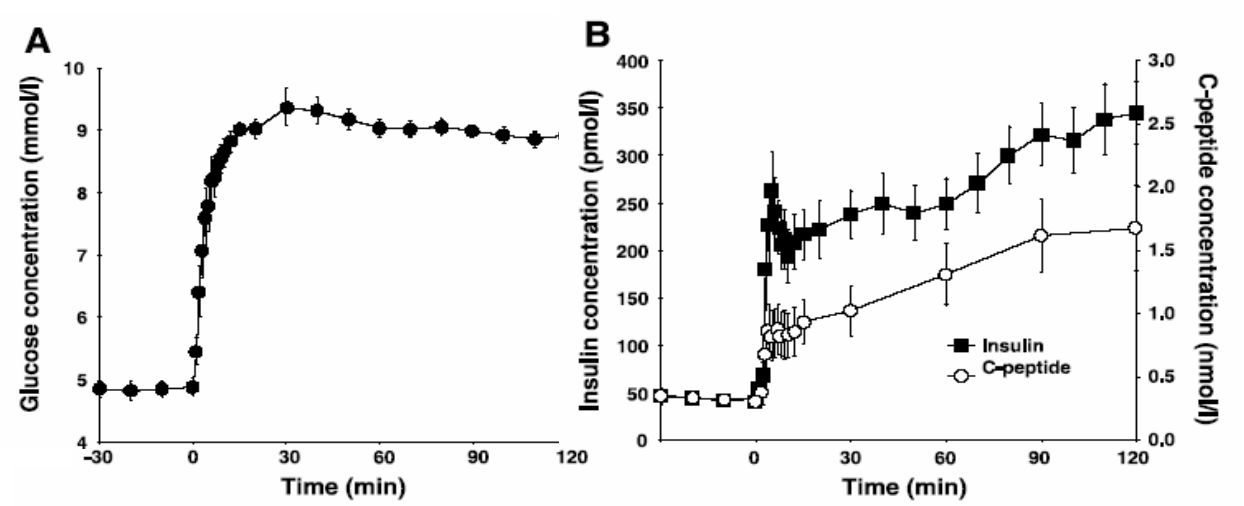

Figure 1-2 Insulin and glucose concentrations in healthy subjects during a hyperglycemic clamp study. [Source: Caumo et al, Am J Physiol Endocrinol Metab, 2004. 287(3): p. E371-85]

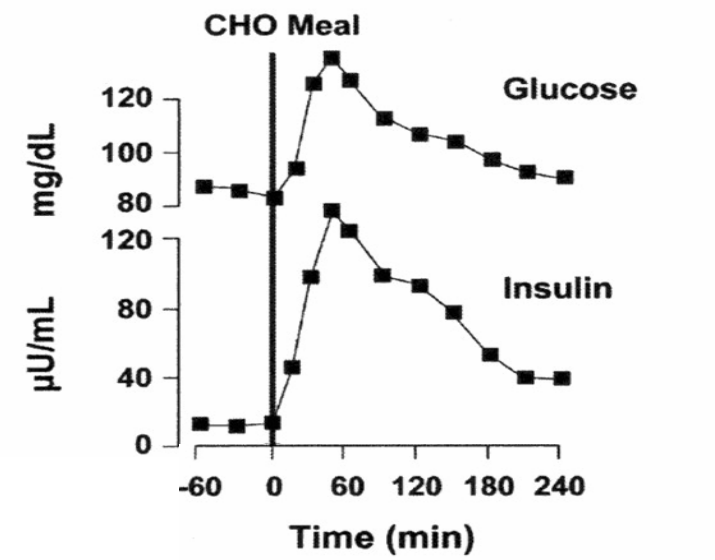

Figure 1-3 Insulin secretion: Non-diabetic subjects [Source: Aronoff, et al. Diabetes Spectrum. 2004;17: 183-90]

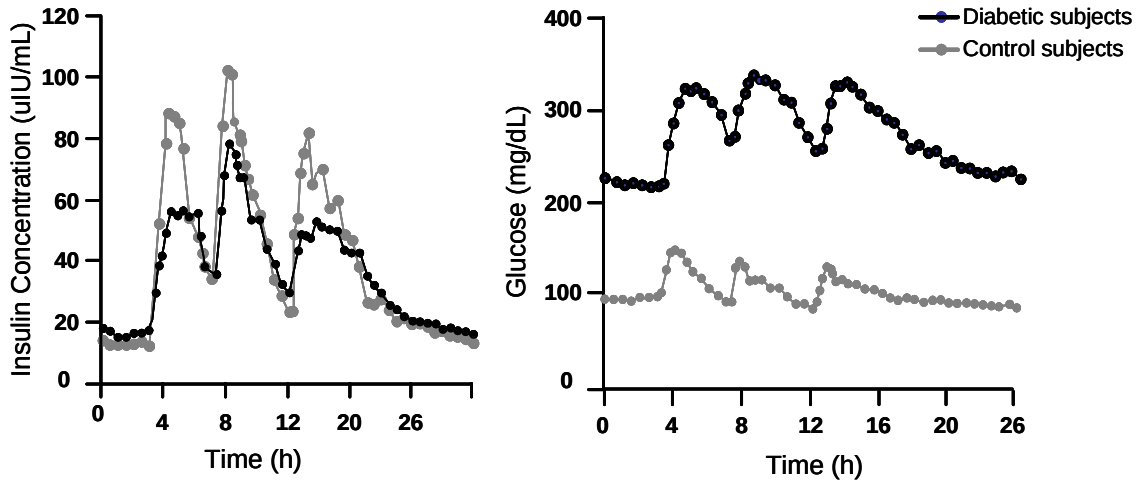

Figure 1-4 Insulin and glucose response in healthy subjects and subjects with type 2 diabetes following meal consumption [Source: Polonsky, K.S., *et al*., N Engl J Med, 1988. 318(19): p. 1231-9]

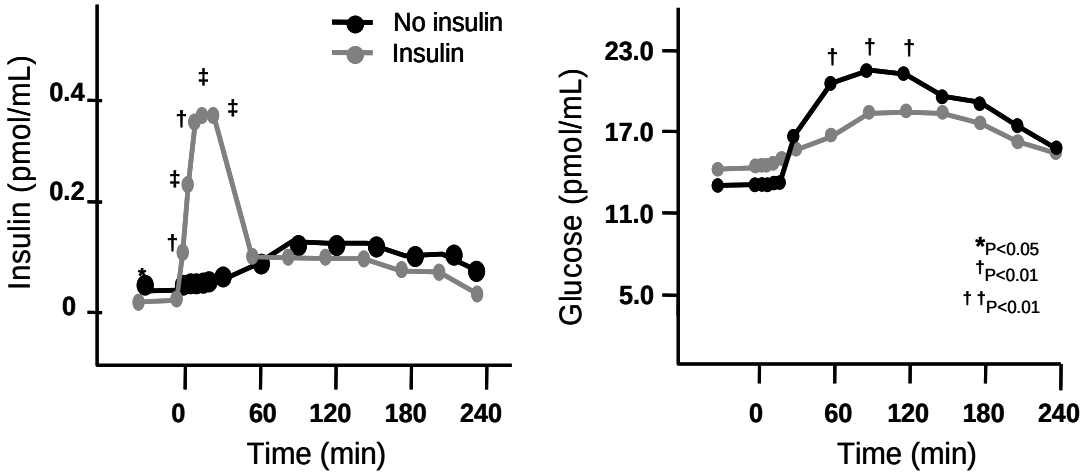

Figure 1-5 Insulin and glucose response in subjects with type 2 diabetes following meal consumption with and without insulin infusion [Source: Luzio *et al*, Diabetes Res, 1991. 16(2): p. 63-7]

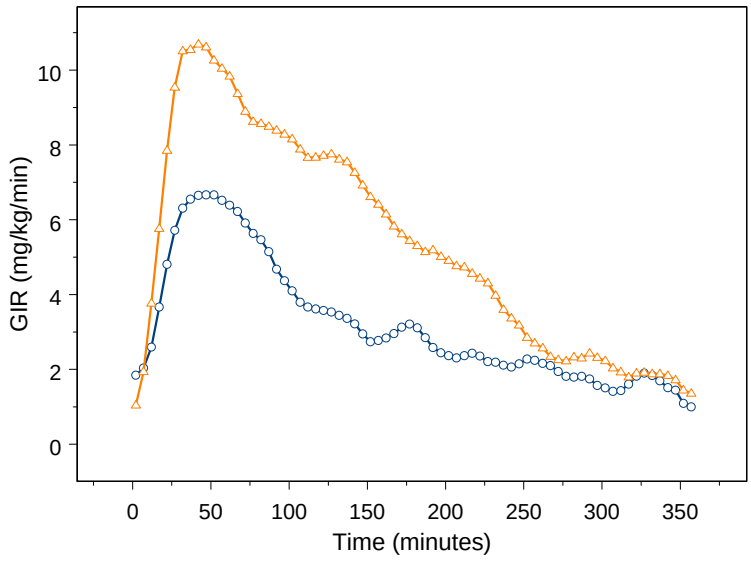

Figure 1-6 GIR vs. time profiles for two different dose strengths of insulin

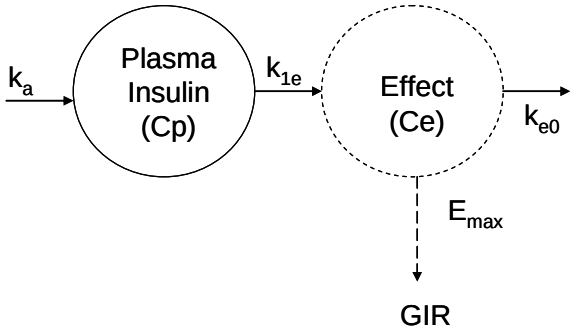

Figure 1-7 Effect compartment model

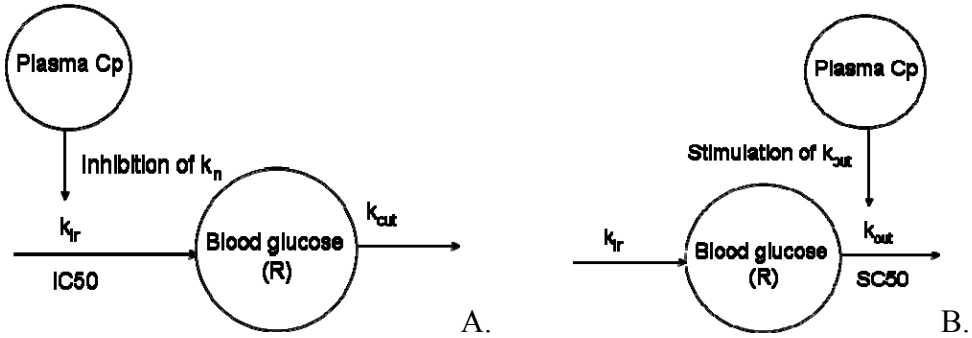

Figure 1-8 Indirect pharmacodynamic models: A) Inhibition and B) Stimulation

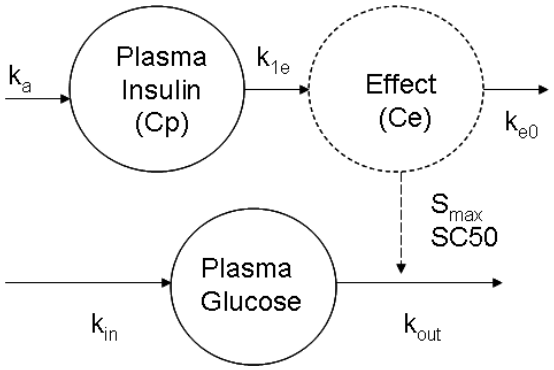

Figure 1-9 Pharmacokinetic/pharmacodynamic model diagram

CHAPTER 2
PHARMACOKINETIC MODEL FOR INTRAVENOUS, SUBCUTANEOUS AND INHALED INSULIN IN HEALTHY SUBJECTS

Background

Insulin disposition following subcutaneous or pulmonary administration has been described by a one compartment pharmacokinetic model [56-61]. Early work also suggested a one compartment model following intravenous administration, but with advances in sensitive and specific analytical methodologies, lower concentrations of insulin could be quantitated. This increased sensitivity enabled the detection of insulin concentrations in the elimination phase, revealing multiple compartment disposition following intravenously administered insulin [55]. However, the slow absorption characteristics of both subcutaneously administered insulin and early formulations for delivery via the pulmonary route obscured the distribution phase and the second compartment. Technosphere® Insulin (TI), a novel, inhaled, regular human insulin (RHI) whose administration by oral inhalation results in rapid absorption and rapid clearance makes it possible to distinguish the second compartment of the insulin pharmacokinetic profile [78].

The aim of the analysis presented here was to develop a pharmacokinetic model for RHI administered via the intravenous, subcutaneous and inhalation routes, and to demonstrate that two compartment disposition is a characteristic of insulin regardless of route of administration, with the route-dependent concentration-time profile differences due primarily to differences in absorption rates.

Materials and Methods

Study Population

Data for this analysis were combined from two separate glucose clamp studies in healthy subjects performed at the same clinical site. Each was a prospective, single-center, open-label, randomized, crossover euglycemic glucose-clamp study in healthy, non-smoking male and

female volunteers, 18–40 years of age, with a body mass index of 18–27 kg/m^2 and normal pulmonary function. Each study was local Ethics Committee reviewed and approved, and all subjects provided written informed consent prior to initiation of any study-related procedures. Prior to entry into either study, all subjects were administered a physical examination, pulmonary function tests, electrocardiography, and laboratory tests, including urinalysis and screening for drugs of abuse.

Study Design and Drug Administration

Both studies utilized a euglycemic glucose clamp procedure performed with the Biostator glucose monitoring and infusion system (Biostator, Life Science Instruments, Elkhart, IN, USA), and a continuous insulin infusion to suppress endogenous insulin production. Following an overnight fast, on each of the treatment days and prior to test article administration, the subjects received a 2-hour constant rate intravenous RHI infusion to establish a serum insulin concentration between 10–15 μU/mL to suppress endogenous insulin secretion. This infusion was continued until the end of each treatment visit. Each subject received a single dose of the test treatment on separate occasions.

Study 1: a three-way crossover euglycemic glucose-clamp study in five subjects to compare the pharmacokinetics and pharmacodynamics of single doses of 100 U of inhaled TI, 10 U RHI administered subcutaneously and 5 U RHI (Actrapid, Novo Nordisk A/S, Bagsvaerd, Denmark) administered intravenously.

Study 2: a four-way crossover euglycemic glucose-clamp study in 12 subjects to compare the pharmacokinetics and pharmacodynamics of three different single doses of inhaled TI with a single dose of 10 U RHI (Actrapid, Novo Nordisk A/S, Bagsvaerd, Denmark).

Blood glucose was kept constant at 90 mg/dL throughout the procedure by a variable infusion of a dextrose solution, controlled by the Biostator. An additional external pump,

controlled by study personnel, was employed if the Biostator could not meet the glucose infusion requirements to maintain euglycemia. If any glucose was provided by the external pump the GIR from the pump was added to the GIR of the Biostator. The subjects were maintained in the fasted state until the end of each treatment visit. The treatment periods were separated by a washout period of 3 to 28 days.

Drug Administration and Insulin Concentrations

TI was administered using a commercially available inhaler (Model M, Boehringer Ingelheim, Ingelheim, Germany) in Study 1, and via the MedTone Dry Powder Inhaler (Model Alpha, MannKind Corporation, Danbury, CT) in Study 2. RHI insulin was administered by subcutaneous injection in the abdomen. All blood samples were drawn from the cubital vein of the arm contralateral to the one used for the continuous insulin infusion and glucose administration via an intravenous catheter. Samples for the determination of insulin concentration were drawn at 120, 90, 60 and 30 minutes before dosing and 0, 1, 3, 7, 12, 20, 30, 45, 60, 90,120, 180, 240, 300 and 360 minutes post-dose, and analyzed for insulin concentration using radioimmunoassay (RIA) with double determinations. C-peptide samples were collected at 120, 60 minutes pre-dose and 0, 30, 60, 180, and 300 minutes post-dose. The samples were cooled in an ice-water bath before centrifugation. After centrifugation the plasma samples were immediately frozen and stored at -80°C until analysis. Glucose infusion rates were registered by the Biostator at every 1 minute from 120 minutes before dosing until 360 minutes post-dose.

Baseline Insulin Correction Methodology

Insulin concentrations collected at 120, 90, 60 and 30 minutes before dosing were averaged, and subtracted from all subsequently observed insulin concentrations. This method adjusted the serum insulin concentrations to account for the ongoing insulin infusion. This correction was conducted before the data was analyzed and used for model development.

Data Excluded from the Pharmacokinetic Analysis

Endogenous insulin secretion was assumed to be completely suppressed following insulin administration. However, to ensure that endogenous insulin suppression lasted for the duration of the sampling period, the serum insulin and C-peptide concentration-time profile for each dosing was examined visually. As expected, in subjects with low exposure to the test treatment, endogenous insulin appeared to be contributing to the curve in the latter part of the study. Due to the small number of samples collected for C-peptide assay, a C-peptide correction method [79] could not be applied to the insulin data, and visual inspection was used to determine insulin concentrations influenced by the endogenous component. As a result of the lower doses administered in Study 2, a higher incidence of elevated C-peptide concentrations was observed in the latter timepoints following TI treatment, particularly in the lower dose groups. All insulin concentrations after 180 minutes post-dose in the 25 U dose group, 240 minutes post-dose in the 50 U dose group, and 300 minutes in the 100 U dose group were excluded, with a total of 51 non-BLQ concentrations excluded from the analysis.

Noncompartmental Pharmacokinetic Analysis and Absolute Bioavailability

Insulin pharmacokinetics were analyzed using noncompartmental methodology using baseline-corrected insulin concentrations. The following PK parameters were derived using WinNonlin v 5.2 (Pharsight Corporation, Mountain View, CA): observed peak insulin concentration (C_{max}), time to peak insulin (t_{max}), and total insulin exposure as measured by the area under the insulin concentration-time curve from time 0 until the last time point with non-zero insulin concentrations ($AUC_{0\text{-last}}$) calculated by the linear-trapezoidal method. The terminal elimination half-life ($t_{1/2}$) was calculated as $\ln(2)/\lambda_z$ in accordance with pharmacokinetic theory [80], where λ_z is the terminal elimination rate constant estimated from log-linear regression analysis of the terminal elimination phase of the concentration-time profile, and $AUC_{0\text{-}\infty}$ was

calculated as $AUC_{0\text{-last}} + C_{last}/\lambda_z$, where C_{last} is the last observed insulin concentration. Noncompartmental parameter values were used to determine starting estimates for pharmacokinetic modeling, and were compared to parameter values estimated by the final model as part of the model fit assessment.

Absolute bioavailability (%F) was determined using the mean dose-normalized insulin $AUC_{0\text{-last}}$ values, expressed as the group average dose-normalized $AUC_{0\text{-last}}$/average dose-normalized $AUC_{0\text{-last}}$ following iv administration.

Pharmacokinetic Model and Data Analysis

The software package NONMEM (Version VI, Level 1.2, NONMEM Project Group, ICON Development Solutions, USA) was used for the population analysis. The ADVAN6 subroutine and first-order (FO) estimation method was used. NONMEM describes the observed concentration-time data in terms of:

- A number of fixed effect parameters, θ, which may include the mean values of the relevant base pharmacokinetic model parameters, or a number of parameters which relate the base model parameters to demographic and other covariates;
- Two types of random effect parameters: (a) ω^2: the variances of the interindividual variability (η) within the population, and (b) σ^2: the variances of the residual intraindividual variability (ε) due to random fluctuations in an individual's parameter values, measurement error, model misspecification, and all sources of error not accounted for by the other parameters.

The population or average values of the parameters, θ, the interindividual variances, ω^2, and the residual variance, σ^2, were estimated by NONMEM. Subject-specific parameters were calculated by NONMEM using the POSTHOC option. These parameters are empirical Bayesian estimates of the individual's true parameters based on the population parameters and the individual's observed concentrations.

Pharmacokinetic base model

Data from all three routes of administration were modeled simultaneously. The PK was described by a two compartment model with one (inhaled) or two sequential (sc insulin) first order absorption processes and first-order elimination [81]. A diagram of the model is presented in Figure 2-1. The model was described by the following differential equations:

$$\frac{dA_1}{dt} = -ka_1 \cdot A_1 \quad (2\text{-}1)$$

$$\frac{dA_2}{dt} = ka_1 \cdot A_1 - ka_2 \cdot A_2 \quad (2\text{-}2)$$

$$\frac{dA_3}{dt} = -ka_{TI} \cdot A_{31} \quad (2\text{-}3)$$

$$\frac{dA_4}{dt} = ka_{TI} \cdot A_3 + ka_2 \cdot A_2 + k_{54} \cdot A_5 - k_{45} \cdot A_4 - k \cdot A_4 \quad (2\text{-}4)$$

$$\frac{dA_5}{dt} = k_{45} \cdot A_4 - k_{54} \cdot A_5 \quad (2\text{-}5)$$

The pharmacokinetic structural model was parameterized in terms of clearance (CL), volume of distribution in the central compartment (V_c), intercompartmental clearance (Q), the volume of distribution in the peripheral compartment (V_p), the first order absorption rate constant for TI (ka_{TI}), the two first order absorption rate constants associated with the sequential absorption for subcutaneously administered insulin ($ka_{sc1}$and ka_{sc2}, depot and a transit compartment) and the absolute bioavailability for subcutaneous insulin and TI (F_{sc}, F_{TI}).

Error model

Fixed effects parameters were used to describe the typical population estimates, and an exponential random effect model was used to describe interindividual variability for each model parameter:

$$\theta_i = \theta^{\eta_i} \quad (2\text{-}6)$$

where θ_i is the estimated parameter value for the i^{th} individual, θ is the fixed effect typical parameter value in the population, and η_i are individual-specific random effects for the i^{th} individual symmetrically distributed with zero mean and variance ω.

A combined proportional and additive error model was used to model the residual unexplained variability, as described by the following equation:

$$Cp_{ij} = \widetilde{C}p_{ij} \cdot (1 + \varepsilon_{1ij}) + \varepsilon_{2ij} \quad (2\text{-}7)$$

where Cp_{ij} is the observed value of the jth plasma concentration of individual i; $\widetilde{C}p_{ij}$ is the predicted j^{th} plasma concentration of individual i; and ε_{ij} is a random variable which represents the discrepancy between the observed and predicted j^{th} concentration.

Considerable interoccasion variability (IOV) was observed within the TI groups, and was attributed to natural variation in inhalation on different occasions, resulting in differences in relative bioavailability at different visits, as described by:

$$F_{TI} = \theta_{FTI}^{\eta_{FTI} + \eta_{OCC1} \cdot OCC1 + \eta_{OCC2} \cdot OCC2 + \eta_{OCC3} \cdot OCC3} \quad (2\text{-}8)$$

where *OCC1*, *OCC2* and *OCC3* are set to 1 at the corresponding occasion and 0 otherwise.

Reparametrization and individual predicted values

Individual-specific values of each pharmacokinetic parameter were obtained by Bayesian analysis with the final model.

$$CL = k \cdot V_4 \quad (2\text{-}9)$$

$$Q = k_{45} \cdot V_4 \quad (2\text{-}10)$$

The following pharmacokinetic parameters could subsequently be calculated for each individual according to the following equations based on compartment modeling theory.

$$\beta = \frac{1}{2}\left[(k_{45} + k_{54} + k) + \sqrt{k_{45} + k_{54} + k + 4k_{54}k}\right] \quad (2\text{-}11)$$

$$\alpha = \frac{1}{2}\left[(k_{45} + k_{54} + k) + \sqrt{k_{45} + k_{54} + k - 4k_{54}k}\right] \quad (2\text{-}12)$$

$$\alpha \ half - life = \frac{0.693}{\alpha} \quad (2\text{-}13)$$

$$\beta \ half - life = \frac{0.693}{\beta} \quad (2\text{-}14)$$

$$absorption \ half - life = \frac{0.693}{k_a} \quad (2\text{-}15)$$

Model fit assessment

Goodness-of-fit was determined by the objective function values (OFV) and visual inspection of scatter plots of predicted versus observed concentrations and weighted residuals. For nested models, hypothesis tests were performed based on the likelihood ratio test, in which the change in OFV approximates the χ^2 distribution. A more complicated model was preferred when the decrease in OFV was more than 3.84 (the critical value for the χ^2 distribution at $p< 0.05$ with 1 degree of freedom).

Covariate analysis

Following the determination of the base population model, potential covariates were examined to determine whether they improved the overall fit and reduced variability in the model. These covariates included age, body weight, body height and BMI. Covariates were initially evaluated for possible relationships with the model estimated pharmacokinetic parameters using the generalized additive model (GAM) procedure in Xpose [82] which incorporates the Akaike Information Criterion (AIC) for covariate identification. Covariates associated with a reduction in the AIC were evaluated using NONMEM in a stepwise manner. Each covariate added to the base model, and the resulting univariate model was then compared to

the reduced model for significant improvement in fit. Covariates were included in the model if the criteria for nested model criteria (a 3.84 point drop in the OFV) was observed ($p<0.05$). Backward elimination was then performed where each covariate was independently removed from the model to confirm its relevance. An increase in the OFV of 6.7 ($p<0.01$) was necessary to confirm that the covariate was significant.

Results

Study Population

All subjects completed the studies and received all scheduled doses. In Study 1, for one subject in the 5 U iv dose group, the insulin concentration time profile did not match the dosing and sampling times, indicating that possible errors may have been made when dosing or sampling times were recorded, and the elapsed time since dose could not be determined with certainty. Since the dosing time could not be determined with certainty, this subject was excluded from the analysis. In Study 2, a subject was excluded from analysis in the 10 U sc treatment group, since three consecutive BLQ values were observed in the pharmacokinetic profile following sc RHI treatment, suggesting a possible analytical error. Furthermore, upon visual inspection of the insulin concentration-time profiles, data from one subject appeared to differ markedly from the other subjects, with almost no insulin exposure within the first few hours post-dose, suggesting that the subject may have had difficulty with inhalation. Statistical analysis determined the subject to be an outlier with respect to at least one pharmacokinetic parameter for each dose group ($p< 0.05$), and consequently, this subject was excluded from all the analysis. Dixon's test was used on all log-transformed pharmacokinetic parameters, with the exception of t_{max}, which was tested using non-transformed values and Tukey's test. A total of 650 insulin concentrations from 16 subjects, and 57 profiles were included in the analysis. Demographic data is summarized in Table 2-1.

Noncompartmental Pharmacokinetic Analysis

Mean insulin concentration-time profiles are presented in Figure 2-2. Noncompartmental pharmacokinetic parameter estimates are presented in Table 2-2. Based on mean dose-normalized $AUC_{0\text{-last}}$, insulin following subcutaneous administration was approximately 53%, and between 10 and 11% following TI administration, and did not appear to depend on TI dose. Terminal insulin half-life and $AUC_{0\text{-}\infty}$ could not be calculated following subcutaneous dosing due to the prolonged absorption from the tissue, and the flip-flop kinetics associated with this route of insulin administration.

Pharmacokinetic Model

A two-compartment open model with one (inhaled) or two sequential (subcutaneous) first order absorption processes and first-order elimination described the insulin concentration data well. The population typical parameter values in the structural model were: clearance, 43.7 L/hr; volume of distribution in the central compartment, 5.11 L; volume of distribution in the peripheral compartment, 31.6 L. These parameter estimates are in close agreement with values reported in literature for intravenous insulin [55]. The base model pharmacokinetic parameter estimates are summarized in Table 2-4.

Covariate analysis

The covariate analysis process is summarized in Table 2-3. A GAM analysis identified BMI as a potential covariate for absorption rate constant associated with sc insulin, and body weight as a potential covariate for volume of distribution in the central compartment; to a lesser extent, age was identified as a potential covariate for the peripheral volume of distribution. Visual inspection of covariate vs. parameter scatter plots and graphs of weighted residuals vs. covariates confirmed these findings. Because different inhalers were used in the two studies, a possible effect on TI bioavailability was examined by adding the effect into the univariate

analysis. The lack of trend seen visually was confirmed by a lack of change in OFV when the covariate was tested.

The results of a stepwise forward addition showed that following the addition of BMI ($p<0.01$) as a covariate to the subcutaneous absorption rate constant, the further addition of weight or subject age on any of the identified parameters did not significantly contribute to the model. BMI effect was described by the following equation:

$$ka_{sc1} = \theta_{kasc1}(1 - \theta_{BMI,kasc1} \cdot (BMI / 23.65) \quad (2\text{-}16)$$

where BMI was centered around the population median value. The addition of this covariate decreased the OFV by 9.41 points and also reduced the interindividual CV% on Ka_{sc1} from 57% to 50% (Tables 2-3 and 2-4).

Final model

The overall model fit was good, with individual predicted versus observed values distributed along the line of unity, and no significant trends in the weighted residuals (Figure 2-3). Thus, the structural and error models appeared to adequately describe insulin pharmacokinetics and explain the variability in the data.

In the final model, the population typical parameter values were: clearance, 43.4 L/hr; volume of distribution in the central compartment, 5.0 L; volume of distribution in the peripheral compartment, 30.7 L. As with the base model, the parameter estimates are in close agreement with values reported in the literature for intravenous insulin [55]. The absolute bioavailability for subcutaneous insulin and TI was 52% and 11%, respectively, matching both results reported with TI [83] and to results reported with sc RHI [84], as well as the results of the noncompartmental analysis (Table 2-2). The pharmacokinetic parameter estimates are summarized in Table 2-4.

The α and β-half-lives of 5 and 93 minutes, respectively, were calculated from the individual predicted parameters and are in close agreement with both the insulin half-life estimates following iv administration reported previously [55] and the terminal half-life approximated following noncompartmental analysis (Table 2-2). The population predicted concentration-time profiles are presented in Figure 2-4. Following intravenous dosing, the distribution phase was approximately thirty minutes. The apparent distribution phase was longer following TI administration, and undistinguishable from the elimination phase following subcutaneous dosing due to the prolonged absorption from the injection site.

Interoccasion variability following TI administration was approximately 30%. The interindividual %CV for all pharmacokinetic parameter estimates ranged from 10 to 52%. The residual error was described by a combined proportional (25.1 %CV) and additive (2.27 μIU/mL) model. Example observed and predicted concentration-time profiles are shown in Figure 2-5 and Figure 2-6.

Discussion

Insulin has been shown to demonstrate a two compartment disposition following intravenous administration, with a previously reported α-half-life of approximately 5-6 minutes [55]. Because the α-phase is short compared to the duration of absorption following subcutaneous administration, the absorption phase obscures the initial distribution, rendering it difficult to distinguish the second compartment. Furthermore, slow absorption dominates the pharmacokinetics of subcutaneously administered insulin in a phenomenon commonly termed "flip-flop" kinetics [59]. As a result of this, the differences in insulin profiles, especially the terminal phase, observed among the various non-iv routes of administration reflect the differences in absorption, not elimination.

Most available assessments of insulin pharmacokinetics use the pharmacokinetic profiles of subcutaneously administered formulations, as this route of administration has been the dominant route since insulin's initiation as a therapeutic agent. Hence, the pharmacokinetic profiles following non-intravenous routes of insulin administration have been described using a one compartment model [57, 59, 85].

TI is a novel inhaled insulin whose unique delivery characteristics result in rapid absorption and systemic clearance, enabling a clearly distinguishable second compartment in its pharmacokinetic profile. This is unique for an insulin formulation, and is thought to be due to the combination of: 1) the quick dissolution of the delivery microparticles upon contact with the lung surface [86]; and, 2) TI is delivered as an insulin monomer to the lung [87], which is the most readily absorbed form of insulin [88]. Because insulin pharmacokinetic properties are expected to be consistent once it is available systemically [89], the inclusion of data from TI and intravenous dosing, both of which have distinct α and β phases in their pharmacokinetic profiles, made it possible to demonstrate the two compartment disposition of all three routes of insulin administration. Furthermore, it allowed for an estimate of the absorption rate differences between TI and subcutaneously administered insulin. A model incorporating two sequential absorption rates and a transit compartment was used to describe the slower absorption seen with the subcutaneously administered insulin. This model was described by Puckett *et al* [81] and was based on the physiology of subcutaneous insulin administration, where the deport compartment represents the subcutaneous tissue, and the second compartment represents the interstitial space.

Interoccasion inhalation variability can result in differences in the bioavailability of treatments administered through the lung. Although this variability may be reduced with

repeated dosing, treatment-naïve or inexperienced subjects may exhibit significant interoccasion differences in exposure. In this analysis, subjects in one of the studies were administered three different doses of TI on three different occasions. The interoccasion variability was successfully modeled to reflect inhalation differences that resulted in a difference in insulin bioavailability, with no difference in other pharmacokinetic parameters. For this group of subjects, the interoccasion variability was estimated by the model to be approximately 30%. Combined with the variability unaccounted for by the interoccasion model (11 %CV), the overall interindividual variability was comparable with that of subcutaneously administered insulin (52 %CV).

Covariate analysis was not expected to result in many findings due to the small number of subjects in this analysis and the fact that the subjects were young, healthy volunteers. However, even in this population, increases in BMI were found to decrease absorption rate when insulin was administered subcutaneously, as reported previously by others [90]. This observation may be attributed to the increased thickness of the subcutaneous tissue in subjects with higher BMI, which slows absorption from the depot compartment. Since this relationship was detected in the healthy population with BMI scores within the normal range, it is expected that a greater impact would be observed on patients taking subcutaneous insulin who have higher BMI, as is often the case in subjects with type 2 diabetes.

Conclusions

Insulin pharmacokinetics were found to be consistent with a two-compartment model, with an approximate distribution phase of about half an hour following intravenous dosing. The apparent distribution phase is longer following TI administration and undistinguishable following subcutaneous dosing due to the prolonged duration of absorption. BMI was found to be a significant covariate on insulin absorption rate following subcutaneous dosing, with an associated decrease in the rate of absorption with increasing BMI. In the model presented here,

differences in the shape of the insulin curve following different routes of administration were successfully attributed to differences in absorption.

Table 2-1 Summary of demographics

Demographic Variable		Value
Age (years)	Mean ± SD	28 ± 4
Weight (kg)	Mean ± SD	76 ± 11
BMI (kg/m2)	Mean ± SD	24 ± 2
Height (cm)	Mean ± SD	179 ± 9
Gender		
Male	N	14
Female	N	2
Race		
Caucasian	N	15
Asian	N	1

Table 2-2 Mean (%CV) noncompartmental pharmacokinetic parameter estimates

Dose Group	t_{max} (h)*	C_{max} (μU/mL)	$AUC_{0\text{-last}}$ (μU/mL·min)	Half-life (h)	$AUC_{0\text{-}\infty}$ (μU/mL·min)	Dose-Normalized $AUC_{0\text{-last}}$ (μU/mL·min)
5 U iv (n=4)	--	--	100.0 (21)	1.7 (23)	103.2 (19)	20.1
10 U sc (n=15)	1.5	30.7 (34)	107.0 (26)	--	--	10.7
25 U TI (n=11)	0.2	54.6 (72)	50.0 (61)	1.1 (61)	57.4 (62)	2.0
50 U TI (n=11)	0.2	105.3 (38)	101.5 (39)	1.3 (31)	111.2 (39)	2.0
100 U TI (n=16)	0.33	240.9 (52)	218.6 (43)	1.4 (57)	230.6 (41)	2.2

* Median presented for t_{max};

Table 2-3 Covariate selection

Covariate Model Tested	OFV	Change in OFV
Base Model	3695.551	
BMI on Kasc1	3686.141	9.410
Body weight on V_c	3694.240	1.311
Age on Vp	3691.658	3.893
BMI on K_{asc1} and Age on V_p	3682.352	3.789

Table 2-4 Population pharmacokinetic parameters of insulin

Pharmacokinetic Parameters	Base Model	Full Model
Parameter	Estimate (%RSE)	Estimate (%RSE)
CL (L/hr)	43.70 (8.6)	43.4 (8.6)
V_c (L)	5.11 (10.0)	5.02 (9.6)
Q (L/hr)	24.5 (15.4)	23.9 (13.3)
V_p (L)	31.6 (18.5)	30.7 (15.4)
ka_{sc1} (hr^{-1})	0.52 (17.3)	2.37 (14.4)
ka_{sc2} (hr^{-1})	1.28 (25.4)	1.04 (22.8)
ka_{TI} (hr^{-1})	2.34 (8.7)	2.35 (8.9)
F_{sc}(%)	53 (13.4)	52 (13.0)
F_{TI} (%)	11 (12.7)	11 (13.0)
BMI covariate effect		0.74 (8.0)
Interindividual and Residual Variability	(%CV)	(%CV)
ω_{CL}	9.2	9.9
ω_{Vc}	37.8	36.9
ω_{Q}	31.5	30.7
ω_{Vp}	29.5	27.7
ω_{kasc1}	57.4	50.1
ω_{kaTI}	19.1	19.6
ω_{Fsc}	23.2	24.1
ω_{FTI}	24.0	23.7
$\omega_{IOV\ FTI}$	30.7	30.2
σ_1	26.1	25.1
σ_2	1.3*	1.51 *

Note: *σ_2 (additive residual error) is expressed in μU/mL; The magnitude of interindividual and residual variability was expressed as CV%, approximated by the square root of the variance estimate.

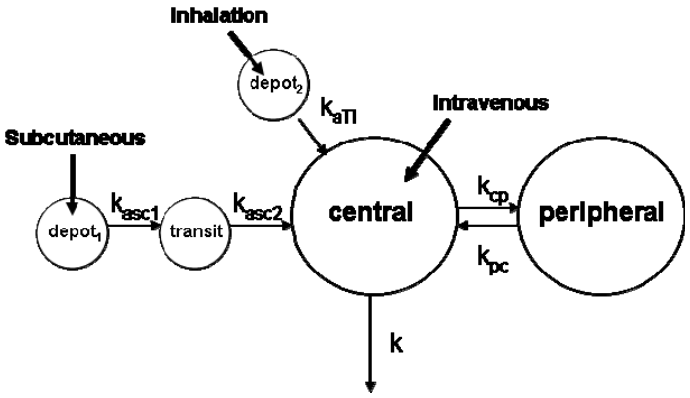

Figure 2-1 Pharmacokinetic model diagram

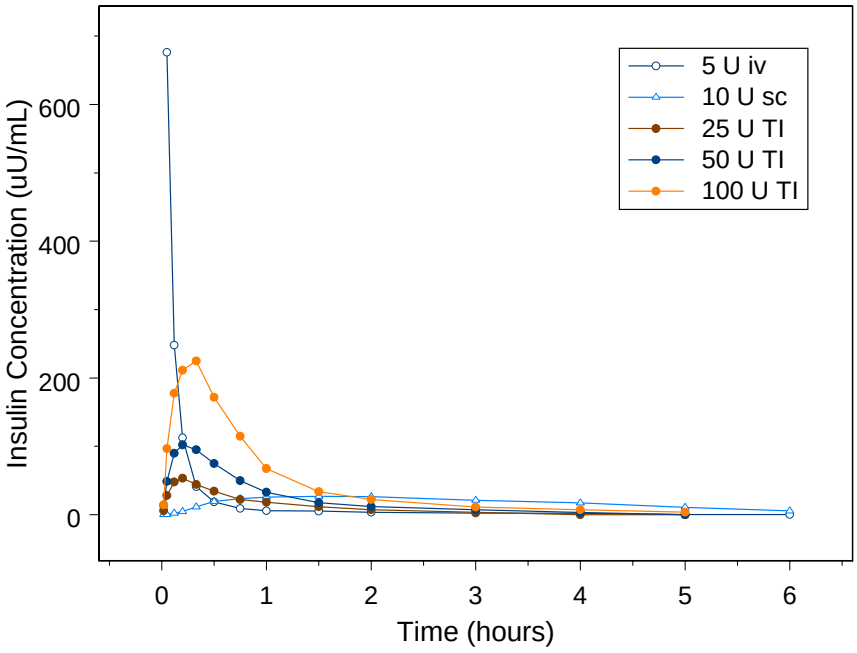

Figure 2-2 Mean insulin concentration-time profiles for all dose groups

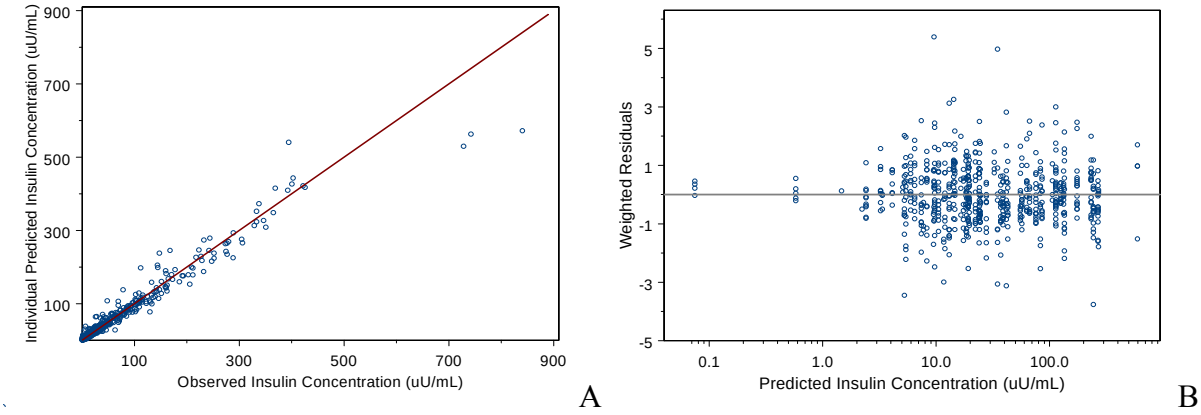

Figure 2-3 Goodness of fit plots. A) Individual predicted versus observed insulin concentrations and B) Predicted insulin concentrations versus weighted residuals

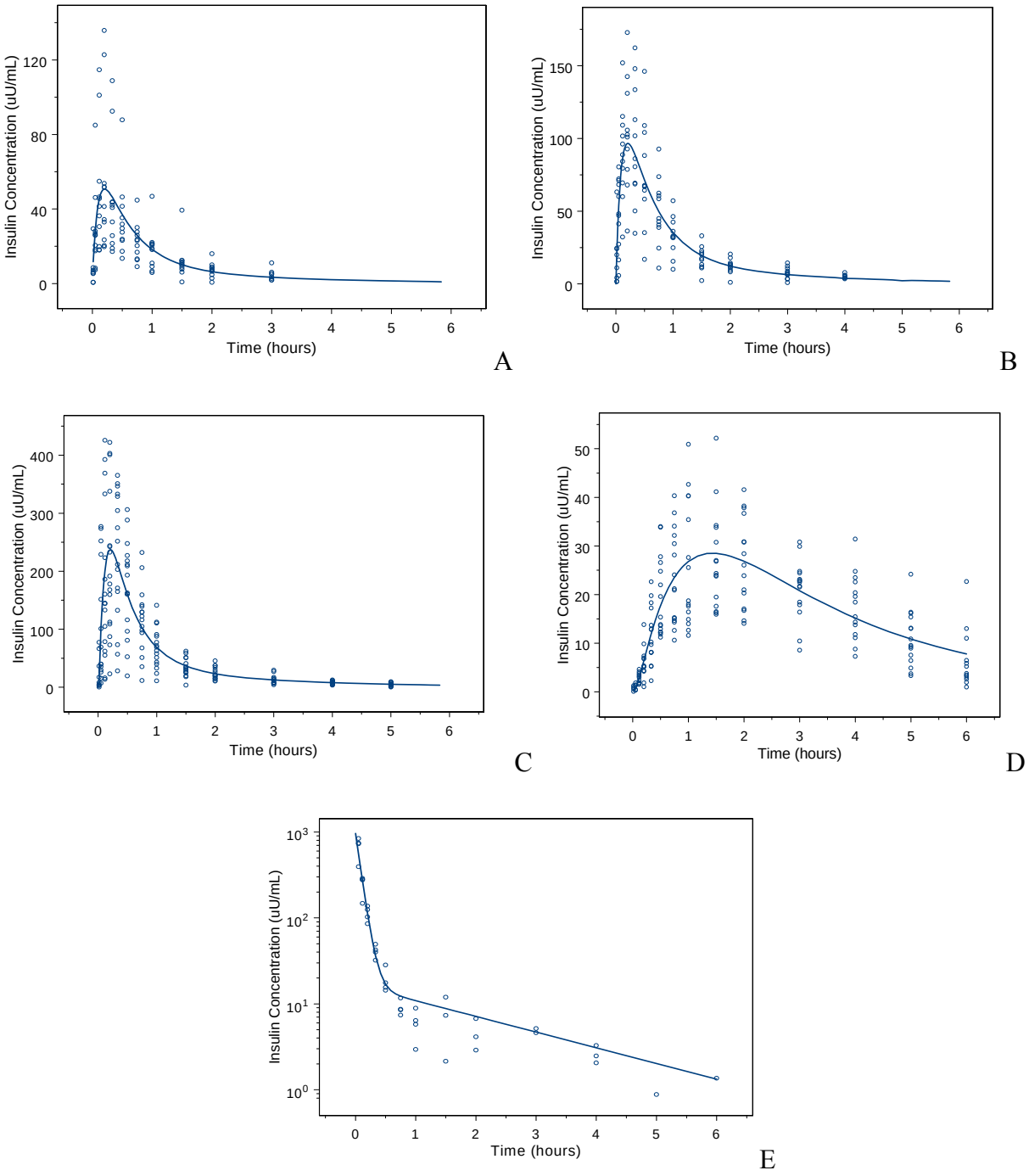

Figure 2-4 Population predicted concentration-time profiles and observed data by dose group. A) TI 25 U dose, B) TI 50 U dose, C) TI 100 U dose, D) subcutaneous RHI 10 U dose, E) intravenous RHI 5 U dose

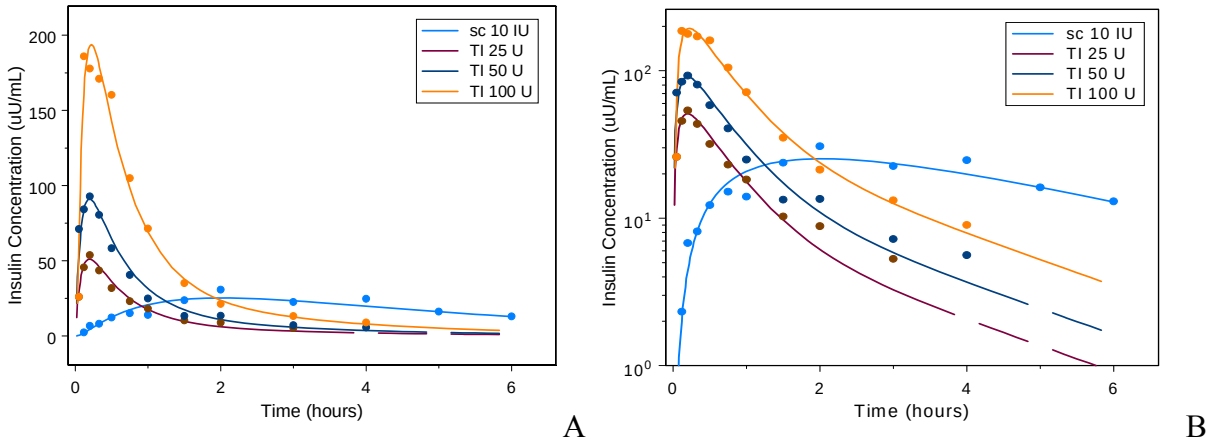

Figure 2-5 Example observed and predicted concentration-time profiles. A) Individual predicted versus observed insulin concentrations for subject 5 (linear scale) and B) Individual predicted versus observed insulin concentrations for subject 5 (log scale)

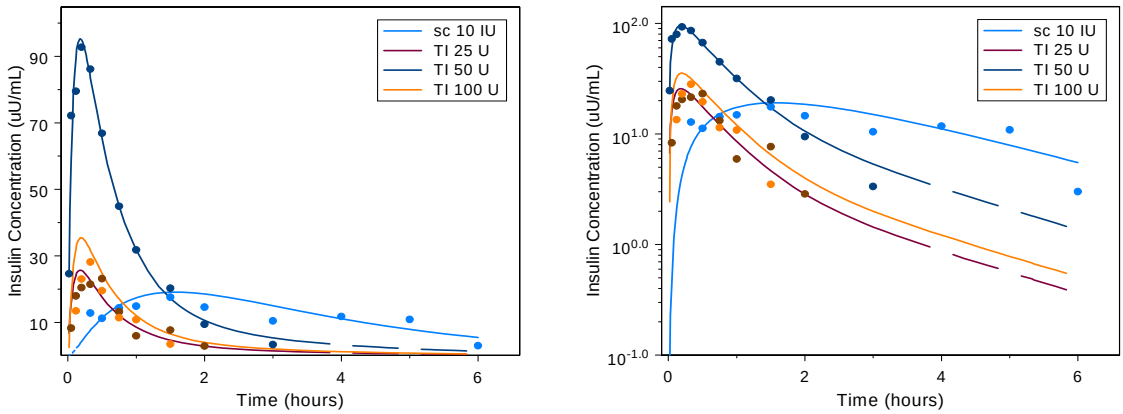

Figure 2-6 Example observed and predicted concentration-time profiles. A) Individual predicted versus observed insulin concentrations for subject 1 (linear scale) and B) Individual predicted versus observed insulin concentrations for subject 1 (log scale)

CHAPTER 3
PHARMACODYNAMIC MODEL FOR INTRAVENOUS, SUBCUTANEOUS AND INHALED INSULIN IN HEALTHY SUBJECTS

Background

The glucose clamp procedure has been used to study biochemical and feedback mechanisms affiliated with diabetes, including determination of insulin sensitivity [47], the effects of exercise [48], and counterregulatory and glucagon responses [49]. More recently, the glucose clamp procedure has been used to study insulin activity [9, 17, 35, 39]. To assess the response to insulin, plasma glucose concentration is held constant at basal levels by a variable glucose infusion. Under these steady-state conditions of euglycemia, the glucose infusion rate equals glucose uptake by all the tissues in the body and is therefore a measure of tissue sensitivity to insulin [14]. By suppressing endogenous insulin secretion one can observe the effects of the administered insulin without confounding additional effect from insulin secreted by the pancreas in response to the administered glucose. An exogenous insulin infusion employed during the study is assumed to completely suppress hepatic glucose production, as well as appreciable insulin secretion, allowing the glucose infusion rate (GIR) to be used as a measure of the pharmacodynamic response to the test treatment insulin only [36]. Numerous pharmacokinetic/pharmacodynamic (PK/PD) models have been developed to establish a relationship between insulin pharmacokinetics and its effect, as assessed by the GIR.

Although considerable efforts have been made to model insulin PK/PD, the pharmacokinetic similarity of most insulin formulations has made it difficult to develop a model which can be applied to pharmacokinetically diverse insulins. Technosphere® Insulin (TI) is a novel inhaled insulin whose unique delivery characteristics result in rapid absorption and systemic clearance, even when compared to rapid acting analogs [91]. The aim of this analysis was to develop a PK/PD model for regular human insulin (RHI) following TI, intravenous and

subcutaneous administration, and to better elucidate the relationship between the vastly different pharmacokinetic profiles of these three insulins with their effect as measured by the GIR.

Materials and Methods

Study Population

Data for this analysis were combined from two glucose clamp studies in healthy subjects performed at the same clinical site. Each study was a prospective, single-center, open-label, randomized, crossover euglycemic glucose-clamp study in healthy, non-smoking male and female volunteers, 18–40 years of age, with a body mass index of 18–27 kg/m^2 and normal pulmonary function. Each study was local ethics committee reviewed and approved, and all subjects provided written informed consent prior to initiating any study-related procedure. Prior to entry into either study, all subjects were administered a physical examination, pulmonary function tests, electrocardiography, and laboratory tests, including urinalysis and screening for drugs of abuse.

Study Design and Drug Administration

Both studies were euglycemic glucose clamp procedures, and were performed utilizing the Biostator glucose monitoring and infusion system (Biostator, Life Science Instruments, Elkhart, IN, USA), and a continuous insulin infusion to suppress endogenous insulin production. Following an overnight fast and prior to test article administration, on each of the treatment days the subjects received a 2-hour constant rate intravenous RHI infusion to establish a serum insulin concentration between 10–15 μU/mL and suppress endogenous insulin secretion. This infusion was continued until the end of each treatment visit. Each subject received a single dose of the test treatment on separate occasions.

Study 1: a three-way crossover euglycemic glucose-clamp study in five subjects to compare the pharmacokinetics and pharmacodynamics of single doses of 100 U of inhaled TI, 10

U RHI administered subcutaneously and 5 U RHI (Actrapid, Novo Nordisk A/S, Bagsvaerd, Denmark) administered intravenously.

Study 2: a four-way crossover euglycemic glucose-clamp study in 12 subjects to compare single dose of 10 U RHI (Actrapid, Novo Nordisk A/S, Bagsvaerd, Denmark) with single doses of 25, 50 and 100 U of TI.

Blood glucose was kept constant at 90 mg/dL throughout the procedure by a variable infusion of a dextrose solution, controlled by the Biostator. If the Biostator could not meet the glucose infusion requirements to maintain euglycemia, an additional, external pump controlled by study personnel was employed. If any glucose was provided by the external pump, that infusion rate was added to the GIR of the Biostator. The subjects remained fasted until the end of the study. The treatment periods were separated by a washout period of 3 to 28 days. Both studies were performed at the same clinical site.

Drug administration and serum insulin concentrations

TI was administered using a commercially available inhaler (Model M, Boehringer Ingelheim, Ingelheim, Germany) in Study 1, and via the MedTone Dry Powder Inhaler (Model Alpha, MannKind Corporation, Danbury, CT) in Study 2. RHI insulin was administered by subcutaneous injection in the abdomen. All blood samples were drawn from the cubital vein of the arm contralateral to the one used for the continuous insulin infusion and glucose administration via an intravenous catheter. Samples for the determination of insulin concentration were drawn at 120, 90, 60 and 30 minutes before dosing and 0, 1, 3, 7, 12, 20, 30, 45, 60, 90,120, 180, 240, 300 and 360 minutes post-dose, and analyzed for insulin concentration using radioimmunoassay (RIA) with double determinations. C-peptide samples were collected at 120, 60 minutes pre-dose and 0, 30, 60, 180, and 300 minutes post-dose. The samples were

cooled in an ice-water bath before centrifugation. After centrifugation the plasma samples were immediately frozen and stored at -80°C until analysis.

Glucose infusion rates and blood glucose concentrations

Glucose infusion rates were registered by the Biostator® every minute from 120 minutes before dosing until 360 minutes post-dose. The blood glucose (BG) measurements of the Biostator were recalibrated at regular intervals (range, 10–30 minutes) by the YSI 2300 STAT Plus™ Glucose Analyzer (YSI Life Sciences, Yellow Springs, OH), which employed the glucose oxidase method. For all subjects, blood glucose concentrations were maintained within the predefined range from the time of dosing until the end of the clamp procedure.

Baseline Correction and Smoothing Methodology

In order to subtract the contribution of the ongoing insulin infusion, serum insulin concentrations were corrected for baseline insulin levels, before being analyzed and used for pharmacokinetic model development. Insulin concentrations collected at 120, 90, 60 and 30 minutes before dosing were averaged, and subtracted from all subsequently observed insulin concentrations. The uncorrected GIR values were smoothed using a 10-minute running average.

Insulin Data for the Pharmacokinetic/Pharmacodynamic Analysis

Individual predicted insulin pharmacokinetic parameters from the pharmacokinetic model (Chapter 2) were used to simulate the insulin concentrations used in the analysis. The pharmacokinetics was described by a two compartment open model with one (inhaled) or two sequential (subcutaneous) first order absorption processes and first-order elimination. Since the pharmacokinetic model was developed using baseline corrected insulin concentrations and the PK/PD analysis targeted exploring the relationship between total insulin concentrations and total GIRs, the simulated insulin values were each added to the baseline used for correction at each

visit. Corresponding insulin and GIR values (every 5 minutes for the first hour and every 10 minutes thereafter) were combined for the analysis.

Pharmacodynamic Model and Data Analysis

The software package NONMEM (Version VI, Level 1.2, NONMEM Project Group, ICON Development Solutions, USA) was used for the population analysis using both the first order conditional estimation method (FOCE) with interaction and the subroutine ADVAN 6.

NONMEM describes the observed effect data in terms of:

- A number of fixed effect parameters, θ, which may include the mean values of the relevant base model parameters, or a number of parameters which relate the base model parameters to demographic and other covariates;
- Two types of random effect parameters: (a) ω^2: the variances of the interindividual variability (η) within the population, and (b) σ^2: the variances of the residual intraindividual variability (ε) due to random fluctuations in an individual's parameter values, measurement error, model misspecification, and all sources of error not accounted for by the other parameters.

The population or average values of the parameters, θ, the interindividual variances, ω^2, and the residual variance, σ^2, were estimated by NONMEM. The η values are independent, identically distributed random errors with a mean of zero and a variance equal to ω^2. Subject-specific parameters were calculated by NONMEM using the FOCE option. These parameters are empirical Bayesian estimates of the individual's true parameters based on the population parameters and the individual's observed concentrations.

Pharmacodynamic model

In a glucose clamp study, blood glucose remains constant and the GIR serves as a surrogate for insulin-mediated glucose disposal and is a natural choice for the pharmacodynamic endpoint. The presence of a hysteresis in insulin effect necessitates that the time element be removed from the model, so that the hysteresis loop can be effectively collapsed. A simple method of correcting nonsteady-state data to the equivalent of steady-state data (so that a

concentration-response curve can be discerned) is the use of an indirect model. In this analysis, the effect-compartment model initially proposed by Sheiner *et al* [70] was used. The effect-compartment model has also previously been successfully applied to similar euglycemic clamp studies [59, 60]. A diagram of the model is presented in Figure 3-1. The pharmacodynamic portion of the model is described by the following equations:

$$\frac{dCe}{dt} = k_{e0} \cdot (Cp - Ce) \tag{3-1}$$

$$GIR = E_0 + \frac{E_{\max} \cdot C_e^{\gamma}}{EC_{50}^{\gamma} + C_e^{\gamma}} \tag{3-2}$$

Equation 3-1 describes the relationship between the observed plasma insulin concentration and the concentration at the effect site. Effectively, k_{e0} is a rate constant which describes the delay in effect. The effect compartment is assumed to receive a negligible mass from the central compartment, thereby not affecting the equations for the insulin pharmacokinetic model. Equation 3-2 establishes the relationship between the GIR and insulin concentration at the effect site. The pharmacodynamic structural model was parameterized in terms of E_0, the baseline GIR value, E_{max}, the maximum glucose infusion rate, EC_{50}, the effect site concentration eliciting 50% of the maximal response, γ the sigmoidicity factor, and Cp and Ce are the plasma and effect site insulin concentrations, respectively.

Error model

Interindividual variability was described by an exponential error model. The intraindividual residual variability of the dependent variable was estimated using an additive error model, as described by the following equation:

$$DV_{ij} = D\tilde{V}_{ij} + \varepsilon_{ij} \tag{3-3}$$

where DV_{ij} is the observed value of the j[th] dependent variable of individual *i*; $\widetilde{DV}_{ij}$ is the predicted j^{th} dependent variable of individual *i*; and ε_{ij} is a random variable which represents the discrepancy between the observed and predicted j^{th} dependent variable value.

Model Fit Assessment

Goodness-of-fit was determined by the objective function values (OFV) and visual inspection of scatter plots of predicted versus observed concentrations as well as the weighted residuals. For nested models, hypothesis tests were performed based on the likelihood ratio test, in which the change in OFV approximates the χ^2 distribution. A more complicated model was preferred when the decrease in OFV was more than 3.84 (the critical value for the χ^2 distribution at $p < 0.05$ with 1 degree of freedom).

Results

Data from both routes of administration were analyzed simultaneously. Mean insulin and GIR-time profiles by dose group are presented in Figure 3-2. When exploring the potential PK/PD model, the relationship between insulin and GIR was first examined by visual inspection. A phase-plot of GIR vs. the plasma insulin concentration, where data points are connected in chronological order, is shown in Figure 3-3 for the pooled data in this analysis. A counter-clockwise hysteresis loop is observed indicating a disconnect between insulin concentrations observed centrally, and insulin action. The temporal dissociation between insulin concentration and GIR clearly differs between TI and subcutaneous insulin, as well as insulin administered intravenously. Interestingly, the maximum effect is similar between all three treatments, but is observed at very different timepoints (40 and 180 minutes post-dose for TI and subcutaneous insulin, respectively, and at 20 minutes following iv administration) and is associated with greatly different insulin concentrations. Furthermore, the delay for subcutaneous insulin is

smaller than that for both TI and insulin administered iv, since the hysteresis loop is clearly smaller for sc insulin.

Pharmacodynamic model: Data from both routes of administration were modeled simultaneously. In Model A, the parameters k_{e0}, EC_{50} and γ were estimated individually for each route of insulin administration, whereas in Model B, a single set of parameters was estimated for all three dosing routes. The baseline GIR (E_0) was assumed to be comparable because the study conditions were similar and the subject pool was homogenous, and E_{max} was assumed to be the same for all treatments, as it is an inherent property of insulin. As a result, no treatment-specific parameter estimates were determined for E_{max} or E_0 in Model A.

Model A: Model A goodness of fit figures are presented in Figure 3-4. The individual predicted versus observed values distributed along the line of unity, and no significant trends in the weighted residuals. The pharmacokinetic parameter estimates are summarized in Table 3-1. Population predicted GIR-time profiles and observed GIR values are shown in Figure 3-5, and representative observed and individual predicted GIR-time profiles are shown in Figure 3-6. The interindividual %CV for all parameter estimates ranged from 23 to 54%. The residual error was described by an additive model.

Population estimates of k_{e0} were 0.7, 1.9 and 1.4 h^{-1} for iv, sc and TI, respectively, and were associated with distribution half-lives of 60, 20 and 30 minutes, respectively. These results indicate that the greatest delay between insulin concentrations observed centrally and insulin effect occur following iv administration, which is in agreement with the relationship observed in Figure 3-3. Gamma estimates were 6.4, 2.5 and 3.2 for iv, TI and sc, respectively, and in close agreement to values previously reported in healthy individuals [55]. The EC_{50} estimated by the

model was associated with the concentration at the effect site (Ce) and was estimated to be 26.6, 41.2 and 32.9 μU/mL.

Model B: For Model B, the overall model fit was good, with individual predicted versus observed values distributed along the line of unity as well, and no apparent trends in the weighted residuals (Figure 3-7). Thus, the structural and error models appeared to adequately describe insulin pharmacodynamics and explain the variability in the data, even without formulations-specific parameter estimates. However, when compared to Model A, Model B goodness of fit plots show more scatter around the line of unity, and lower individual predicted GIR values overall.

In the model, the population typical values were: E_{max}, 13.1 mg/kg/min; EC_{50}, 32.8 μU/mL; gamma, 3.0 and k_{e0} of 1.6 hr^{-1}. The interindividual %CV for all parameter estimates ranged from 28 to 47%. The residual error was described by an additive model, and the residual error had a greater magnitude in Model B (2 mg/kg/min) when compared to Model A (1.68 mg/kg/min), indicating that more of the observed variability was explained by the treatment-specific parameters and associated interindividual variability in Model A.

The pharmacokinetic parameter estimates are summarized in Table 3-2. Population predicted GIR-time profiles and observed GIR values are shown in Figure 3-8, and representative observed and individual predicted GIR-time profiles are shown in Figure 3-9.

Discussion

The effects of different insulin doses and treatments are often evaluated by comparing the shape and area under the GIR vs. time curve. As a result, numerous attempts have been made to model the insulin-effect relationship as derived from clamp study data to more fully understand the differential effects. GIR data have been assessed using a variety of physiologically-based and empirical models, including indirect [56, 57, 72] and effect compartment models [55, 59,

60]. However, previous work focused on either one insulin formulation, insulins with similar pharmacokinetic properties, or explicitly estimated different pharmacodynamics for insulins with different pharmacokinetics. Hence, the models developed provided limited use towards predictions of the effects of insulins with dissimilar insulin concentration profiles than those included in the model. The purpose of the current work was to develop a model that would be simple and non-specific, allowing for the prediction of insulin effect based on insulin pharmacokinetics alone and, thus, applicable to insulins with differing pharmacokinetic properties. To accomplish this, three insulins with differing pharmacokinetic properties were used in model development.

As a first step, a model was developed (Model A), with individualized estimates for k_{e0}, EC_{50} and γ for each formulation. This model was used to obtain reasonable initial estimates for Model B, in which one set of parameters was estimated for all three insulins. Since the predictive performance of Model A was expected to be better, a comparison could be made as to the fit of Model B using magnitude of residual variability and individual fits. Treatment-specific values for insulin E_{max} and E_0 were not estimated in Model A, as they were assumed to be comparable between treatments.

Model A parameter estimates varied most notably in the gamma parameter, with the highest value associated with intravenous insulin administration. The other parameter which varied considerably following intravenous administration was k_{e0}, which was lowest in this treatment, and associated with the longest central to effect site equilibration half-life. This is most likely due to the relatively quickly changing insulin concentrations following this route of administration, but comparable delay in insulin effect for all three treatments, thus resulting in an apparent difference in k_{e0}. However, due to the small number of subjects in each treatment

group, in particular only 4 subjects receiving iv insulin, the treatment-specific parameter estimate differences may not be conclusive, and should be used with caution for predictive purposes.

In Model B, pharmacodynamic parameter variability ranged from 27 to 52%, with the greatest variability observed on γ, the sigmoidicity factor. This was an expected result, since Model A estimated different γ values for the three insulins, and others who estimated formulation-specific differences in insulin formulations saw the greatest differences in pharmacokinetically different insulins in γ and EC_{50} estimates [60]. The population k_{e0} estimate of 1.7 was similar to the estimates for both TI and sc insulin in Model A. This is most likely attributable to the overwhelming majority of the data being obtained following non-iv administration. Nonetheless, the same γ and k_{e0} estimates were able to relate fairly well very different insulin concentration-time profiles to the GIR.

Model B attempts to simultaneously model the concentration-GIR relationship of insulins with very different pharmacokinetic properties, without individualizing the pharmacodynamic parameters for each formulation. Given the lack of such a model in the literature, this would appear to be the first model constructed in this manner. Although empirical in nature, it is the potential predictive ability of Model B that makes it uniquely valuable, and future work could focus on applying the model to external datasets to determine its accuracy in predicting insulin effect. Using this model, the pharmacokinetic insulin profile can be used to determine the pharmacodynamics, resulting in a straightforward simulation of the activity of insulins with varying pharmacokinetic properties. Although the simple nature of the model is a benefit, it is also a drawback in that the model slightly underpredicts the GIR around the time of peak effect in some patients, especially in subjects who exhibit a quick and high rise in insulin. In the data assessed here, the model fit is less predictive of maximum effect in certain subjects in the 100 U

TI dose group, and to a greater extent in subjects receiving insulin intravenously. Under these conditions, the fit is better in Model A, where the formulation-specific parameter estimates are better able to fit the data. However, some underprediction still exists, and the reason for this observation may be due to insulin effect having two components: the stimulation of glucose disposal and the inhibition of glucose production [76]. The simple nature of the E_{max} model cannot account for two processes; it may describe insulin concentration-related glucose disposal, which is expected to follow a receptor-driven model, but it is unable to account for changes in insulin effects on hepatic glucose production, which are more immediate and associated with a threshold insulin value [9].

In most cases, the model performs well and is reasonable, with its only weakness being the underprediction at specific conditions. An area of model improvement would be to attempt to account for this additional "hump" in the GIR curve, however, such a modification may detract from the simple nature of the model. Because the population used in this analysis was comprised of healthy volunteers with normal insulin sensitivity, the impact on liver glucose output would be expected to be higher than in a diabetic subject, where some of the sensitivity is lost. It is therefore possible that the extent of the underprediction may be lessened in the diabetic population. Additional research that would greatly help improve this model would be the comparison of its applicability in the diabetic population, whose insulin sensitivity may be compromised.

Conclusions

Insulin pharmacodynamics during a glucose clamp procedure in healthy subjects were found to be well described by a simple E_{max} model when a hypothetical effect compartment was used to collapse the hysteresis in insulin effect. The model was able to successfully describe the GIR response to three pharmacokinetically diverse insulin formulations.

Table 3-1 Model A insulin population pharmacodynamic parameter estimates

Parameter	Intravenous Estimate (%RSE)	Subcutaneous Estimate (%RSE)	Inhaled Estimate (%RSE)
E_0 (mg/kg/min)	2.7 (10.8)	2.7 (10.8)	2.7 (10.8)
E_{max} (mg/kg/min)	14.6 (14.1)	14.6 (14.1)	14.6 (14.1)
EC_{50}	26.6 (18.1)	32.9 (12.1)	41.2 (16.5)
K_{e0} (h^{-1})	0.7 (13.9)	1.9 (6.5)	1.4 (12.4)
gamma	6.4 (35.4)	3.2 (24.3)	2.5 (19.1)
Interindividual and Residual Variability	%CV	%CV	%CV
ω_{E0}	41.6	41.6	41.6
ω_{Emax}	38.3	38.3	38.3
ω_{EC50}	31.0	40.2	31.6
ω_{Ke0}	23.2	17.4	50.3
ω_{gamma}	54.1	42.5	39.9
ω_{IOV}	41.6	41.6	41.6
σ_1	1.68	1.68	1.68

Note: *σ_1 (additive residual error) is expressed in mg/kg/min; The magnitude of interindividual and residual variability was expressed as % CV, approximated by the square root of the variance estimate.

Table 3-2 Model B insulin population pharmacodynamic parameter estimates

Pharmacodynamic Parameters	
Parameter	Estimate (%RSE)
E_0 (mg/kg/min)	2.9 (12.4)
E_{max} (mg/kg/min)	13.1 (10.0)
EC_{50}	32.8 (11.9)
K_{e0} (h^{-1})	1.6 (7.7)
gamma	3.0 (17.6)
Interindividual and Residual Variability	%CV
ω_{E0}	41.6
ω_{Emax}	33.8
ω_{EC50}	46.7
ω_{Ke0}	28.1
ω_{gamma}	35.2
σ_1	2.0

Note: *σ_1 (additive residual error) is expressed in mg/kg/min; The magnitude of interindividual and residual variability was expressed as CV%, approximated by the square root of the variance estimate.

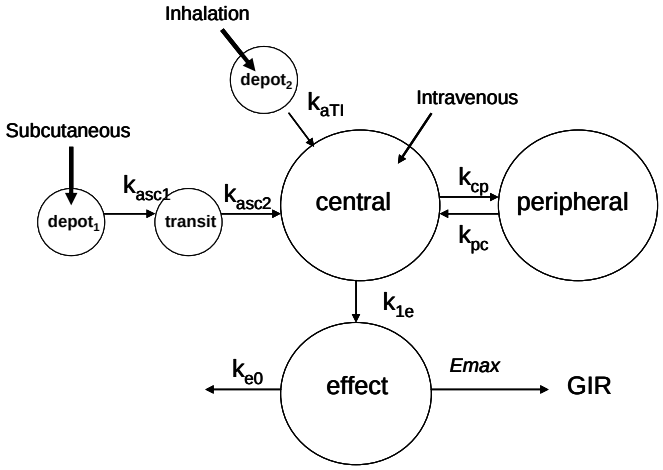

Figure 3-1 Pharmacokinetic/pharmacodynamic model diagram

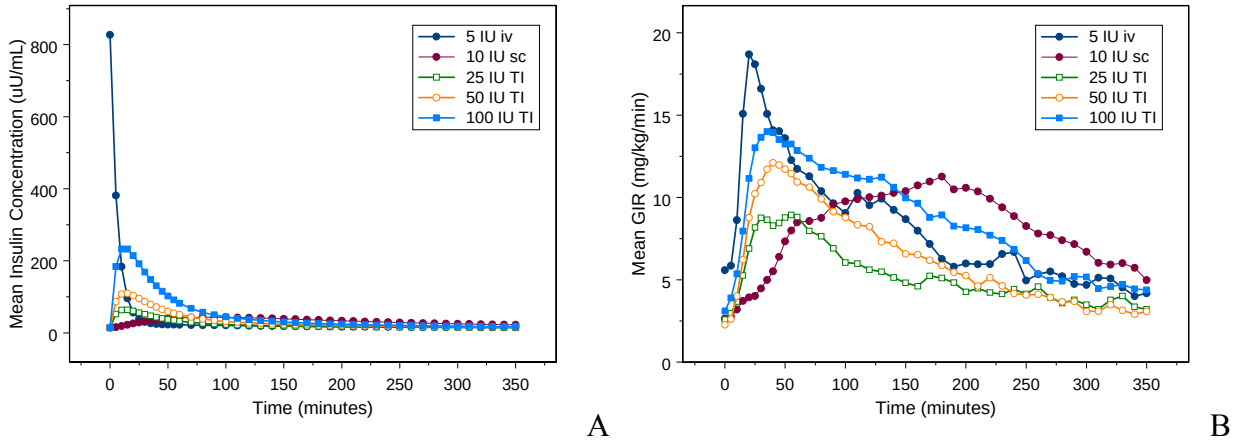

A B

Figure 3-2 Mean insulin and GIR-time profiles by dose group. A) Mean individual predicted insulin concentrations by dose and B) Mean observed GIR by dose group

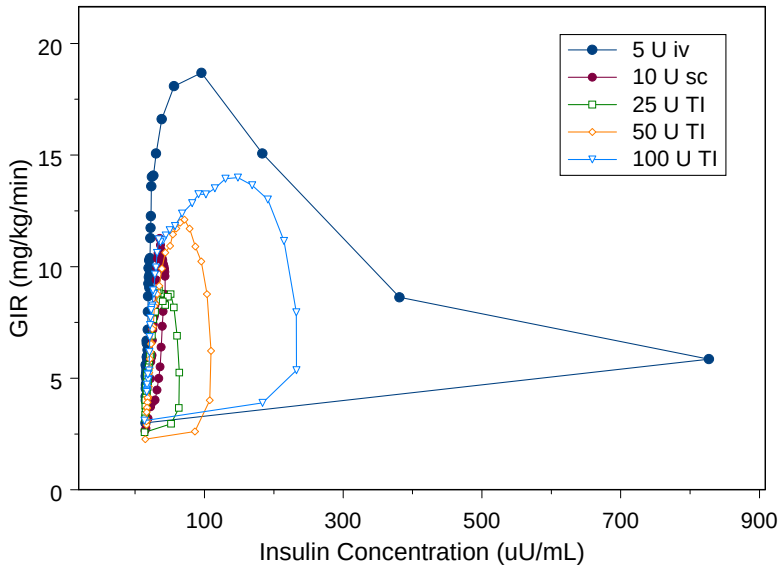

Figure 3-3 Hysteresis in the insulin-GIR relationship

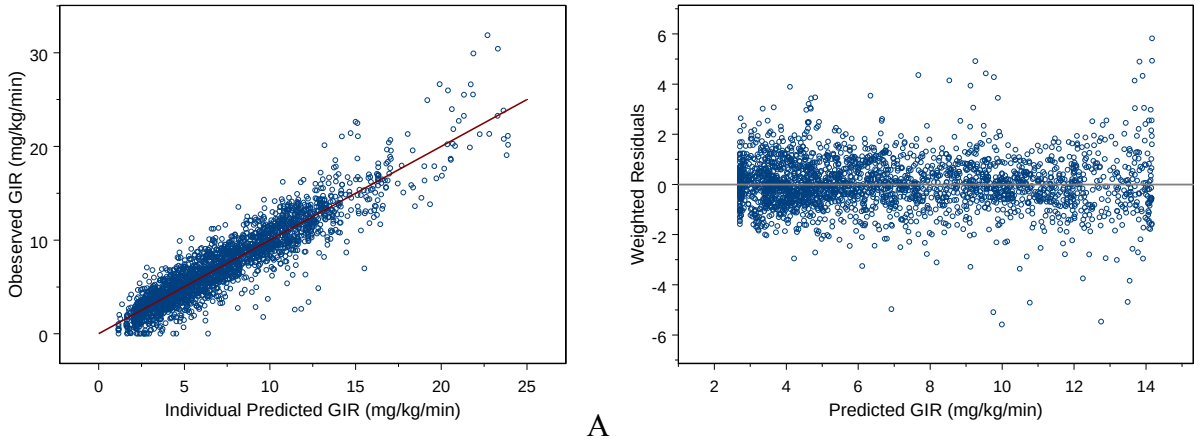

A B

Figure 3-4 Goodness of fit plots for Model A. A) Individual predicted GIR versus observed GIR and B) GIR values versus weighted residuals

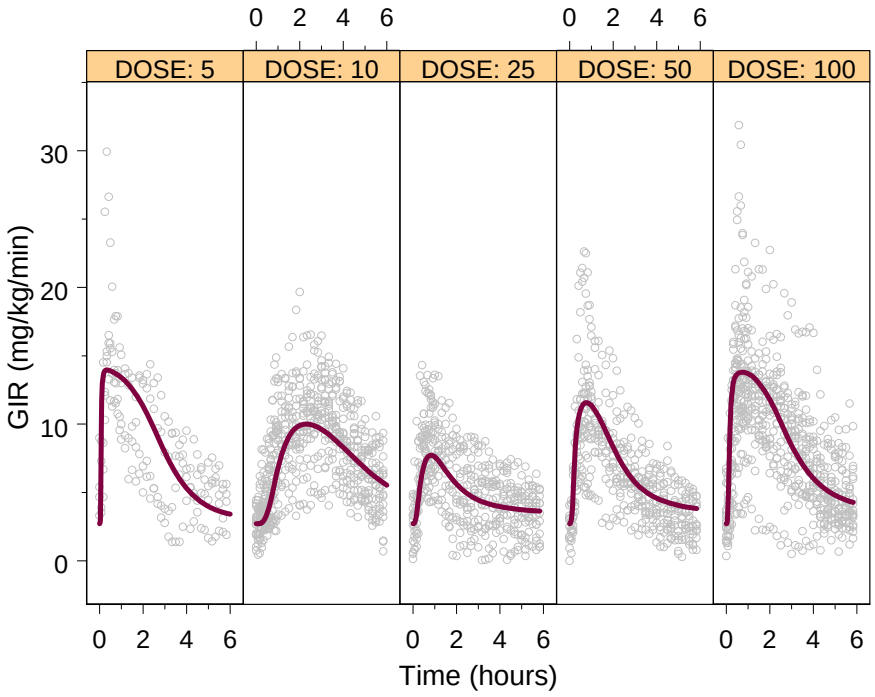

Figure 3-5 Model A: Population predicted and observed GIR values by dose group

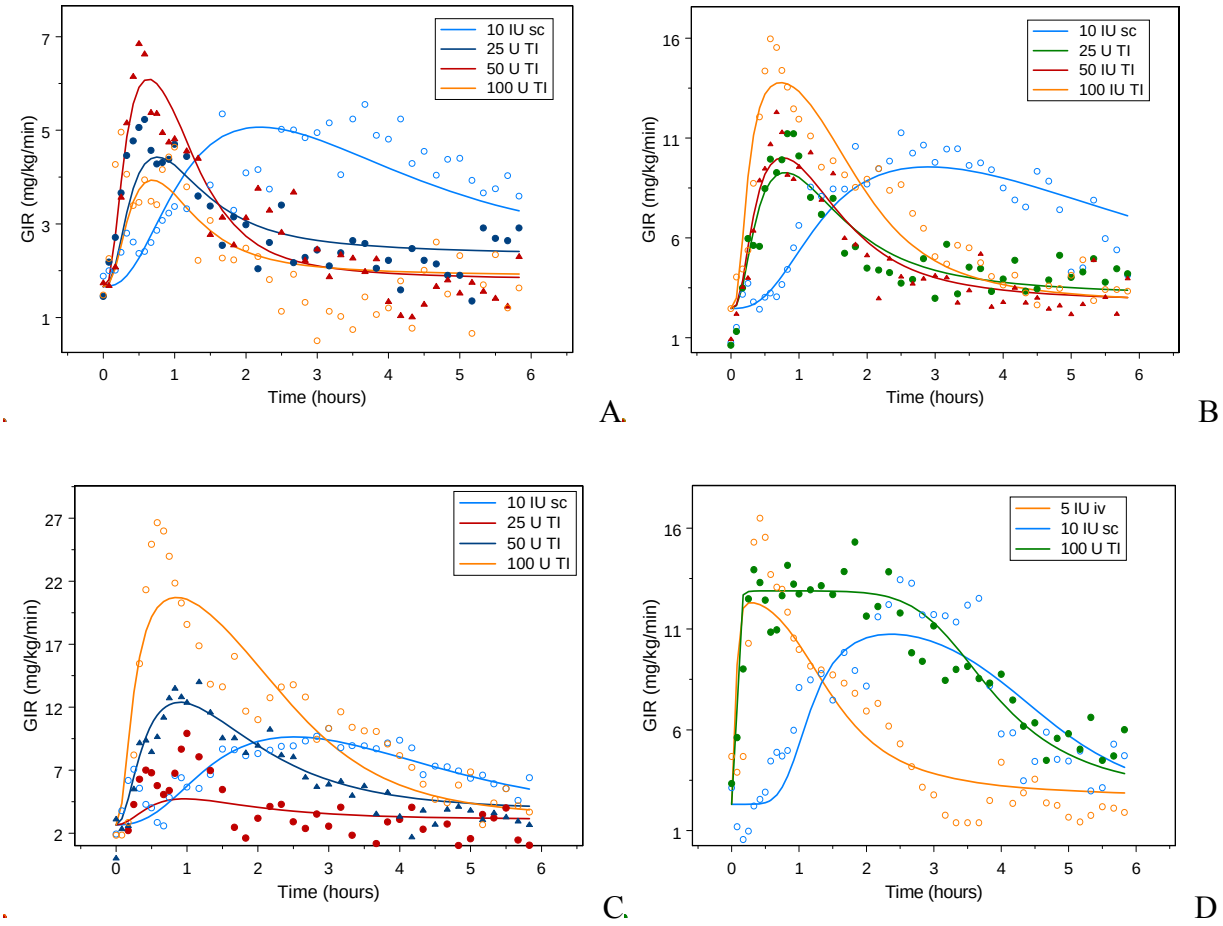

Figure 3-6 Model A: Model predicted and observed GIR values in four subjects

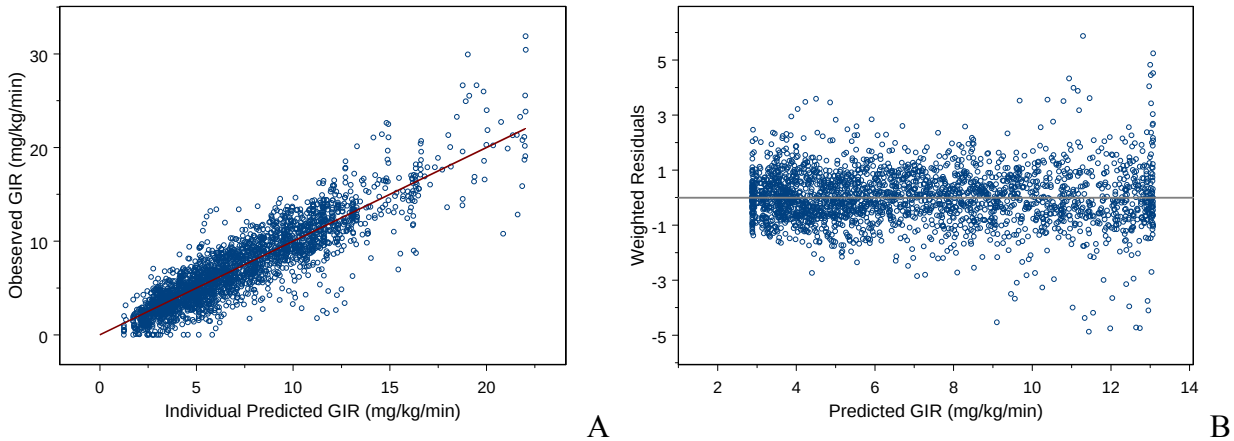

Figure 3-7 Goodness of fit plots for Model B. A) Individual predicted GIR versus observed GIR and B) GIR values versus weighted residuals

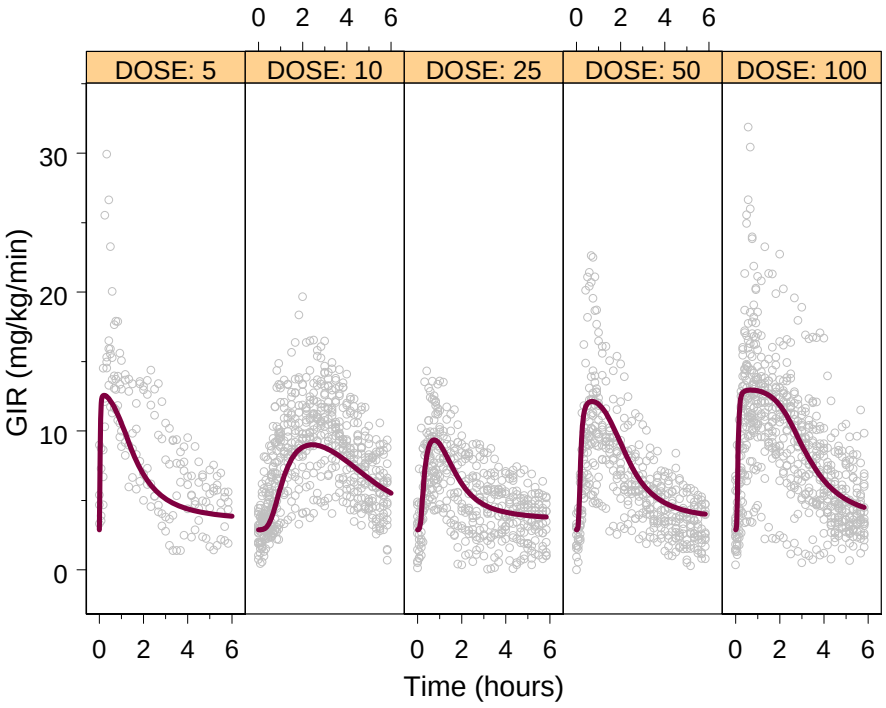

Figure 3-8 Model B: Population predicted (red) and observed (gray) GIR values by dose group

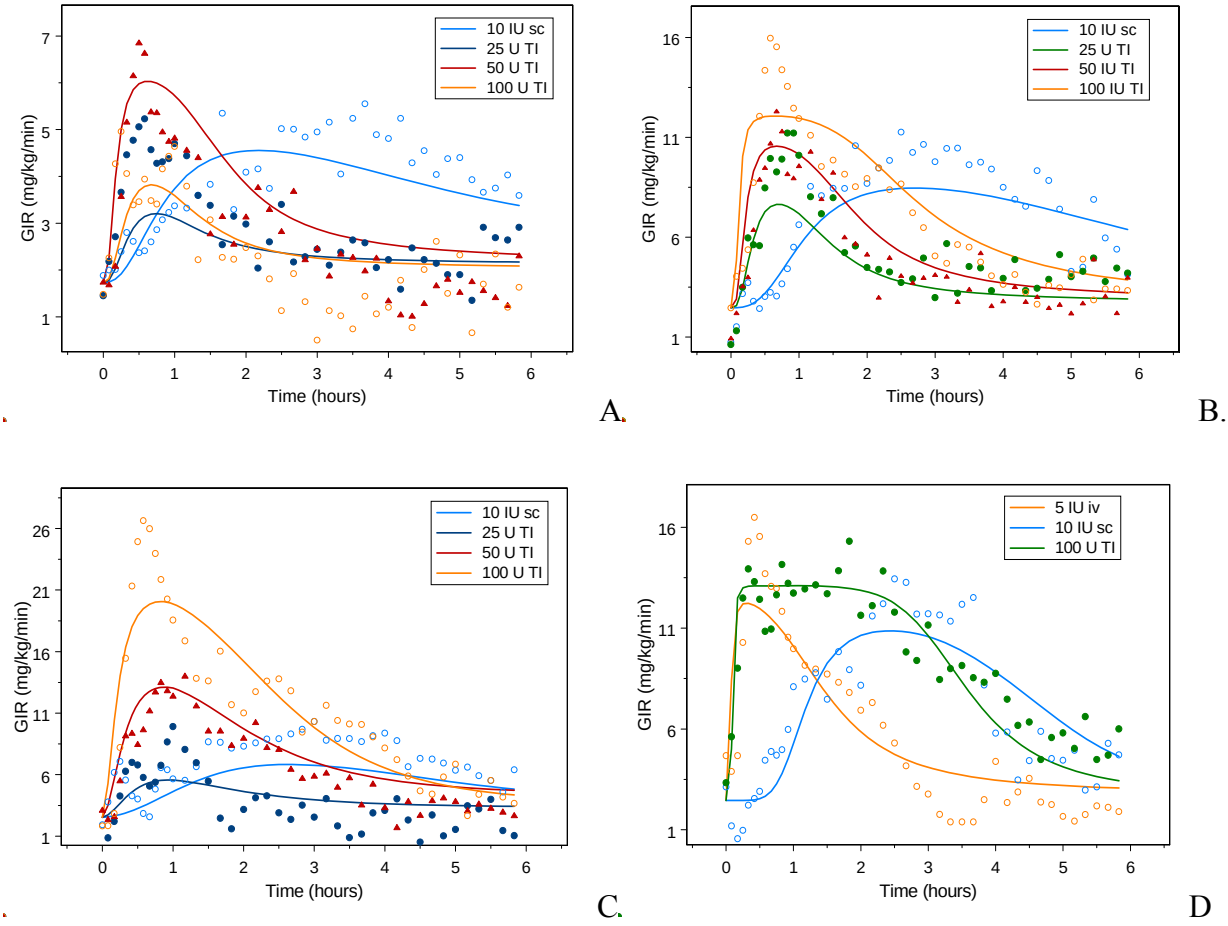

Figure 3-9 Model B: Predicted and observed GIR values in four subjects

CHAPTER 4
POPULATION PHARMACOKINETIC MODEL FOR SUBCUTANEOUSLY ADMINISTERED REGULAR HUMAN INSULIN, INSULIN LISPRO AND INHALED INSULIN IN HEALTHY AND DIABETIC SUBJECTS

Background

Until recently, the majority of therapeutic insulins administered via non-intravenous routes have been described by a one compartment pharmacokinetic model, as both the distribution phase and second compartment have been obscured by slow absorption characteristics. Technosphere® Insulin (TI) is a novel inhaled regular human insulin (RHI) whose unique delivery mechanism results in rapid absorption and rapid clearance, making it possible to distinguish the second compartment in its pharmacokinetic profile [78]. The inclusion of data following TI dosing has made it possible to attribute the differences in the shape of the insulin curve, following various routes of administration, to differences in absorption. As such, insulin disposition following subcutaneous, pulmonary and intravenous administration has been described by a two compartment pharmacokinetic model combining data from all three routes of administration (Chapter 2).

Having established that insulin pharmacokinetics can be modeled using a two compartment model, and that subcutaneously administered and inhaled insulin can be modeled together, the aim of this analysis was to develop a population pharmacokinetic model for RHI and insulin lispro administered via the subcutaneous route, and TI administered via inhalation. Population pharmacokinetic modeling has become a staple in all areas of pharmacokinetic research, and can be particularly useful in finding trends and relationships between covariates and pharmacokinetic parameters, as well as identifying and quantifying sources of variability [92]. Although insulin has been used as therapy for more than 80 years, no larger scale population analysis has been performed combining healthy subjects and subjects with diabetes and a large range of

demographic covariates. In this analysis, data from healthy, type 1 and type 2 diabetic subjects was combined, and the model was used to determine the relative bioavailability of the three formulations and to identify any significant covariates associated with insulin pharmacokinetics.

Materials and Methods

Study Population and Study Design

A population pharmacokinetic model of insulin was developed using data from four studies. Three studies were prospective, open-label, randomized, crossover, euglycemic glucose clamp studies in non-smoking male and female healthy volunteers and subjects with type 2 diabetes. One study was a meal challenge in subjects with type 1 diabetes. Prior to entry into any study, all subjects provided written informed consent and were then given a physical examination, pulmonary function tests, electrocardiography and laboratory tests, including urinalysis and screening for drugs of abuse. All studies were approved by the local ethics committee. The data from all four studies were combined for modeling purposes, with a total of 103 subjects included in the model and 213 pharmacokinetic profiles.

All of the studies were conducted in a crossover fashion, where each subject received a single dose of each treatment studied. In all studies, TI was administered using the MedTone dry powder inhaler, with the exception of Study 1, where TI was administered using a commercially available inhaler (Model M, Boehringer Ingelheim, Ingelheim, Germany). Samples for the determination of insulin, lispro and c-peptide concentrations were drawn from the cubital vein in the contralateral arm to that used for the insulin infusion and glucose administration, and analyzed using a radioimmunoassay (RIA). A brief description of the study design and methods follows.

Healthy volunteers

Study 1: This was a three-way crossover euglycemic glucose-clamp study in five subjects to compare the pharmacokinetics and pharmacodynamics of single doses of 100 U of inhaled TI, 10 U RHI administered subcutaneously and 5 U RHI (Actrapid, Novo Nordisk A/S, Bagsvaerd, Denmark) administered intravenously.

Study 2: This was a four-way crossover euglycemic glucose-clamp study in 12 subjects to compare the pharmacokinetics and pharmacodynamics of three different single doses of inhaled TI with a single dose of 10 U RHI (Actrapid, Novo Nordisk A/S, Bagsvaerd, Denmark). RHI insulin was administered by subcutaneous injection in the abdominal region. Blood glucose was kept constant at 90 mg/dL throughout the glucose clamp by a variable infusion of a dextrose solution. Samples for the determination of insulin concentration were drawn at 120, 90, 60 and 30 minutes before dosing and 0, 1, 3, 7, 12, 20, 30, 45, 60, 90,120, 180, 240, 300 and 360 minutes post-dose, and C-peptide concentrations were collected at 120 and 60 minutes pre-dose and 0, 30, 60, 180, and 300 minutes post-dose. The subjects were kept fasted until the end of the study. The treatment periods were separated by a washout period of 3 and 28 days.

Type 2 diabetic subjects

Study 3: This was a prospective, randomized, open label, single site study in 12 non-smoking, male and female subjects with a diagnosis of type 2 diabetes mellitus for ≥12 months, a stable antidiabetic regimen with insulin for the previous 3 months and HbA1c ≤ 8.5%, to compare the pharmacokinetics and pharmacodynamics of two doses of TI (60 and 90 U) with a single dose of 10 U lispro (Humalog™, Eli Lilly & Co.). Six subjects received 60 U TI and the other six subjects received 90 U TI. All twelve subjects received lispro insulin administered by subcutaneous injection in the abdominal region. Following an overnight fast, the subjects received, on each of the treatment days, a constant rate intravenous infusion of either RHI or

insulin lispro (opposite of the type of insulin to be used in dosing) during a 4-6-hour run-in period in order to suppress endogenous insulin production. This infusion was continued until the end of the clamp procedure. Blood glucose was kept constant at 110 (±10) mg/dL throughout the last 60 minutes of the run-in period, and for 480 minutes post-dosing via the glucose clamp using the Biostator®. Samples for insulin and insulin lispro concentration determination were drawn at 310, 20 and 5 minutes before dosing and at time 0, 5, 10, 15, 20, 30, 45, 60, 75, 90, 105, 120, 150, 180, 210, 240, 300, 360, 420 and 480 minutes post-dose. The patients were kept fasted until the end of each treatment visit. The treatment periods were separated by a washout period of 7 to 21 days. The studies in healthy and type 2 diabetic were performed at the same clinical site.

Type 1 diabetic subjects

Study 4: This was an open label, prospective, randomized study in 75 non-smoking male and female subjects with type 1 diabetes (HbA1c<11%) and normal pulmonary function, to compare the pharmacokinetics of a 30 U cartridge delivered using two different models of the MedTone Inhaler. The last dose of long-acting insulins or intermediate-acting insulins was taken in the morning on the day before TI administration. Subsequently, subjects were instructed to manage their BG with intermittent injections of RAA. Subjects utilizing continuous subcutaneous insulin infusion pumps were instructed to replace their usual insulin with NovoRapid (Novo Nordisk, Denmark) the day before treatment. All subjects were administered TI directly before the start of a meal (12 oz. Boost® Plus). Samples for insulin and insulin lispro concentration determination were drawn at 30, 20, 10 minutes prior to dosing and 0, 3, 6, 9, 12, 15, 20, 25, 30, 45, 60, 75, 90, 105, 120, 150, 180, and 240 minutes after drug administration. The treatment periods were separated by a washout period of 1 day.

Baseline Correction Methodology

In order to subtract the contribution of the ongoing insulin infusion (studies 1 and 2) and detectable concentrations of insulin still washing out from the system (studies 3 and 4), serum insulin concentrations were corrected for baseline insulin levels before being analyzed and used for model development. Any baseline-corrected value below zero was set equal to zero. Due to the differing study conditions, different baseline-correction strategies had to be used:

Studies 1 and 2: Insulin concentrations collected at 120, 90, 60 and 30 minutes before dosing were averaged, and subtracted from all subsequently observed insulin concentrations.

Study 3: Baseline correction was applied to account for any endogenous insulin that was not fully suppressed with the baseline infusion. For the TI group, all insulin concentrations were corrected by subtracting the mean of the values in the later time points (300–480 minutes) from each individual time point for each subject. At these time points, most subjects' insulin concentration-time profiles were observed to be reasonably flat and uninfluenced by exogenous contribution.

Study 4: In accordance with the study analysis plan, the mean concentration of the -30 through 0 time points was used as baseline. Of the 150 profiles, 13 profiles on day 1 had a mean of > 3.6 μU/mL as a baseline, and on day 2, only 7 subjects had a baseline > 3.6 μU/mL.

Data Excluded from the Pharmacokinetic Analysis

For studies 1 and 2, each serum insulin and C-peptide concentration-time profile was examined visually together. Due to the lower doses administered in Study 2, a higher incidence of elevated C-peptide concentrations was observed in the latter time points following TI treatment, particularly in the lower dose groups. All insulin concentrations after 180 minutes post-dose in the 25 U dose group, 240 minutes post-dose in the 50 U dose group, and 300 minutes in the 100 U dose group were excluded, since endogenous insulin appeared to be

contributing to the curve in the latter part of the study, with a total of 51 non-BLQ concentrations excluded from the analysis. A further 21 concentrations were excluded for pharmacokinetic implausibility, such as concentrations below the quantifiable limit in close proximity to the C_{max}, or unexpectedly high concentrations at the end of the profile. One subject from study 2 was excluded from the entire analysis, and another a subject was excluded from analysis in the 10 U sc treatment group, since three consecutive BLQ values were observed in the pharmacokinetic profile following sc RHI treatment, suggesting a possible analytical error. A total of 15 profiles were excluded due to lack of test treatment exposure or incomplete dosing and/or sampling information.

Noncompartmental Pharmacokinetic Analysis and Absolute Bioavailability

Insulin pharmacokinetics were analyzed using noncompartmental methodology using baseline-corrected insulin concentrations. The following PK parameters were derived using WinNonlin v 5.2 (Pharsight Corporation, Mountain View, CA): observed peak insulin concentration (C_{max}), time to peak insulin (t_{max}), and total insulin exposure as measured by the area under the insulin concentration-time curve from time 0 until the last timepoint with non-zero insulin concentrations ($AUC_{0\text{-}last}$) as calculated by the linear-trapezoidal method. The terminal elimination half-life ($t_{1/2}$) was calculated as $\ln(2)/\lambda_z$ in accordance with pharmacokinetic theory [80], where λ_z is the terminal elimination rate constant estimated from log-linear regression analysis of the terminal elimination phase of the concentration-time profile, and $AUC_{0\text{-}\infty}$ was calculated as $AUC_{0\text{-}last} + C_{last}/\lambda_z$, where C_{last} is the last observed insulin concentration. Noncompartmental parameter values were used to determine starting estimates for pharmacokinetic modeling, and were compared to parameter values estimated by the final model as part of the model fit assessment.

Relative bioavailability (%F) was determined using the mean dose-normalized insulin $AUC_{0\text{-last}}$ values, expressed as the group average dose-normalized $AUC_{0\text{-last}}$/average dose-normalized $AUC_{0\text{-last}}$ following lispro administration.

Statistical Analysis

Dose-normalized insulin $AUC_{0\text{-}\infty}$ was used in order to investigate possible TI exposure differences between studies. Statistical differences were concluded if the average log transformed $AUC_{0\text{-}\infty}$ values were found statistically different by the one-way ANOVA technique, which was performed with the null hypothesis that the study average values are the same, at the α=0.05 level. The alternative hypothesis was that some of the group means differ from each other.

In the event that statistical differences were found by ANOVA, Tukey's pairwise comparison method was used to determine which pairs of studies differ. The family error rate was set to 5%. Results were presented as a set of confidence intervals for the difference between pairs of means, from which the following conclusions were drawn: 1) if an interval does not contain zero, there is a statistically significant difference between the corresponding means and 2) if the interval does contain zero, the difference between the means is not statistically significant.

It was necessary to test the variances of the dose-normalized, log-transformed $AUC_{0\text{-}\infty}$ values in the four studies for homogeneity in order to accept the results of the ANOVA analysis, since homogeneity of variances is one of the ANOVA assumptions. Levene's test was performed under the null hypothesis that the variances are the same and an alternative hypothesis that the at least one of the variances was different from the others. The data were tested at the α=0.05 level. The results of the statistical tests were obtained using MINITAB (v.15.1.30.0).

Population Pharmacokinetic Analysis

The software package NONMEM (Version VI, Level 1.2, NONMEM Project Group, ICON Development Solutions, USA) was used for the population analysis. NONMEM describes the observed concentration-time data in terms of:

- A number of fixed effect parameters, θ, which may include the mean values of the relevant base pharmacokinetic model parameters, or a number of parameters which relate the base model parameters to demographic and other covariates;
- Two types of random effect parameters: (a) ω^2: the variances of the interindividual variability (η) within the population, and (b) σ^2: the variances of the residual intraindividual variability (ε) due to random fluctuations in an individual's parameter values, measurement error, model misspecification, and all sources of error not accounted for by the other parameters.

The population or average values of the parameters, θ, the interindividual variances, ω^2, and the residual variance, σ^2, were estimated by NONMEM. The η values are independent, identically distributed random errors with mean of zero and a variance equal to ω^2. Subject-specific parameters were calculated by NONMEM using the POSTHOC (FO method) option. These parameters are empirical Bayesian estimates of the individual's true parameters based on the population parameters and the individual's observed concentrations.

Pharmacokinetic base model

Data from all three routes of administration were modeled simultaneously. The PK was described by a two compartment model with one (inhaled) or two sequential (subcutaneous) first order absorption processes and first-order elimination. A diagram of the model is presented in Figure 4-1.

The model was described by the following differential equations:

$$\frac{dA_1}{dt} = -ka_1 \cdot A_1 \quad (4\text{-}1)$$

$$\frac{dA_2}{dt} = ka_1 \cdot A_1 - ka_2 \cdot A_2 \quad (4\text{-}2)$$

$$\frac{dA_3}{dt} = -ka_{TI} \cdot A_{31} \quad (4\text{-}3)$$

$$\frac{dA_4}{dt} = ka_{TI} \cdot A_3 + ka_2 \cdot A_2 + k_{54} \cdot A_5 - k_{45} \cdot A_4 - k \cdot A_4 \quad (4\text{-}4)$$

$$\frac{dA_5}{dt} = k_{45} \cdot A_4 - k_{54} \cdot A_5 \quad (4\text{-}5)$$

The pharmacokinetic structural model was parameterized in terms of clearance (CL), volume of distribution in the central compartment (V_c), intercompartmental clearance (Q), the volume of distribution in the peripheral compartment (V_p), the first order absorption rate constant for TI (ka_{TI}), the two first order absorption rate constants associated with the sequential absorption for subcutaneously administered insulin ($ka_{sc1}$and ka_{sc2}, depot and a transit compartment), sequential absorption for subcutaneously administered lispro ($ka_{LI1}$and ka_{LI2}), and the absolute bioavailability for subcutaneous insulin, lispro and TI (F_{sc}, F_{LI}, F_{TI}).

Error model

Fixed effects parameters were used to describe the typical population estimates, and an exponential random effect model was used to describe interindividual variability for each model parameter:

$$\theta_i = \theta^{\eta_i} \quad (4\text{-}6)$$

where θ_i is the estimated parameter value for the i^{th} individual, θ is the fixed effect typical parameter value in the population, and η_i are individual-specific random effects for the i^{th} individual symmetrically distributed with zero mean and variance ω.

A combined proportional and additive error model was used to model the residual unexplained variability, as described by the following equation:

$$Cp_{ij} = \widetilde{C}p_{ij} \cdot (1 + \varepsilon_{1ij}) + \varepsilon_{2ij} \quad (4\text{-}7)$$

where Cp_{ij} is the observed value of the jth plasma concentration of individual *i*; $\widetilde{C}p_{ij}$ is the predicted j^{th} plasma concentration of individual *i*; and ε_{ij} is a random variable which represents the discrepancy between the observed and predicted j^{th} concentration.

Considerable interoccasion variability (IOV) was observed within the TI groups, and was attributed to natural variability in inhalation on different occasions, resulting in differences in relative bioavailability at different visits, as described by:

$$F_{TI} = \theta_{FTI}^{\eta_{FTI}+\eta_{OCC1}\cdot OCC1+\eta_{OCC2}\cdot OCC2+\eta_{OCC3}\cdot OCC3} \tag{4-8}$$

where *OCC1*, *OCC2* and *OCC3* are set to 1 at the corresponding occasion and 0 otherwise.

Reparameterization and individual predicted values

Individual-specific values of each pharmacokinetic parameter were obtained by Bayesian analysis with the final model.

$$CL = k \cdot V_4 \tag{4-9}$$

$$Q = k_{45} \cdot V_4 \tag{4-10}$$

The following pharmacokinetic parameters could subsequently be calculated for each individual according to the following equations based on compartment modeling theory.

$$\beta = \frac{1}{2}\left[(k_{45} + k_{54} + k) + \sqrt{k_{45} + k_{54} + k + 4k_{54}k}\right] \tag{4-11}$$

$$\alpha = \frac{1}{2}\left[(k_{45} + k_{54} + k) + \sqrt{k_{45} + k_{54} + k - 4k_{54}k}\right] \tag{4-12}$$

$$\alpha\ half - life = \frac{0.693}{\alpha} \tag{4-13}$$

$$\beta\ half - life = \frac{0.693}{\beta} \tag{4-14}$$

Model Fit Assessment

Goodness-of-fit was determined by the objective function values (OFV) and visual inspection of scatter plots of predicted versus observed concentrations as well the weighted residuals. For nested models, hypothesis tests were performed based on the likelihood ratio test, in which the change in OFV approximates the χ^2 distribution. A more complicated model was preferred when the decrease in OFV was more than 3.84 (the critical value for the χ^2 distribution at $p < 0.05$ with 1 degree of freedom).

Covariate Analysis

Following the determination of the base population model, potential covariates were examined to determine whether they improved the overall fit and reduced variability in the model. These covariates included age, body weight, BMI, disease status (healthy, type of diabetes), gender, study effect and insulin type. Furthermore, the pulmonary function values: forced expiratory volume in one second (FEV_1) and percent of predicted FEV_1 (National Health and Nutrition Examination Survey [NHANES III]) were assessed for possible effect on TI parameters. Covariates were initially evaluated for possible relationships with the model estimated pharmacokinetic parameters using the generalized additive model (GAM) procedure in Xpose [82]. Covariates associated with a reduction in the Akaike Information Criterion (AIC) were evaluated using NONMEM in a stepwise manner. Each covariate added to the base model, and the resulting univariate model was then compared to the reduced model for significant improvement in fit. Covariates were included in the model if a 3.84 point drop in the OFV was observed ($p<0.05$). Backward elimination was then performed where each covariate was independently removed from the model to confirm its relevance. An increase in the OFV of 6.7 ($p<0.01$) was necessary to confirm that the covariate was significant.

Model Validation

The precision of the population pharmacokinetic model parameter estimates was assessed by establishing 95% confidence intervals (CI) using a nonparametric bootstrap analysis (Wings for NONMEM; Version 409d) [93]. Subjects were selected repeatedly and at random, with replacement, from the dataset to create a new dataset with the same number but different combination of subjects. The bootstrap resampling was repeated 200 fold and only runs that converged successfully were used for the analysis. The 95% CI was calculated for each pharmacokinetic parameter by using the 2.5th and 97.5th percentile from 200 bootstrap estimates. The final population pharmacokinetic parameter estimates were compared with the bootstrap estimates.

Results

Patient population

A total of 3,227 insulin concentrations from 103 subjects and 213 profiles were included in the analysis. The ADVAN6 subroutine and first-order estimation method were used. Subject demographic data is summarized in Table 4-1.

Noncompartmental Analysis

Mean insulin concentration-time profiles are presented in Figure 4-2. Noncompartmental pharmacokinetic parameter estimates are presented in Table 4-2. Based on mean $AUC_{0\text{-last}}$, the relative bioavailability of TI was approximately 12% and 20% compared to lispro and RHI, respectively, and approximately 60% when RHI was compared to lispro. However, the latter estimate is most likely artificially low, since RHI was sampled only until 6 hours, and lispro was sampled until 8 hours post-dose. Terminal elimination half-life and $AUC_{0\text{-}\infty}$ could not be calculated following subcutaneous dosing of either RHI or lispro due to the prolonged absorption from the tissue, and the flip-flop kinetics associated with this route of insulin administration.

Exposure in study 4 (30 U TI dose) appeared to be approximately 30% to 40% lower when compared to other studies, based on dose-normalized $AUC_{0-\infty}$. The difference was found to be statistically significant when the dose-normalized insulin $AUC_{0-\infty}$ was compared using a one-way ANOVA.

Statistical Analysis

ANOVA test for equality of means

The aim of this study was to detect possible statistical differences in average insulin exposure in the four studies included in the analysis. A one-way ANOVA was performed with the null hypothesis that the group average dose-normalized exposure is the same. The null hypothesis was rejected at the $\alpha=0.05$ level, with a p value of < 0.001 and associated test statistic $F= 9.55$, in favor of the alternative hypothesis, that some of the group means are different.

Differences in means between the four studies

In light of the ANOVA outcome that statistical differences exist between the studies, the four studies were compared using Tukey's pairwise comparison method, and a family error rate of 5%. Results are presented in Table 4-3 as a set of confidence intervals for the difference between pairs of means. From the results presented in Table 4-3, a difference is observed between insulin exposure between studies 1 and 4, 2 and 4 as well as 3 and 4, indicating that exposure was different in study 4 (30 U TI dose) when compared to the other studies, as suggested by the results of the noncompartmental parameter values presented in Table 4-2.

The analysis was repeated without data from study 4, to test for differences between the mean exposure in the other studies. A one-way ANOVA was performed on the reduced dataset, with the null hypothesis that the group average dose-normalized exposure is the same. The null hypothesis could not be rejected at the $\alpha=0.05$ level, with a p value of 0.271, and the mean exposure between studies 1, 2 and 3 were concluded to be no different from each other.

Levene's test was performed to test the variances of the four studies for homogeneity. The null hypothesis of equal variances could not be rejected at the α=0.05 level, with a p value of 0.175. Therefore, the variances met the homogeneity assumption.

Population Pharmacokinetic Analysis

Base model

A two-compartment open model with one (inhaled) or two sequential (subcutaneous) first order absorption processes and first-order elimination described the insulin concentration data well. The lower exposure in study 4 was incorporated in the base model. The population typical values were: apparent clearance, 53.3 L/hr; apparent volume of distribution in the central compartment, 4.6 L; apparent volume of distribution in the peripheral compartment, 37 L; and relative bioavailability of subcutaneous RHI and TI estimated at 75% and 14%, respectively, with an approximate 50% lower exposure in study 4. The base model pharmacokinetic parameter estimates are summarized in Table 4-6.

The overall model fit was good, with individual predicted versus observed values distributed along the line of unity, and no significant trends in the weighted residuals (Figure 4-3 and Figure 4-4). Thus, the structural and error models appeared to adequately describe insulin pharmacokinetics and explain the variability in the data.

Covariate analysis

A GAM analysis identified the following potential covariates: body weight on insulin clearance, age on the volumes of distribution and TI absorption rate, BMI on subcutaneous absorption, FEV_1, body weight and gender on TI absorption rate, and body weight and age as covariates on TI bioavailability. Visual inspection of covariate vs. parameter scatter plots were also used for covariate identification. All potential covariates were included in a univariate analysis, where each covariate was added to the base model, and assessed in terms of OFV

reduction as well as overall reduction in variability. A summary of the univariate analysis is presented in Table 4-4.

The results of the univariate analysis showed that the addition of age as a covariate to the pulmonary absorption rate significantly improved the model ($p<0.01$). However, once age had been accounted for, the further addition of gender and weight did not significantly contribute to the model as the addition of gender resulted in an increased %RSE associated with the TI ka estimate as well as an increase in the interindividual variability, and the addition of weight did not result in a further decrease in OFV. Hence, neither gender nor weight was not included in further model building. Age effect on TI absorption rate was described by a power model.

$$ka_{TI} = \theta_{kaTI} \cdot Age/36^{-\theta_{age}} \quad (4\text{-}15)$$

In agreement with results reported earlier (Chapter 2), BMI was found to be negatively correlated with subcutaneous absorption rate, and was described by a linear model.

$$ka_{sc} = \theta_{kasc} + (BMI - 24) \cdot \theta_{BMI} \quad (4\text{-}16)$$

Both age and BMI were centered at the population mean value. The addition of age decreased the OFV by 98.9 points (Table 4-4) and the addition of BMI decreased the OFV by 22.2 points (Table 4-4).

Following the inclusion of age on the central volume of distribution, further addition of age on the peripheral volume did not contribute to the model, resulting in no further decrease in OFV. The addition of age decreased the OFV by 36.5 (Table 4-4). Age was modeled using a linear model, where age was centered at the population mean.

$$V_C = \theta_{Vc} + (Age - 36) \cdot \theta_{age} \quad (4\text{-}17)$$

The remaining significant covariates were each tested for inclusion in the final model using stepwise forward addition. Following the inclusion of age on TI ka, age on the central volume of

distribution and BMI on subcutaneous absorption rate, weight was no longer a significant covariate associated with clearance (OFV decrease of 0.235). The significance of each of the remaining covariates was confirmed by backwards elimination from the full model and is summarized in Table 4-5. Each of the three covariates was found to contribute to the model ($p<0.01$) and all three were retained in the final model.

Final model

The inclusion of the covariates to the base model resulted in a better fit, with an improved distribution of individual predicted versus observed values along the line of unity, and no significant trends in the weighted residuals (Figure 4-5 and Figure 4-6). The bioavailability relative to lispro for subcutaneous insulin and TI was 72% and 14%. Interoccasion variability following TI administration was approximately 31%. The interindividual %CV for all pharmacokinetic parameter estimates ranged from 10.7 to 82.5%. The residual error was described by a combined proportional (20.2 %CV) and additive (0.87 μU/mL) model. The pharmacokinetic parameter estimates are summarized in Table 4-6.

The final model was used to simulate insulin concentration-time profiles following administration of 60 U of TI to subjects at age 20, 35 and 65, as well as subjects with BMI values of 20, 23 and 26 kg/m^2, receiving 10 U RHI. Due to the small range of BMI in the RHI treated group, and the possible non-linear relationship that may exist beyond the range studied, no simulations were preformed for BMI values not used in the model development. The magnitude of the covariate effects is depicted in Figure 4-7.

Model Validation

A nonparametric bootstrap was used to evaluate the stability and precision of the final model parameters. Due to the long run times associated with the final model, the bootstrap analysis was limited to 200 runs. One hundred ninety-two runs that converged successfully were

used for further analysis. The final parameter estimates are presented in Table 4-6. Overall, the median bootstrap structural and covariate parameter values matched the population typical values well. The confidence interval around the age covariate associated with the volume of distribution was very close to zero at the lower limit, suggesting that the relationship may be data-set specific, and that it should be used with caution for predictive purposes.

Discussion

In this population pharmacokinetic analysis, data from subcutaneous administration of lispro and RHI was combined with data following inhalation (TI). TI administration results in rapid absorption and a rapid systemic clearance, with a clearly distinguishable second compartment in its pharmacokinetic profile. The inclusion of data following TI dosing has made it possible to attribute the differences in the shape of the insulin curve following the different routes of administration to differences in absorption [94]. In agreement with previously reported results, insulin pharmacokinetics were found to be consistent with a two-compartment model [94].

In this analysis, data from subjects with type 1 and type 2 diabetes treated with TI and lispro were combined with data from healthy individuals dosed with TI and subcutaneously administered insulin. The inclusion of lispro in the model was appropriate, since lispro has been shown to exhibit almost identical pharmacokinetics as RHI when administered intravenously [37], and its more rapid apparent clearance can be attributed to its more rapid absorption rate. The inclusion of lispro data in the model allowed for an estimate of the absorption rate differences between TI, subcutaneously administered insulin as well as lispro. As expected, TI was characterized by the quickest absorption rate, followed by lispro and RHI. Both subcutaneously administered insulins were adequately described by two sequential first order absorption rate constants, as described by Puckett *et al* [81] in a model based on the physiology

of subcutaneous insulin administration, where the depot compartment represents the subcutaneous tissue, and the second compartment represents the interstitial space. This model of insulin absorption was applied to data from healthy volunteers, as described in Chapter 2. Absorption rate estimates for both TI and subcutaneous RHI were almost identical to the previously developed model, as expected, since the current population model included the data from healthy volunteers used in the earlier analysis (Chapter 2). As also expected, the lispro absorption rate was estimated to be faster than following RHI, indicating that the rapid dissociation of lispro into the readily absorbable monomeric form increases its absorption rate from the subcutaneous tissue. An ideal design to better explore this difference between the two subcutaneous forms of insulin would be a crossover study, which would greatly diminish the interindividual variability that is inherent with subcutaneous dosing and would allow for a better comparison between the two treatments.

The inclusion of data from an inhaled product in the model made it necessary to account for the considerable interoccasion variability associated with pulmonary drug administration. Inhalation differences from day to day can result in differences in the bioavailability of treatments administered through the lung, and although this variability may be reduced with repeated dosing, treatment-naïve or inexperienced subjects may exhibit significant interoccasion differences in exposure. In this analysis, subjects in one of the studies were administered three different doses of TI on three different occasions and in another study, subjects were administered TI on two different occasions. The interoccasion variability was successfully modeled to reflect inhalation differences that resulted in a difference in insulin bioavailability, with no difference in other pharmacokinetic parameters. For this group of subjects, the

interoccasion variability was estimated by the model to be approximately 29%, which is similar to values reported previously (Chapter 2).

In this analysis, relative bioavailability of TI and subcutaneous RHI was estimated by fixing lispro bioavailability to 1. The absolute bioavailability of lispro has been reported to be between 55-77%, and has been shown to be significantly greater than that of RHI [37]. In the model presented here, subcutaneous RHI and TI are estimated to have a relative bioavailability of 72 and 14%, respectively. Assuming the lispro absolute bioavailability to be 77%, as reported in literature, the parameter estimates presented here match well with those estimated in an analysis reported earlier (Chapter 2), with an absolute bioavailability adjusted systemic clearance of 40.3 L/hr (previously reported 43.4 L/hr), a central volume of distribution of 3.7 L (reported 5.0 L) and a peripheral volume of distribution of 28 L (reported 30 L). The relative bioavailability of TI to RHI was 19.4%, in close agreement with previous results where it was found to be 21% [94].

The final population model included age as a significant covariate positively correlated with insulin volume of distribution in the central compartment, and negatively correlated with the TI absorption rate. Pulmonary absorption rate was found to decrease with age, and appeared to be independent of any age-associated decreases in pulmonary function, as FEV_1 did not contribute to the model significantly when tested in the univariate analysis. Visual inspection of the relationship of age and TI absorption rate revealed asymptotic tendencies with increasing age. The power model appeared to fit the data well, indicating that the extent of the effect would be self-limiting. This finding could be beneficial to older patients, who often times experience a slower gut transit time when compared to younger patients. High and fast insulin peaks, such as those seen with TI, might cause a mismatch in insulin peak and glucose appearance from the

meal, causing early hypoglycemic events in older patients. The slightly longer absorption and lower overall insulin peak will result in a decreased likelihood of such an event in this population.

Unlike differences in age, pulmonary function differences were not found to affect either the pulmonary absorption rate or bioavailability following TI administration. The fact that the analysis did not identify either FEV_1 or percent of predicted FEV_1 as covariates was not an unexpected result, since the inclusion criteria into the studies in this analysis required pulmonary function in the normal range. An interesting addition to the model would be the inclusion of subjects with moderately or even severely impaired pulmonary function, to further investigate any potential relationship.

Increases in BMI were found to decrease absorption when insulin was administered subcutaneously, as reported previously by others [90]. This observation may be attributed to the increased thickness of the subcutaneous tissue in subjects with higher BMI, which slows absorption from the depot compartment. The small number of subjects, narrow BMI range and homogenous nature of the healthy population makes it difficult to extrapolate these results, however, it is expected that a greater impact would be observed on patients taking subcutaneous insulin who have higher BMI, as is often the case in subjects with type 2 diabetes.

In this analysis, the inclusion of the covariates associated with the disease state was difficult and complicated, since data from each population was derived from a different study. Furthermore, different baseline correction methods, which may influence some parameter estimates, were used in each study. Addition of more data to the model may help overcome this issue and would strengthen the validity of the analysis.

Overall, the median bootstrap structural and covariate parameter values matched the population typical values well, adding a stronger level of confidence in the results. However, the confidence interval around the age covariate associated with the volume of distribution was very close to zero at the lower limit, suggesting that the relationship may be data-set specific, and that it should be used with caution for predictive purposes. The bootstrap results of the interindividual and residual error estimates suggest that the accuracy of final model estimates of variability may be limited, and that a larger set of data may be necessary for an accurate assessment of the variability in a model which describes the pharmacokinetics of a highly variable substance. Furthermore, the bulk of the data in this analysis was obtained following TI administration, making it difficult to truly gage the variability associated with subcutaneous dosing due to the relatively small number of patients dosed via this route. This is a shortcoming of the model developed, and assessment of variabilities is very likely representative of only the population used in model development. Finally, it is possible that there are relationships which may account for some of the variability that were impossible to detect with the number of subjects included in the analysis, a problem further compounded by the fact that certain potential covariates were only derived from one study.

Conclusions

Data from four studies were included in a population pharmacokinetic analysis of insulin. In agreement with previously reported results, insulin pharmacokinetics were found to be consistent with a two-compartment model. Following subcutaneous dosing, both sc RHI and lispro were characterized by two sequential first order absorption rates. No significant differences in insulin pharmacokinetics were observed between the healthy, type 1 and type 2 diabetic populations. Age was identified as a significant covariate associated with the volume of distribution in the central compartment, where volume was found to increase with increasing

age. Age was also found to be related to the rate of pulmonary absorption, with increasing age associated with a decrease in absorption rate. Increased BMI was found to be associated with a decrease in insulin absorption rate following subcutaneous administration.

Table 4-1 Summary of demographics and baseline characteristics

Demographic Variable		
Diabetes Status	Parameter	Value
Healthy	N (# of profiles)	16 (57)
Type 1 diabetic	N (# of profiles)	75 (136)
Type 2 diabetic	N (# of profiles)	12 (20)
Gender		
Male	N	55
Female	N	48
Race		
Caucasian	N	102
Asian	N	1
Age (years)	Mean ± SD	36 ± 12
Weight (kg)	Mean ± SD	72 ± 13
BMI (kg/m^2)	Mean ± SD	24 ± 3
Height (cm)	Mean ± SD	171 ± 10
FEV_1 (L)	Mean ± SD	4 ± 1
Percent of predicted FEV_1 (%)	Mean ± SD	98 ± 12

Table 4-2 Mean (%CV) noncompartmental insulin pharmacokinetic parameter estimates

Dose Group	t_{max} (h)*	C_{max} (µU/mL)	Half-life (h)	AUC_{0-4} (µU/mL·min)	AUC_{0-last} (µU/mL·min)	$AUC_{0-\infty}$ (µU/mL·min)	Dose-Normalized $AUC_{0-\infty}$
10 U RHI (n=15)	1.50	30.7 (34)	--	85.2 (30)	107.0 (26)	--	
10 U lispro (n=9)	1.25	55.5 (21)	--	147.6 (17)	180.3 (15)	--	--
25 U TI (n=11)	0.20	54.6 (72)	1.1 (61)	52.8 (61)	50.0 (61)	57.4 (62)	2.0
30 U TI (n=139)	0.20	52.0 (54)	1.1 (59)	40.2 (47)	40.2 (47)	42.6 (48)	1.4
50 U TI (n=11)	0.20	105.3 (38)	1.3 (31)	102.6 (40)	101.5 (39)	111.2 (39)	2.0
60 U TI (n=6)	0.25	163.1 (43)	1.5 (53)	132.6 (43)	134.1 (43)	139.5 (41)	2.3
90 U TI (n=6)	0.25	217.9 (41)	1.2 (46)	166.9 (35)	168.7 (34)	170.2 (34)	1.9
100 U TI (n=16)	0.33	240.9 (52)	1.4 (57)	213.6 (44)	218.6 (43)	230.6 (41)	2.2

* Median presented for t_{max};

Table 4-3 Tukey 95% simultaneous confidence intervals

	Compared to Study	Lower limit of Conf. interval	Center Value	Upper limit of Conf. interval
Study 1	2	-0.4808	-0.1915	0.09782
	3	-0.4861	-0.1652	0.15573
	4	-0.6342	-0.3599	-0.08549
Study 2				
	3	-0.1769	0.0263	0.22956
	4	-0.2849	-0.1683	-0.05176
Study 3				
	4	-0.376	-0.1947	-0.01338

Table 4-4 Univariate analysis

Covariate Model Tested	OFV	Change in OFV
Base Model	13760.76	--
Age on Vc	13724.22	36.538
Weight on CL	13749.57	11.196
Age on Vp	13760.26	0.502
BMI on ka_{sc}	13738.54	22.223
Age on ka_{TI}	13661.83	98.936
Weight on ka_{TI}	13761.16	-0.393
Sex on ka_{TI}	13737.91	22.856
FEV_1 on ka_{TI}	13761.31	-0.547
FEV_1 on TI F	13761.39	-0.625
Age on TI F	13762.00	-1.238
Body weight on TI F	13760.89	-0.124

Table 4-5 Final model: Backwards elimination

Model	OFV	Change in OFV
Final model	13641.22	
Final model-age on TI ka	13707.17	-65.945
Final model-age on V	13659.93	-18.709
Final model-BMI on sc RHI ka	13657.96	-16.736

Table 4-6 Population pharmacokinetic parameter estimates of insulin

Pharmacokinetic Parameters	Base Model	Full Model	Bootstrap
Parameter	Estimate (%RSE)	Estimate (%RSE)	Median (95% CI)
CL (L/hr)	53.3 (10.0)	52.30 (9.6)	51.9 (43.0, 69.7)
V_c (L)	4.6 (13.5)	4.64 (12.8)	4.79 (3.83, 6.38)
Q (L/hr)	23.9 (12.9)	23.00 (12.4)	23.3 (18.0, 30.3)
V_p (L)	37.0 13.9)	36.40 (14.0)	34.8 (25.7, 47.7)
ka_{sc1} (hr^{-1})	0.6 (47.9)	0.68 (24.9)	0.76 (0.43, 1.20)
ka_{LI1} (hr^{-1})	0.7 (28.3)	0.73 (36.5)	0.72 (0.44, 1.22)
ka_{sc2} (hr^{-1})	1.0 (48.9)	0.91 (22.4)	0.88 (0.57, 1.60)
ka_{LI2} (hr^{-1})	1.4 (26.3)	1.27 (34.5)	1.28 (0.78, 2.15)
ka_{TI} (hr^{-1})	2.6 (5.4)	2.39 (5.0)	2.44 (2.21, 2.71)
F_{sc} **	0.75 (13.3)	0.72 (12.3)	0.71 (0.58, 0.90)
F_{LI} **	1 fixed	1 fixed	--
F_{TI} **	0.14 (16.1)	0.14(15.9)	0.14 (0.10, 0.19)
Lower BA of study 4	0.07 (28.6)	0.07 (28.2)	0.08 (0.05, 0.13)
Age on Vc		0.02 (81.8)	0.02 (0.001, 0.06)
Age on ka_{TI}		-0.48 (20.9)	-0.47 (-0.69, -0.31)
BMI on ka_{sc}		0.10 (38.7)	0.13 (0.04, 0.42)
Interindividual and Residual Variability			
ω_{CL}	33.3	30.7	52.8 (33.3, 111)
ω_{Vc}	83.5	82.5	90.8 (80.1, 97.6)
ω_{Q}	70.1	62.6	77.6 (60.6, 108)
ω_{Vp}	63.9	63.0	77.7 (61.0, 116)
ω_{kasc}	26.6	21.8	46.2 (28.8, 57.1)
ω_{kaLI}	11.5	10.7	32.8 (6.7, 45.1)
ω_{kaTI}	28.1	19.4	43.2 (5.6, 50.2)
ω_{Fsc}	13.3	13.5	41.2 (8.0, 75.8)
ω_{FTI}	--	0.0	--
$\omega_{IOV\ FTI}$	28.9	30.9	58.2 (45.4, 67.3)
σ_1	20.9	20.2	44.8 (42.4, 54.2)
σ_2 *	0.85	0.87	0.91 (0.8, 1.05)

Note: *σ_2 (additive residual error) is expressed in μU/mL; The magnitude of interindividual and residual variability was expressed as CV%, approximated by the square root of the variance estimate. ** F is reported as relative bioavailability to lispro.

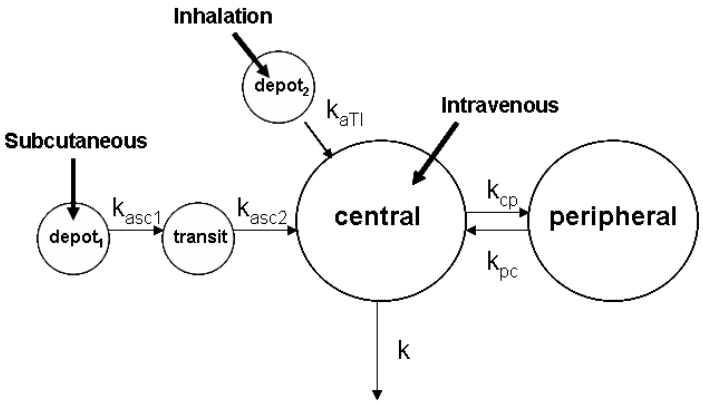

Figure 4-1 Pharmacokinetic model diagram

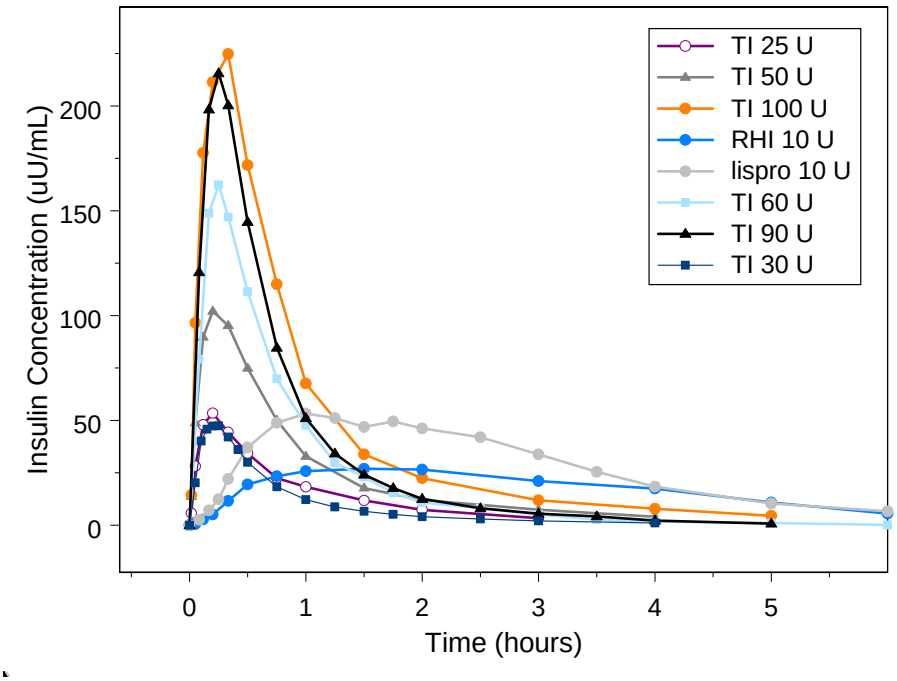

Figure 4-2 Mean insulin concentration-time profiles by dose and treatment

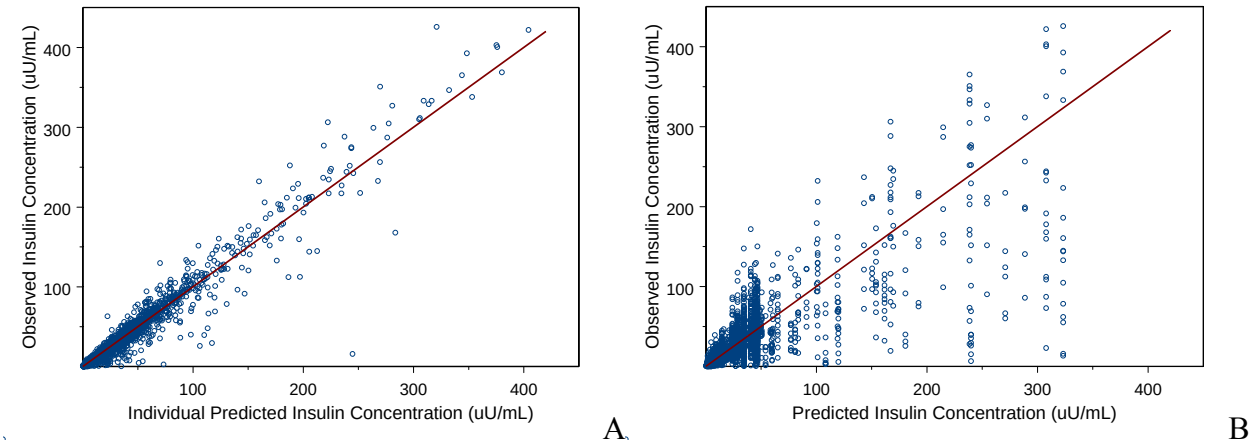

Figure 4-3 Goodness of fit plots of predicted and individual predicted insulin concentrations. A) Base model individual predicted versus observed insulin concentrations and B) Base model predicted insulin concentrations versus observed insulin concentrations

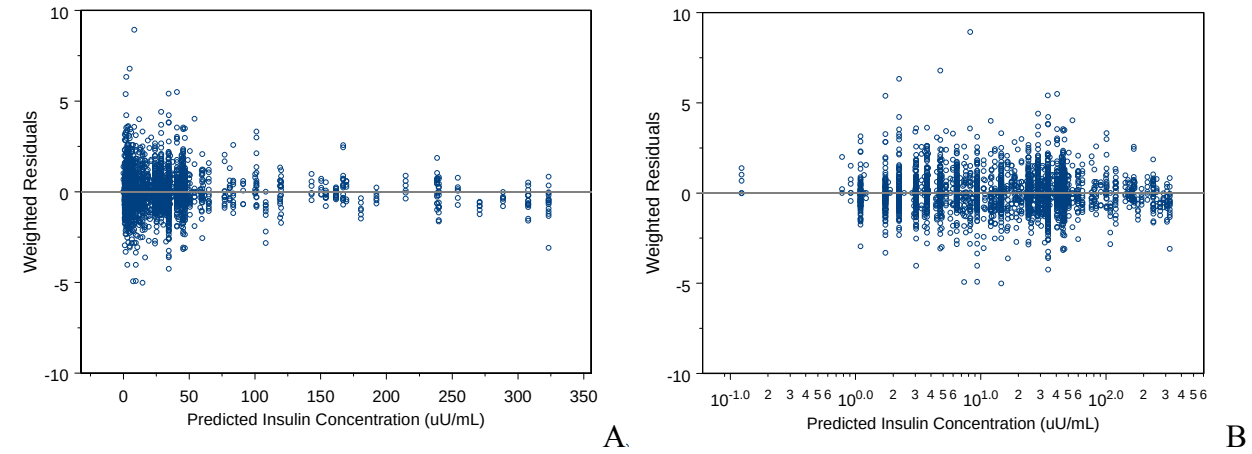

Figure 4-4 Goodness of fit plots of weighted residuals. A) Base model predicted insulin concentrations versus weighted residuals (linear scale) and B) Base model predicted insulin concentrations versus weighted residuals (log scale)

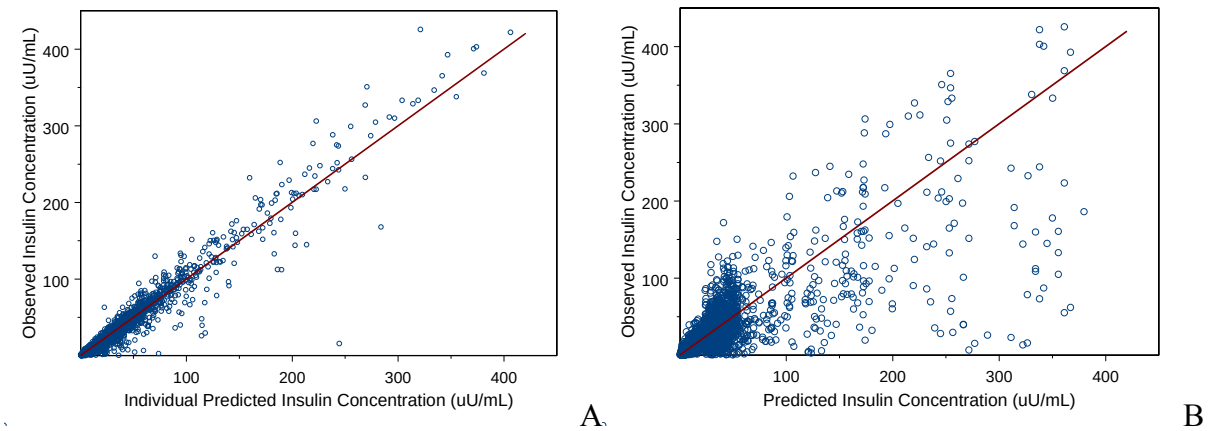

Figure 4-5 Goodness of fit plots of predicted and individual predicted insulin concentrations. A) Individual predicted versus observed insulin concentrations and B) Predicted insulin concentrations versus weighted residuals

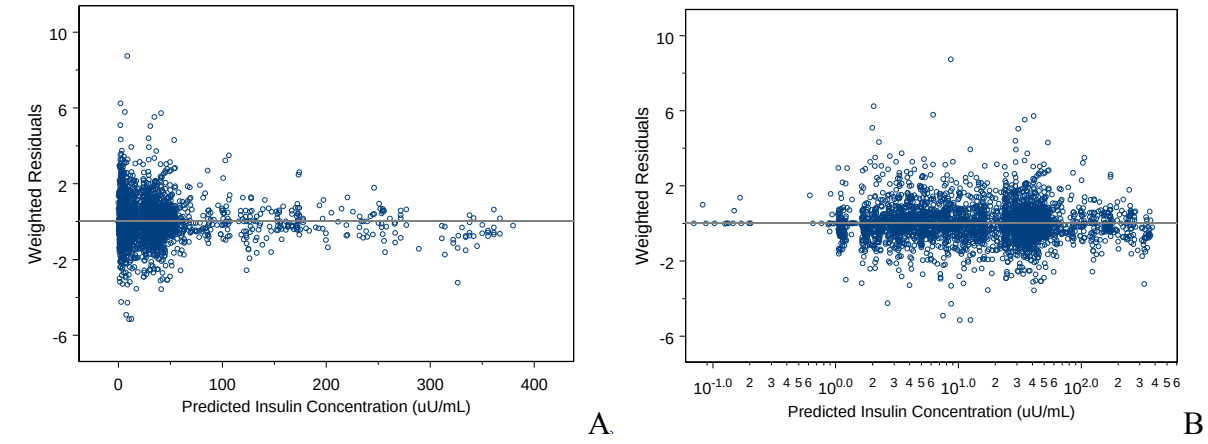

Figure 4-6 Goodness of fit plots of weighted residuals. A) Final model predicted insulin concentrations versus weighted residuals (linear scale) and B) Predicted insulin concentrations versus weighted residuals (log scale)

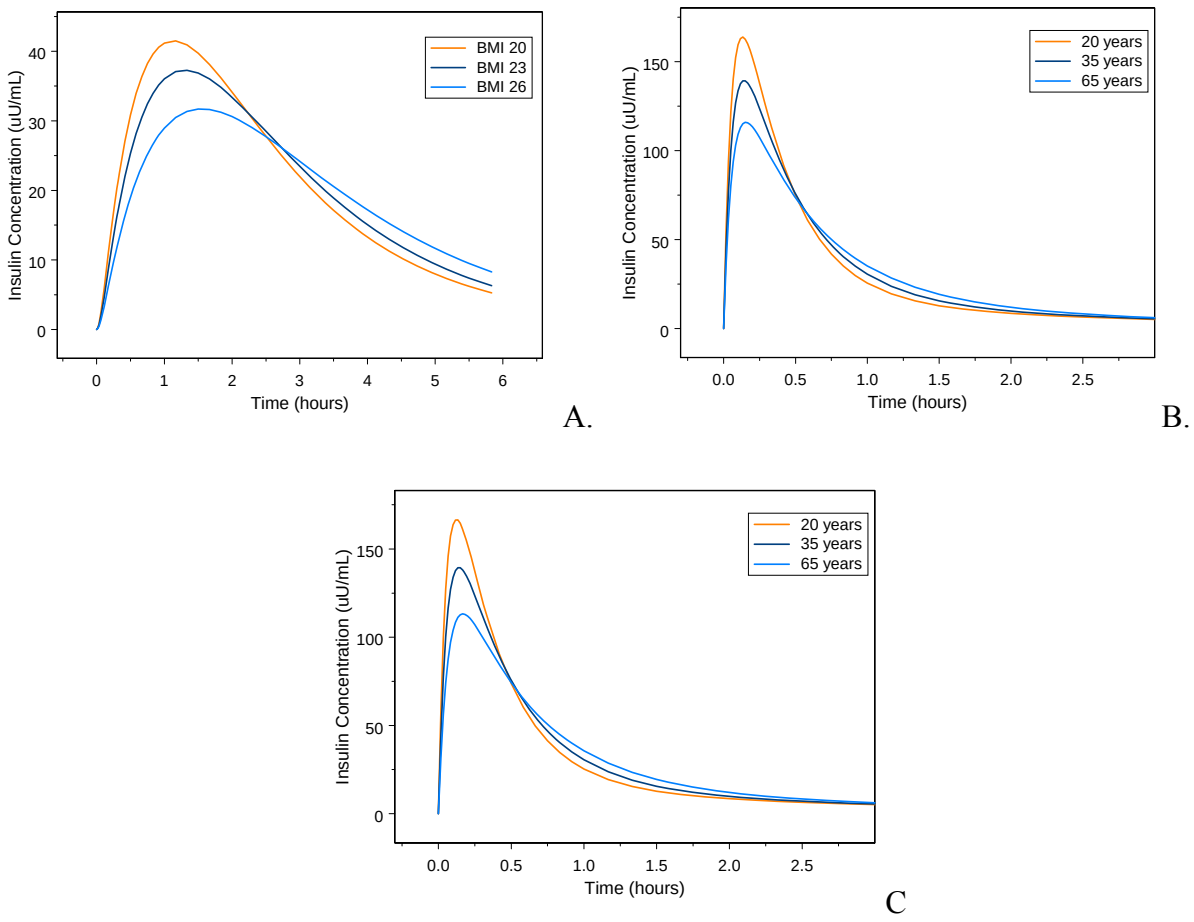

Figure 4-7 Simulated covariate effect on insulin pharmacokinetics. A) BMI effect on subcutaneous absorption rate B) Age effect on V_c C) Age effect on TI absorption and V_c

CHAPTER 5
PHARMACODYNAMIC MODEL FOR SUBCUTANEOUSLY ADMINISTERED REGULAR HUMAN INSULIN, INSULIN LISPRO, AND INHALED INSULIN IN HEALTHY VOLUNTEERS AND TYPE 2 DIABETIC SUBJECTS

Background

The glucose clamp procedure has been used extensively to study insulin activity [9, 17, 35, 39]. During this procedure, patients are administered a fixed insulin infusion, while at the same time receiving a varying infusion rate of glucose to counteract insulin's action and maintain a constant glycemic state. Suppressing endogenous insulin secretion with the insulin infusion is critical to distinguishing between the effects of the administered insulin and insulin secreted by the pancreas in response to the administered glucose. As it is assumed that the exogenous insulin infusion completely suppresses hepatic glucose production as well as appreciable insulin secretion, the glucose infusion rate (GIR) can be used as a measure of the pharmacodynamic response to the administered insulin [36]. This procedure allows for the direct measure of insulin effects by determining the amount of glucose required to maintain blood glucose concentrations within a defined range.

A pharmacokinetic/pharmacodynamic (PK/PD) model was developed for insulin concentrations and the GIR in healthy subjects (Chapter 3). In order to expand the model to the relevant population, glucose clamp data from subjects with type 2 diabetes was included in the analysis. Subjects with type 2 diabetes exhibit decreased insulin sensitivity [95], and it is expected that the pharmacodynamic response in this population will be different from non-diabetics. The aim of this analysis was the development of a PK/PD model for RHI administered via the inhalation route so as to better refine 1) the model parameter estimates as they differ between a population with type 2 diabetes and healthy subjects, and 2) the impact that the disease state has on insulin effect as measured by the GIR.

Materials and Methods

Study Population

Data from three glucose clamp studies were combined for this analysis. The first two studies were conducted in healthy volunteers, and the third study was conducted in type 2 diabetic subjects. Each study was a prospective, single-center, open-label, randomized, crossover euglycemic glucose clamp study in non-smoking male and female volunteers with normal pulmonary function. All three studies were performed at the same clinical site. Each was approved by the local ethics committee and was carried out in accordance with the principles of the Declaration of Helsinki and of Good Clinical Practice. Subjects gave written informed consent prior to randomization.

Prior to entry into the studies, all subjects were given a physical examination, pulmonary function tests, electrocardiography, and laboratory tests, including urinalysis and screening for drugs of abuse. All blood samples were drawn from a forearm vein via an intravenous catheter, placed in the cubital vein of the arm contralateral to the one used for the continuous insulin infusion and glucose administration.

For this analysis, only TI data was used since this was the only treatment used in both the healthy subjects and the subjects with type 2 diabetes, thus only handling of TI data is described. However, for completeness, the study conduct for the studies is described in full, including all treatments.

Study Design and Insulin Concentrations

Healthy volunteers

Both studies were euglycemic glucose clamp procedures performed with the Biostator glucose monitoring and infusion system (Biostator, Life Science Instruments, Elkhart, IN, USA), and a continuous insulin infusion to suppress endogenous insulin production. Following an

overnight fast, on each of the treatment days, the subjects received a constant rate intravenous infusion of RHI during a 2-hour run-in period to establish a serum insulin concentration of 10–15 μU/mL. This infusion was continued until the end of the study. Each subject received a single dose of the test treatment on separate occasions.

Study 1: This was a three-way crossover euglycemic glucose-clamp study in five subjects to compare the pharmacokinetics and pharmacodynamics of single doses of 100 U of inhaled TI, 10 U RHI administered subcutaneously and 5 U RHI (Actrapid, Novo Nordisk A/S, Bagsvaerd, Denmark) administered intravenously.

Study 2: This was a four-way crossover euglycemic glucose-clamp study in 12 subjects to compare the pharmacokinetics and pharmacodynamics of three different single doses of inhaled TI with a single dose of 10 U RHI (Actrapid, Novo Nordisk A/S, Bagsvaerd, Denmark).

TI was administered using a commercially available inhaler (Model M, Boehringer Ingelheim) in study 1, and using the MedTone Dry Powder Inhaler (MannKind Corporation, Danbury, CT) in study 2. RHI insulin was administered by subcutaneous injection in the abdominal region. Samples for insulin concentration determination were drawn at 120, 90, 60 and 30 minutes before dosing and 0, 1, 3, 7, 12, 20, 30, 45, 60, 90,120, 180, 240, 300 and 360 minutes post-dose, and analyzed for insulin concentration using radioimmunoassay (RIA) with double determinations. C-peptide concentrations were collected at 120 and 60 minutes pre-dose and 0, 30, 60, 180, and 300 minutes post-dose. The samples were cooled in an ice-water bath before centrifugation. After centrifugation the plasma samples were immediately frozen and stored at -80°C until analysis. Blood glucose was kept constant at 90 (±10) mg/dL throughout the glucose clamp by a variable infusion of a dextrose solution. The patients were kept in a fasted

state until the end of each treatment visit. The treatment periods were separated by a washout period of 3 and 28 days.

Type 2 diabetic subjects

Study 3: This was a prospective, randomized, open label, single site study in 12 non-smoking, male and female subjects with a diagnosis of type 2 diabetes mellitus for ≥12 months, stable antidiabetic regimen with insulin for the previous 3 months and HbA1c ≤ 8.5%, to compare the pharmacokinetics and pharmacodynamics of two doses of TI (60 and 90 U) with a single dose of 10 U lispro (Humalog™, Eli Lilly & Co.). Six subjects received 60 U TI and the other six subjects received 90 U TI. All twelve subjects received lispro administered by subcutaneous injection in the abdominal region. Following an overnight fast, on each of the treatment days, the subjects received a constant rate intravenous infusion of either RHI or lispro (opposite of the type of insulin to be used in dosing) during a 4-6-hour run-in period to suppress endogenous insulin production and to obtain target blood glucose levels of 110 mg/dL. This infusion was continued until the end of the clamp procedure. Blood glucose was kept constant at 110 (±10) mg/dL throughout the glucose clamp by the Biostator®. Samples for insulin and lispro concentration determination were drawn at 310, 20 and 5 minutes before dosing and at time 0, 5, 10, 15, 20, 30, 45, 60, 75, 90, 105, 120, 150, 180, 210, 240, 300, 360, 420 and 480 minutes post-dose. The patients were kept in a fasted state until the end of each treatment visit. The treatment periods were separated by a washout period of 7 to 21 days.

Glucose Infusion Rates and Blood Glucose Concentrations

Glucose infusion rates were registered by the Biostator® every minute from 120 minutes before dosing until 360 minutes post-dose (studies 1 and 2) and from 60 minutes before dosing until 480 minutes post-dose (study 3). If the glucose pump could not meet the glucose infusion requirements, an additional external pump controlled by study personnel, was employed. The BG

measurements of the Biostator® were recalibrated at regular intervals (range, 10–30 minutes) by the YSI 2300 STAT Plus™ Glucose Analyzer (YSI Life Sciences, Yellow Springs, OH), which employed the glucose oxidase method.

Baseline Correction

Studies 1 and 2: Insulin concentrations collected at 120, 90, 60 and 30 minutes before dosing were averaged, and subtracted from all subsequently observed insulin concentrations, to account for any incomplete endogenous insulin suppression and the constant insulin infusion. Any resulting negative values were set to zero.

Study 3: Baseline correction was applied to account for any endogenous insulin that was not fully suppressed with the baseline infusion. All insulin concentrations were corrected by subtracting the mean of the values in the later time points (300–480 minutes) from each individual time point for each subject. At these time points, most subjects' insulin concentration-time profiles were observed to be reasonably flat and uninfluenced by exogenous contribution.

GIR Smoothing Methodology

For the pharmacodynamic analysis, GIR values were smoothed using a 10-minute running average. For the noncompartmental GIR analysis, GIR values were first baseline-corrected, where GIR values from 60 minutes prior to dosing were averaged, and subtracted from all subsequently observed GIR values. Resulting negative values were set to 0, and the data was smoothed using a 10 minute running average.

Insulin Data for the Pharmacokinetic/Pharmacodynamic Analysis

Individual predicted insulin pharmacokinetic parameters from the pharmacokinetic model were used to simulate the insulin concentrations used in the analysis. Since the pharmacokinetic model was developed using baseline corrected insulin concentrations and the PK/PD analysis targeted exploring the relationship between total insulin concentrations and total GIRs, the

simulated insulin values were each added to the baseline used for correction at each visit. GIR and insulin values ever 5 minutes for the first hour and every 10 minutes thereafter were combined for the analysis.

Data Excluded from the Pharmacokinetic Analysis

For studies 1 and 2, each serum insulin concentration-time profile was examined visually together with C-peptide concentrations. Due to the lower doses administered in study 2, a higher incidence of elevated C-peptide concentrations was observed in the latter timepoints following TI treatment, particularly in the lower dose groups. All insulin concentrations after 180 minutes post-dose in the 25 U dose group, 240 minutes post-dose in the 50 U dose group, and 300 minutes in the 100 U dose group were excluded, since endogenous insulin appeared to be contributing to the curve in the latter part of the study, with a total of 51 non-BLQ concentrations were excluded from the analysis. One subject from study 2 was excluded from the analysis.

Noncompartmental Pharmacokinetic and Pharmacodynamic Analysis

Insulin pharmacokinetics were analyzed using noncompartmental methodology using baseline-corrected insulin concentrations. The following PK parameters were derived using WinNonlin v 5.2 (Pharsight Corporation, Mountain View, CA): observed peak insulin concentration (C_{max}), time to peak insulin (t_{max}), and total insulin exposure as measured by the area under the insulin concentration-time curve from time 0 until the last time point with non-zero insulin concentrations ($AUC_{0\text{-}last}$), calculated by the linear-trapezoidal method. The terminal elimination half-life ($t_{1/2}$) was calculated as $\ln(2)/\lambda_z$ in accordance with pharmacokinetic theory [80], where λ_z is the terminal elimination rate constant estimated from log-linear regression analysis of the terminal elimination phase of the concentration-time profile, and $AUC_{0\text{-}\infty}$ was calculated as calculated as $AUC_{0\text{-}last} + C_{last}/\lambda_z$, where C_{last} is the last observed insulin concentration. Noncompartmental parameter values were used to determine starting estimates for

pharmacokinetic modeling, and were compared to parameter values estimated by the final model as part of the model fit assessment.

Insulin pharmacodynamic (GIR) parameters were derived using WinNonlin v 5.2. The following parameters were determined from the 10 minute running average smoothed GIR data: observed peak GIR (GIR_{max}), time to peak GIR (GIR t_{max}), and the area under the GIR-time curve from time 0 until time t (GIR_{0-t} AUC), calculated by the linear-trapezoidal method.

Statistical Analysis

Dose-normalized log transformed insulin $AUC_{0-\infty}$ was used in order to investigate dose-proportionality. Dose-proportionality could not be concluded if the average dose-normalized $AUC_{0-\infty}$ values were found statistically different by a one-way ANOVA technique, which was performed with the null hypothesis that the dose average log transformed $AUC_{0-\infty}$ values are the same, at the α=0.05 level. The alternative hypothesis was that some of the group means differ from each other.

It was necessary to test the variances of the five dose groups for homogeneity in order to accept the results of the ANOVA analysis, since homogeneity of variances is one of the ANOVA assumptions. Levene's test was both performed under the null hypothesis that the variances are the same and an alternative hypothesis that the at least one of the variances was different from the others. The data were tested at the α=0.05 level. The results of the statistical tests were obtained using MINITAB (v.15.1.30.0).

Linear regression was used to assess whether or not the 90% CI around the intercept included 0. The CI was calculated as he average ± 1.96 · standard error of the mean (SEM).

Pharmacokinetic/Pharmacodynamic Model and Data Analysis

The software package NONMEM (Version VI, Level 1.2, NONMEM Project Group, ICON Development Solutions, USA) was used for the population analysis using both the first order (FO) and the first order conditional estimation method (FOCE).

NONMEM describes the observed concentration-time data in terms of:

- A number of fixed effect parameters, θ, which may include the mean values of the relevant base pharmacokinetic model parameters, or a number of parameters which relate the base model parameters to demographic and other covariates;
- Two types of random effect parameters: (a) ω^2: the variances of the interindividual variability (η) within the population, and (b) σ^2: the variances of the residual intraindividual variability (ε) due to random fluctuations in an individual's parameter values, measurement error, model misspecification, and all sources of error not accounted for by the other parameters.

The population or average values of the parameters, θ, the interindividual variances, ω^2, and the residual variance, σ^2, were estimated by NONMEM. The η values are independent, identically distributed random errors with mean of zero and a variance equal to ω^2. Subject-specific parameters were calculated by NONMEM using the POSTHOC (FO method) option. These parameters are empirical Bayesian estimates of the individual's true parameters based on the population parameters and the individual's observed concentrations.

Pharmacokinetic and pharmacodynamic model

Data from both studies were modeled simultaneously, but the pharmacokinetic and pharmacodynamic models were developed sequentially. The pharmacokinetics was described by a two compartment open model with first order absorption and was parameterized in terms of apparent clearance (CL/F), volume of distribution in the central compartment (V_c/F), the apparent intercompartmental clearance (Q/F), the volume of distribution in the peripheral compartment (V_p/F) and the first order absorption rate constant (ka). NONMEM library

subroutines ADVAN4 and TRANS4 were used. A diagram of the combined PK/PD model is presented in Figure 5-1.

In the PD model, the GIR was used as the dependent variable. When exploring the potential PK/PD model, the relationship between insulin and GIR was first examined by visual inspection. The pharmacodynamic model was described by the following differential equations:

$$\frac{dCe}{dt} = k_{e0} \cdot (Cp - Ce) \tag{5-1}$$

$$GIR = E_0 + \frac{E_{\max} \cdot C_e^{\gamma}}{EC_{50}^{\gamma} + C_e^{\gamma}} \tag{5-2}$$

Equation 5-1 describes the relationship between the observed plasma insulin concentration and the concentration at the effect site. Effectively, k_{e0} is a rate constant which describes the delay in effect. The effect compartment is assumed to receive a negligible mass from the central compartment, thereby not affecting the equations for the insulin pharmacokinetic model. Equation 5-2 establishes the relationship between the GIR and insulin concentration at the effect site. The pharmacodynamic structural model was parameterized in terms of E_0, the baseline GIR value, E_{max}, the maximum glucose infusion rate, EC_{50}, the effect site concentration eliciting 50% of the maximal response, γ the sigmoidicity factor, and Cp and Ce are the plasma and effect site insulin concentrations, respectively.

Error model

Interindividual variability was described by an exponential error model. The intraindividual residual variability of insulin plasma concentration was estimated using a proportional and additive error model (PK) and additive error model (PD).

Results

Patient Population

A total of 621 insulin concentrations from 28 subjects and 50 profiles were included in the analysis. Demographic data is summarized in Table 5-1.

Pharmacokinetic and Pharmacodynamic Results

Noncompartmental analysis

Mean baseline corrected insulin and uncorrected GIR-time profiles are presented in Figure 5-2 and the PK and PD parameters are presented in Table 5-2 and Table 5-3, respectively.

Pharmacokinetics: The average time-insulin concentration time profiles increased with increasing dose for insulin following TI administration, and t_{max} and half-life remained relatively constant with dose (Table 5-2). Insulin exposure following TI, as measured by insulin AUC_{0-360} and $AUC_{0-\infty}$ increased in a proportional manner with increasing dose with the doubling of the dose resulting in an approximate doubling in exposure. An ANOVA and linear regression (Figure 5-3) analyses were performed to assess the relationship between dose and insulin exposure. Log-transformed dose-normalized insulin $AUC_{0-\infty}$ was analyzed using a one way ANOVA, with no differences found between the dose groups ($p=0.985$). Levene's test was performed to test the variances of the four studies for homogeneity. The null hypothesis of equal variances could not be rejected at the $\alpha=0.05$ level, with a p value of 0.968. Therefore, the variances met the homogeneity assumption. Due to the high variability observed in this parameter, the r-squared value resulting from the linear regression was only 0.5061, even with the regression line falling very closely to the mid-points of the parameter values. The intercept estimate was of 1.5216, slope estimate of: 2.2 and associated $p < 0.0001$. The 90% CI around the intercept (-36.66, 39.7) included 0, and hence dose-proportionality was concluded.

Pharmacodynamics: A phase-plot of GIR vs. the plasma insulin concentration, where data points are connected in chronological order, is shown in Figure 5-4 for the pooled data in this analysis. A counter-clockwise hysteresis loop is observed indicating a disconnect between insulin concentrations observed centrally and insulin action. Unlike the pharmacokinetic profiles, the GIR profiles did not appear dose-proportional from visual inspection (Figure 5-2). This was confirmed by an inspection of the baseline-corrected GIR parameters, where both the mean GIR_{max} and mean GIR $AUC_{0\text{-}360}$ were lower in subjects with type 2 diabetes (Table 5-3).

Differences in study conditions and patient population resulted in lower GIRs in the subjects with type 2 diabetes. Furthermore, little difference was observed in the mean GIR response between the 60 and 90 U dose groups (Table 5-3), suggesting that the differences in mean concentrations seen in this small sample size did not result in readily discernable mean differences in GIR response.

Pharmacokinetic and pharmacodynamic analysis

Pharmacokinetic model: A two-compartment open model with first order absorption processes and first-order elimination described the insulin concentration data well. The overall model fit was good, with individual predicted versus observed values distributed along the line of unity, and no significant trends in the weighted residuals (Figure 5-5). Thus, the structural and error models appeared to adequately describe insulin pharmacokinetics and explain the variability in the data. The population typical values were: apparent clearance, 466 L/hr; apparent volume of distribution in the central compartment, 38.2 L; apparent volume of distribution in the peripheral compartment, 258 L, an intercompartmental clearance of 171 L/hr and an absorption rate of 2.0 h^{-1}. The base model pharmacokinetic parameter estimates are summarized in Table 5-4.

Pharmacodynamic model: For the pharmacodynamic analysis, parameter values estimated by Model A (Chapter 3) developed using data from healthy subjects, were used as starting values. To account for the different blood glucose clamp settings, the E_0 was estimated separately for the two groups. To explore and evaluate the differences in the response between the two groups, all other parameters were estimated separately, with the exception of E_{max}, which was fixed to the value estimated for the healthy population. The limited range of values and small N associated with the data from the type 2 population made the estimation of this parameter difficult, and work previously performed strongly suggests that insulin E_{max} would not be affected by the disease state [96]. Parameter estimates are presented in Table 5-5.

The overall model fit was good, with individual predicted versus observed values distributed along the line of unity, and no significant trends in the weighted residuals (Figure 5-6) for either the healthy (blue) or type 2 diabetic (orange) subjects. Thus, the structural and error models appeared to adequately describe insulin pharmacodynamics and explain the variability in the data. Individual predicted GIR values overlaid with observed values for all subjects in the analysis are presented in Figure 5-7.

Discussion

Glucose clamp studies have been used to compare the activity of insulins, and GIR data have been assessed using a variety of modes, including indirect [56, 57, 72] and effect compartment models [55, 59, 60]. In previous work, an E_{max} model was used to describe the PK/PD relationship of insulins with different pharmacokinetics (Chapter 3). Because of its simplicity, and because the different insulins were modeled simultaneously, the pharmacodynamic parameter estimates from the model developed allow for the prediction of insulin effect completely based on insulin pharmacokinetics alone, and can therefore be used to predict the effect of insulins with differing pharmacokinetic properties. However, data from

healthy subjects was used for model development, and the pharmacodynamic parameters may not apply to subjects with type 2 diabetes, who exhibit decreased insulin sensitivity [95].

The work presented here expands the model to the relevant population by including glucose clamp data from subjects with type 2 diabetes. As seen previously, when the pharmacodynamic parameters were estimated independently for each insulin formulation (Chapter 3), inter- and intra-individual errors decreased when compared to the model where parameter estimates were not individualized for each formulation, and the model resulted in improved fit. In this analysis, in order to improve the accuracy of the fits and better elucidate the difference between healthy individuals and subjects with diabetes, only TI data was included in the analysis.

Noncompartmental analysis of the PK data showed that dose-proportionality was maintained when the healthy individual data was combined with data following TI administration to subjects with type 2 diabetes. The two compartment pharmacokinetic model fit the data well, without any need to account for differences in disease state between the subjects, and the pharmacokinetic parameter estimates were almost identical to parameter estimates obtained in a model incorporating only the data from the healthy volunteers. However, the response, assessed from the mean GIR curve and the noncompartmental pharmacodynamic parameters, did not appear proportional. In fact, the response was lower, on average, in subjects with type 2 diabetes receiving the 90 U TI dose than healthy volunteers receiving 50 U TI.

Although it is impossible to compare the data directly due to the different glucose clamp setting (90 mg/dL in healthy subjects and 110 mg/dL in subjects with type 2 diabetes), the difference in response appears markedly different between the two populations in light of the relatively small difference in the target glucose concentration. A literature search was conducted

to try to establish the effect that different clamp settings would have on the GIR parameters in comparable populations, so that an adjustment could be made in the model; however, no published results which would be applicable were found. Baseline correction for the difference in the glucose needed to maintain the target glucose concentration was therefore assumed to account for the differences in the clamp settings, so that the data could be compared. Although a simplification of the system, the clamp settings were not very different and hence, were not expected to account for the dramatic differences observed. Following baseline correction, the GIR response was still visibly lower in the type 2 diabetic population. This result is not unexpected due to the insulin resistance observed in subjects with type 2 diabetes, and a decreased response in the diabetic population has been demonstrated previously [96].

When the data was modeled, the pharmacodynamic parameter estimates obtained in the healthy volunteers (Chapter 3) were used as starting estimates for the model. All of the parameters were estimated separately for the two groups, with the exception of E_{max}, which was fixed to the value estimated for the healthy population. The limited range of values and small N associated with the data from the type 2 population made the estimation of this parameter difficult. Although there is a sound basis for this approach in work previously performed by Rizza [96] and the model fit was very good, an valuable improvement to the model would be the addition of more data from diabetic subjects, so that the insulin E_{max} could be estimated independently in this population.

Most of the pharmacodynamic parameters were similar for both groups (γ=2.5 and 2.7 for the healthy and type 2 diabetic subjects, respectively, and a k_{e0} of 1.4 and 1.8 h^{-1}, respectively). The lack of a large difference in k_{e0} suggests that the distribution time is not affected to a large extent by disease state. However, the EC_{50} and estimate was found to be clearly increased in the

diabetic population. In this set of subjects with diabetes, the magnitude of difference was approximately a three-fold increase in EC_{50}, indicating a significant decrease in insulin sensitivity.

Conclusions

Insulin pharmacodynamics were found to be well described by a simple E_{max} model, after a hypothetical effect compartment was used to collapse the hysteresis in insulin effect observed during clamp procedures in healthy and type 2 diabetic subjects. The EC_{50} parameter estimate was found to be approximately three-fold higher for subjects with type 2 diabetes, most likely due to the insulin resistance that is associated with this disease state.

Table 5-1 Summary of demographics and baseline characteristics

Demographic Variable		Value
Diabetes Status	N (number of profiles)	
Healthy	N	16 (38)
Type 2 diabetic	N	12 (12)
Gender		
Male	N	24
Female	N	4
Race		
Caucasian		27
Asian	N	1
Age (years)	Mean ± SD	40 ± 15
Weight (kg)	Mean ± SD	82 ± 13
BMI (kg/m^2)	Mean ± SD	26 ± 4
Height (cm)	Mean ± SD	178 ± 8
FEV_1 (L)	Mean ± SD	4 ± 1
Percent of predicted FEV_1 (%)	Mean ± SD	99 ± 13

Table 5-2 Mean (%CV) noncompartmental pharmacokinetic parameter estimates

Dose Group	t_{max} (h)*	C_{max} (µU/mL)	$AUC_{0\text{-last}}$ (µU/mL·min)	Half-life (h)	$AUC_{0\text{-}\infty}$ (µU/mL·min)	Dose-Normalized $AUC_{0\text{-}\infty}$
25 U TI (n=11)	0.20	54.6 (72)	50.0 (61)	1.1 (61)	57.4 (62)	2.0
50 U TI (n=11)	0.20	105.3 (38)	101.5 (39)	1.3 (31)	111.2 (39)	2.0
60 U TI (n=6)	0.25	163.1 (43)	134.1 (43)	1.5 (53)	139.5 (41)	2.3
90 U TI (n=6)	0.25	217.9 (41)	168.7 (34)	1.2 (46)	170.2 (34)	1.9
100 U TI (n=16)	0.33	240.9 (52)	218.6 (43)	1.4 (57)	230.6 (41)	2.2

* Median presented for t_{max};

Table 5-3 Mean (%CV) pharmacodynamic parameters

Dose (U)	GIR t_{max} (min)	GIR_{max} (uncorrected) (mg/kg/min)	GIR $AUC_{0\text{-}360}$ (uncorrected) (mg/kg)	GIR_{max} (corrected) (mg/kg/min)	GIR $AUC_{0\text{-}360}$ (corrected) (mg/kg)
25 (n=11)	50	9.9 (28)	1857 (38)	8.1 (32)	1221 (44)
50 (n=11)	45	13.2 (36)	2230 (32)	11.1 (38)	1490 (36)
60 (n=6)	43	8.7 (26)	1183 (29)	7.6 (29)	825 (28)
90 (n=6)	43	9.1 (57)	1228 (42)	8.2 (54)	933 (41)
100 (n=16)	38	16.1 (39)	3032 (36)	13.8 (43)	2220 (40)

Table 5-4 Population pharmacokinetic parameters of insulin

Pharmacokinetic Parameters	Parameter Values	Interindividual and Residual Variability	
Parameter	Estimate (%RSE)	Parameter	%CV
CL (L/hr)	466.0 (9.7)	ω_{CL}	33.6
V_c (L)	38.2 (19.3)	ω_{Vc}	72.9
Q (L/hr)	171.0 (13.9)	ω_{Q}	64.0
V_p (L)	258.0 (21.8)	ω_{Vp}	67.3
ka_{TI} (hr^{-1})	2.0 (7.4)	ω_{ka}	22.2
		$\omega_{IOV\ FTI}$	35.4
		σ_1	24.6
		σ_2	1.42*

Note: *σ_2 (additive residual error) is expressed in μU/mL; The magnitude of interindividual and residual variability was expressed as CV%, approximated by the square root of the variance estimate.

Table 5-5 Pharmacodynamic parameters of insulin in healthy and type 2 diabetic subjects

Parameter	Healthy Subjects Parameter Estimate (%RSE)	Type 2 Diabetic Subjects Parameter Estimate (%RSE)
E_0 (mg/kg/min)	2.5 (17.1)	1.4 (15.2)
E_{max} (mg/kg/min)	14.4 (14.5)	14.4 fixed
EC_{50}	39.9 (15.2)	121.0 (6.5)
K_{e0} (h^{-1})	1.4 (14.9)	1.8 (16.4)
gamma	2.5 (16.0)	2.7 (16.7)
Interindividual and Residual Variability	%CV	%CV
ω_{E0}	49.5	39.9
ω_{Emax}	37.0	58.8
ω_{EC50}	39.0	--
ω_{Ke0}	49.5	53.0
ω_{gamma}	44.6	49.3
σ_1	1.80	1.16

Note: *σ_1 (additive residual error) is expressed in mg/kg/min; The magnitude of interindividual and residual variability was expressed as CV%, approximated by the square root of the variance estimate.

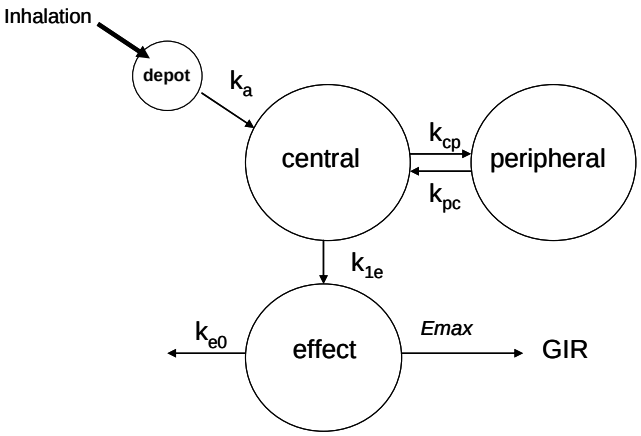

Figure 5-1 Pharmacokinetic/pharmacodynamic model diagram

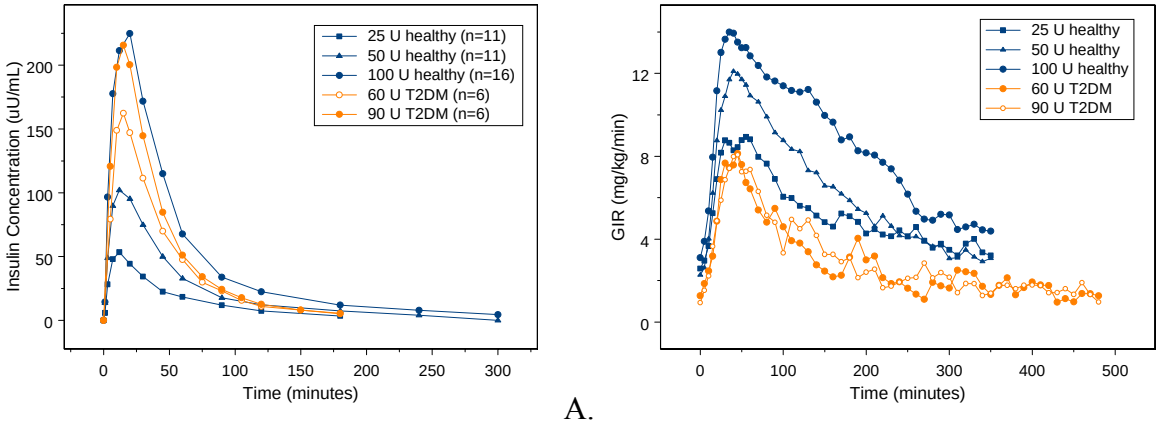

A. B.

Figure 5-2 Insulin and GIR-time profiles. A) Mean individual insulin concentrations by dose group and B) Mean observed GIR by dose group

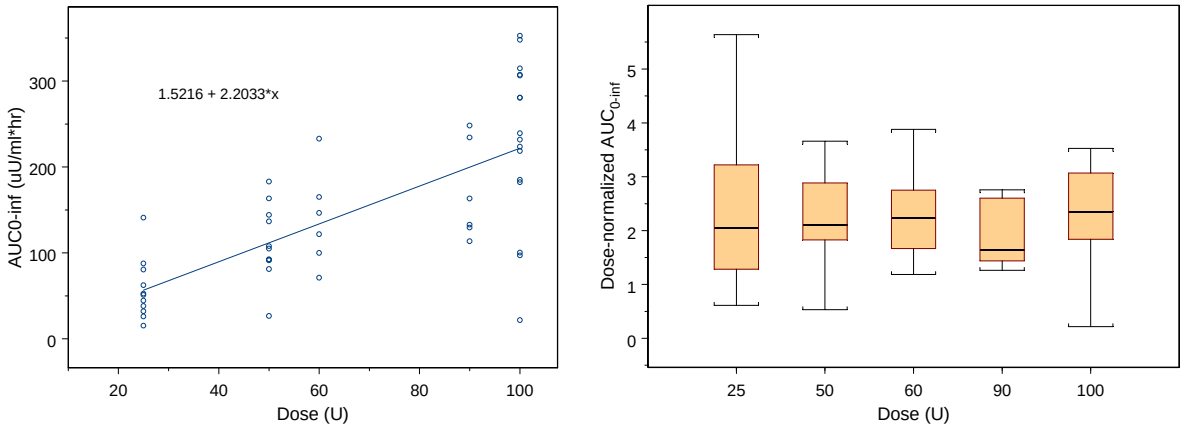

Figure 5-3 Dose proportionality assessment. A) Dose vs. insulin $AUC_{0-\infty}$ with regression line and B) Dose-normalized $AUC_{0-\infty}$ vs. dose as box and whisker plots with median

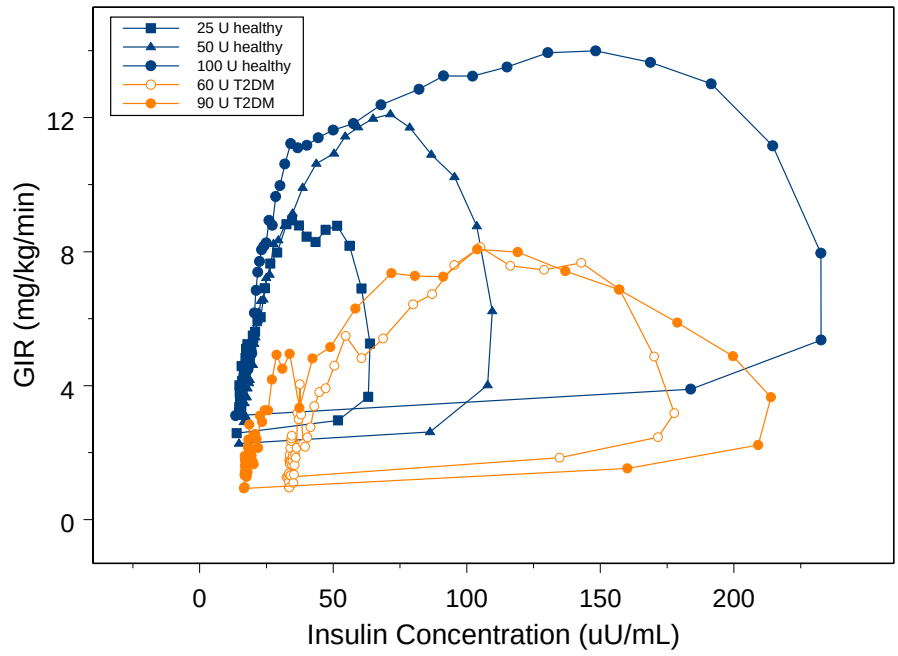

Figure 5-4 Hysteresis in the insulin-GIR relationship for healthy and type 2 diabetic subjects

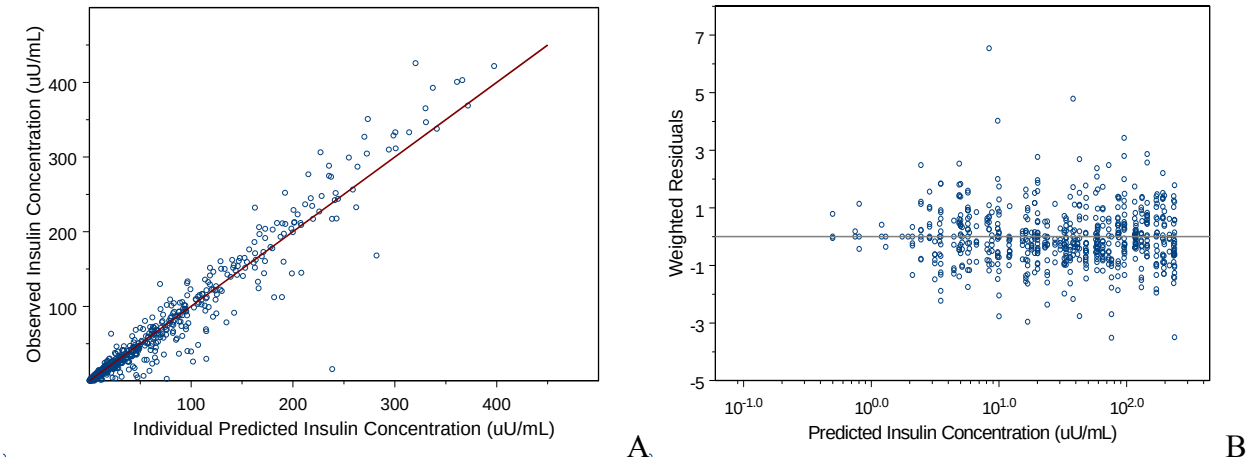

Figure 5-5 Goodness of fit plots for the pharmacokinetic model. A) Model individual predicted versus observed insulin concentrations and B) Model predicted insulin concentrations versus weighted residuals

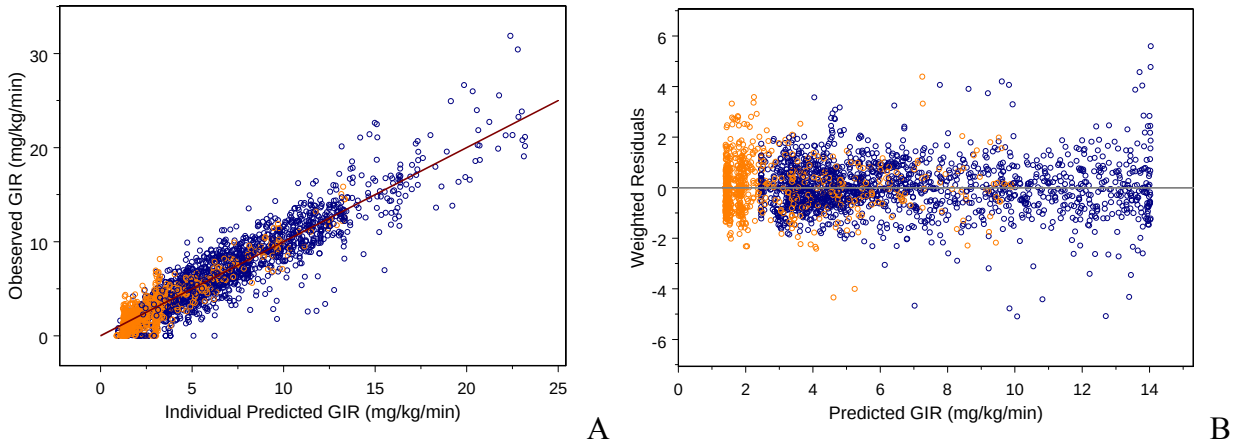

Figure 5-6 Goodness of fit plots for the pharmacodynamic model. A) Individual predicted GIR versus observed GIR and B) GIR values versus weighted residuals (orange=type 2, blue=healthy)

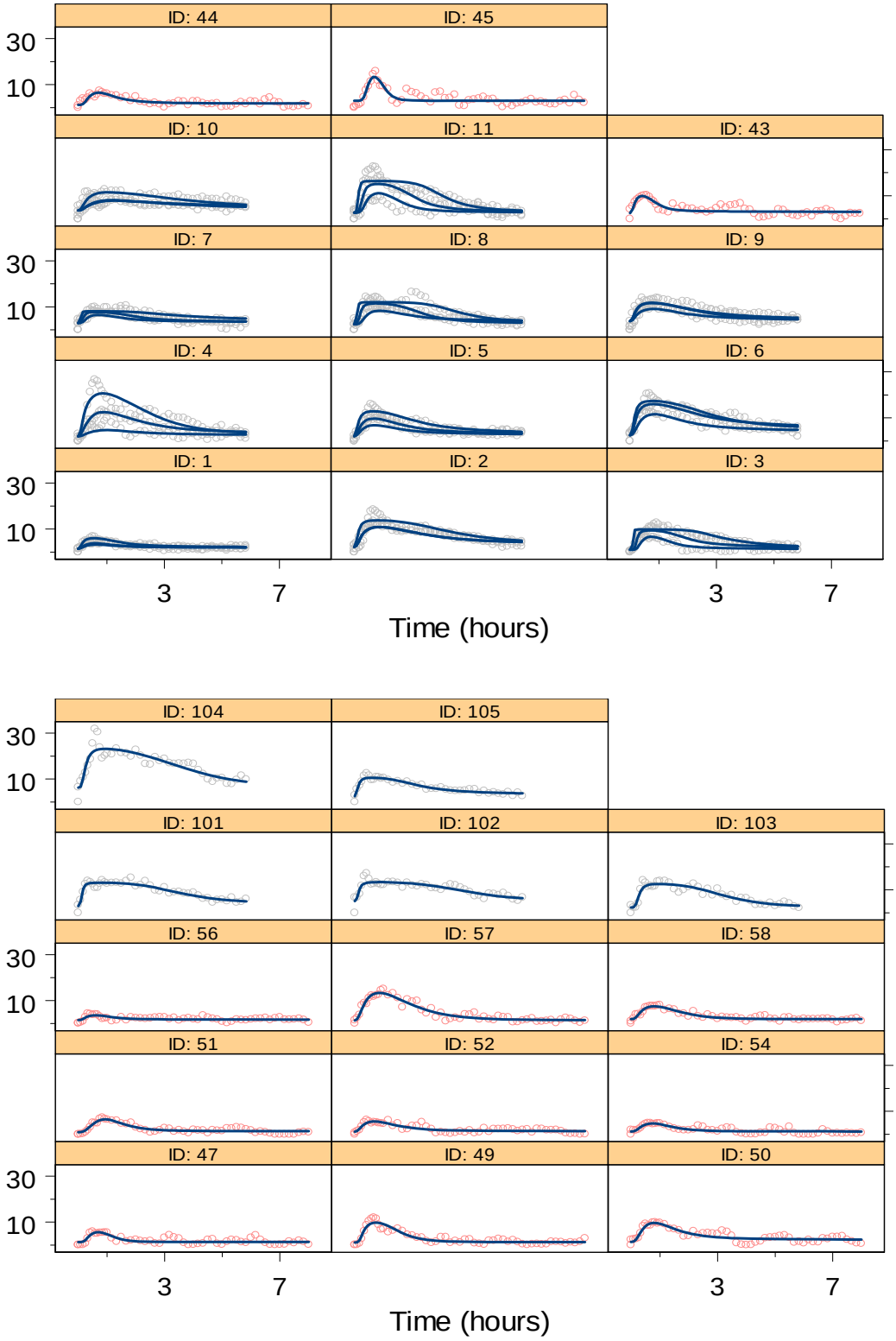

Figure 5-7 Individual predicted GIR versus observed GIR by subject (gray symbols=healthy subjects; red symbols=type 2 subjects)

CHAPTER 6
CONCLUSIONS

The purpose of this research was to develop population pharmacokinetic (PK) and pharmacokinetic/pharmacodynamic (PK/PD) models for insulins with different PK properties, and to characterize and bridge the PK and PD properties of a quickly absorbed inhaled insulin, subcutaneous insulin and insulin administered intravenously, using a population approach in healthy and type 2 diabetic subjects. The models examined were empirical in nature, and the PD response was based on GIR data derived from glucose clamp studies. The PK and PK/PD models were developed first in healthy volunteers and then expanded to include subjects with diabetes.

The first aim was to characterize insulin pharmacokinetics. Following intravenous dosing, insulin is characterized by multiple compartment disposition [55], however, the slow absorption characteristics of subcutaneously administered insulin obscure the distribution phase in what is termed "flip-flop" kinetics, where elimination is driven by a slower absorption process [38], making it impossible to model the second compartment. Technosphere® Insulin (TI) is a novel inhaled regular human insulin (RHI) whose unique delivery mechanism results in rapid absorption and rapid clearance, making it possible to distinguish the second compartment of its pharmacokinetic profile [78]. Because insulin pharmacokinetic properties are expected to be consistent once it is available systemically, the inclusion of data from TI and intravenous dosing, both of which have distinct α and β phases in their pharmacokinetic profiles, made it possible to demonstrate the two compartment disposition of all three routes of insulin administration.

Data from two studies was pooled for the analysis, with a total of 16 healthy subjects treated with insulin administered intravenously, subcutaneously and via the lung while undergoing a euglycemic glucose clamp procedure. Insulin absorption following pulmonary

administration was rapid and well described by a first order absorption rate constant; however, two sequential absorption rates and a transit compartment were used to describe the slower absorption seen with the subcutaneously administered insulin. Following intravenous dosing, the distribution phase was approximately thirty minutes. The apparent distribution phase was longer following TI administration, and undistinguishable from the elimination phase following subcutaneous dosing due to the prolonged duration of absorption.

In the final model, the population typical values were: clearance, 43.4 L/hr; volume of distribution in the central compartment, 5.0 L; volume of distribution in the peripheral compartment, 30.7 L. The absolute bioavailability for subcutaneous insulin and TI was 52% and 11%, respectively, matching both results reported with TI [83] and sc RHI [84]. The α and β-half-lives were calculated from the individual predicted parameters, and were 5 and 93 minutes, respectively, which are in close agreement with insulin half-life estimates following iv administration reported previously [55]. Interoccasion variability in bioavailability following TI administration was approximately 30%, indicating moderate differences in insulin exposure on different dosing occasions. Overall, the variability in insulin bioavailability was similar between the two non-iv treatments.

Covariate analysis identified BMI as a significant covariate on insulin absorption rate following subcutaneous dosing, with decreased absorption with increasing BMI, as previously reported by others [90]. This finding may be attributed to the increased thickness of the subcutaneous tissue in subjects with higher BMI, which slows absorption from the depot compartment. No other covariates were identified, but due to the homogenous nature of the subject population, covariate analysis was limited.

The population model was expanded to include data from subjects with both type 1 and type 2 diabetes, as well as data following administration of lispro in Aim 3. The same PK model was used to describe the data as in the first aim, and insulin PK was found to be consistent with a two-compartment model. The inclusion of lispro in the model was appropriate, since lispro has been shown to exhibit almost identical pharmacokinetics as RHI when administered intravenously [37], and its more rapid apparent clearance can be attributed to its more rapid absorption rate. As expected, TI was characterized by the quickest absorption rate, followed by lispro and RHI. Both subcutaneously administered insulins were adequately described by two sequential first order absorption rate constants.

In the model developed, subcutaneous RHI and TI are estimated to have a relative bioavailability of 72% and 14%, respectively, when compared to lispro. Assuming the lispro absolute bioavailability to be 77%, as reported in literature, the parameter estimates match well with those estimated in an analysis reported earlier (Chapter 2), with an absolute bioavailability adjusted systemic clearance of 40.3 L/hr (previously reported 43.4 L/hr), a central volume of distribution of 3.6 L (reported 5.0 L) and a peripheral volume of distribution of 28 L (reported 30.7 L).

Covariate analysis identified age as an important covariate positively correlated with insulin volume of distribution in the central compartment. Age was also found to have significant effect on the rate of pulmonary absorption when insulin was administered into the lung, with a decrease in pulmonary absorption with increasing age, independently of any age-associated decreases in pulmonary function. This finding could be beneficial to older patients, who have a slower gut transit time and longer absorption period compared to younger patients. In older patients, high and fast insulin peaks might cause a mismatch in insulin peak and glucose

appearance from the meal, causing early hypoglycemic events, but a slightly longer absorption and lower overall insulin peak will result in less likelihood of early hypoglycemia. Increases in BMI were associated with a decrease in insulin absorption rate following subcutaneous administration. The small number of subjects, narrow BMI range and homogenous nature of the healthy population makes it difficult to extrapolate these results, however, it is expected that a greater impact would be observed on patients taking subcutaneous insulin who have higher BMI, as is often the case in subjects with type 2 diabetes.

The second aim was to characterize the pharmacodynamics of the data included in Aim 1. The data originated from two glucose clamp studies, and the glucose infusion rate (GIR) was used as the pharmacodynamic endpoint. Data following intravenous, subcutaneous and pulmonary administration was modeled simultaneously. An E_{max} model was found to describe the data well when the hysteresis was first collapsed using an effect compartment. In the first model (Model A), treatment specific EC_{50}, k_{e0} and γ were modeled. The parameter estimates varied most notably in the γ parameter, with the highest value associated with intravenous insulin administration. The other parameter which varied considerably following intravenous administration was k_{e0}, which was lowest in this treatment, and associated with the longest central to effect site equilibration half-life. This is most likely due to the relatively quickly changing insulin concentrations following this route of administration, but comparable delay in insulin effect for all three treatments.

In the second model (Model B), no treatment-specific differences were assumed. Pharmacodynamic parameter variability ranged from 27 to 52%, with the greatest variability observed on γ, the sigmoidicity factor. This was an expected result, since this is the parameter that varied most between treatments in the first model. The residual error was described by an

additive model in both models A and B, and the residual error had a greater magnitude in Model B (2 mg/kg/min) when compared to Model A (1.68 mg/kg/min), indicating that more of the observed variability was explained by the treatment-specific parameters and associated interindividual variability in Model A.

Although the simple nature of the second model is a benefit, it is also a drawback in that the model underpredicts the GIR around the time of peak effect in some patients, especially in subjects who exhibit a quick and high rise in insulin. Hence, the model fit is less predictive of maximum effect in certain subjects in the 100 U TI dose group, and to a greater extent, in subjects receiving insulin intravenously. The reason for this observation may be due to the fact that insulin effect has two components: the stimulation of glucose disposal, as well as inhibition of hepatic glucose production [76], and the simple nature of the model cannot account for both. It appears that the model may describe insulin concentration-related glucose disposal, which is expected to follow a receptor-driven E_{max} model, it is unable to account for changes in insulin effects on hepatic glucose production, which are more immediate and associated with a threshold insulin value [9].

The effects of exogenous insulins are often compared based on the shape of, and area under the GIR vs. time curve, and numerous attempts have been made to model the insulin-GIR relationship. However, previous work focused on either one or similar insulin formulations, or explicitly estimated different pharmacodynamics for insulins with different pharmacokinetics, providing limited use towards predicting insulin effect for insulins other than those included in the model. The potential predictive ability of Model B makes it unique since it can easily be applied to simulate the activity of insulins with varying pharmacokinetic properties. In most

cases, the model performs well and is reasonable, with its only weakness being the underprediction at specific conditions.

The PD model was expanded to include glucose clamp data from subjects with type 2 diabetes, who, due to their disease state, exhibit decreased insulin sensitivity [95]. In this analysis, in order to improve the accuracy of the fits and better elucidate the difference between healthy individuals and subjects with diabetes, only TI data was included in the model. The PK model was developed first, with a good fit of a two compartment model, and with no difference in the PK between the two populations. This finding was confirmed by a noncompartmental analysis, which showed that dose-proportionality for both insulin AUC and C_{max} in the pooled dataset.

However, the response, assessed from the mean GIR curve and the noncompartmental pharmacodynamic parameters, did not appear proportional. Although it is impossible to compare the data directly due to the different target glucose concentrations during the clamp for the two populations, the difference in response appeared markedly different between the two groups, even though the blood glucose target differed only slightly. This result is not unexpected due to the insulin resistance observed in subjects with type 2 diabetes. When the data was modeled, the insulin EC_{50} estimate was found to be approximately three-fold higher in the diabetic population, and was indicative of a significant decrease in insulin sensitivity due to the disease state. Little difference was observed in k_{e0}, which suggests that the distribution time is largely independent of the disease state.

In conclusion, insulin was found to be well described by a two compartment pharmacokinetic model, with the differences in the insulin profiles attributable to absorption differences for the different routes of administration. Insulin pharmacodynamics were well

described by an E_{max} model, related to effect site concentration. Some underprediction of the GIR resulted with high and quick insulin peaks. Model fit was better when the model estimated different EC_{50}, k_{e0} and γ values for each of the insulin formulations, however, when one common set of parameters were used, the model still described the data well, with a modestly greater underprediction of the GIR associated at some peaks, in particular, those associated with intravenous dosing. Although the increase in underprediction is a weakness of the simpler model, its ability to predict insulin effect based on insulin pharmacokinetics alone makes the model much more useful in practical applications. The extension of this model to subjects with type 2 diabetes found this population to have an approximately three-fold higher EC_{50} when compared to healthy subjects, most likely due to the decreased insulin sensitivity associated with the disease state.

LIST OF REFERENCES

[1] Economic costs of diabetes in the U.S. In 2007. Diabetes Care. 2008; **31**: 596-615

[2] Wild S, Roglic G, Green A, Sicree R, King H. Global prevalence of diabetes: estimates for the year 2000 and projections for 2030. Diabetes Care. 2004; **27**: 1047-1053

[3] Weyer C, Bogardus C, Mott DM, Pratley RE. The natural history of insulin secretory dysfunction and insulin resistance in the pathogenesis of type 2 diabetes mellitus. The Journal of Clinical Investigation. 1999; **104**: 787-794

[4] The relationship of glycemic exposure (HbA1c) to the risk of development and progression of retinopathy in the diabetes control and complications trial. Diabetes. 1995; **44**: 968-983

[5] Rother KI. Diabetes treatment--bridging the divide. The New England Journal of Medicine. 2007; **356**: 1499-1501

[6] Goodman LS, Gilman A, Brunton LL, Lazo JS, Parker KL. Goodman & Gilman's the Pharmacological Basis of Therapeutics. 11th edn. New York: McGraw-Hill, 2006.

[7] Matveyenko AV. Liver Cells Listening to Beta Cells. American Diabetes Association 69th Scientific Sessions. New Orleans, 2009

[8] Guyton AC, Hall JE. Textbook of medical physiology. 11th edn. Philadelphia: Elsevier Saunders, 2006.

[9] Cherrington AD, Sindelar D, Edgerton D, Steiner K, McGuinness OP. Physiological consequences of phasic insulin release in the normal animal. Diabetes. 2002; **51 Suppl 1**: S103-108

[10] Wyne KL. Free fatty acids and type 2 diabetes mellitus. The American Journal of Medicine. 2003; **115 Suppl 8A**: 29S-36S

[11] Boden G, Lebed B, Schatz M, Homko C, Lemieux S. Effects of acute changes of plasma free fatty acids on intramyocellular fat content and insulin resistance in healthy subjects. Diabetes. 2001; **50**: 1612-1617

[12] McGarry JD. Banting lecture 2001: dysregulation of fatty acid metabolism in the etiology of type 2 diabetes. Diabetes. 2002; **51**: 7-18

[13] Polonsky KS, Given BD, Hirsch LJ*, et al.* Abnormal patterns of insulin secretion in non-insulin-dependent diabetes mellitus. The New England Journal of Medicine. 1988; **318**: 1231-1239

[14] DeFronzo RA, Tobin JD, Andres R. Glucose clamp technique: a method for quantifying insulin secretion and resistance. The American Journal of Physiology. 1979; **237**: E214-223

[15] Lerner RL, Porte D, Jr. Relationship between intravenous glucose loads, insulin responses and glucose disappearance rate. The Journal of Clinical Endocrinology and Metabolism. 1971; **33**: 409-417

[16] Porte D, Jr., Pupo AA. Insulin responses to glucose: evidence for a two pool system in man. The Journal of Clinical Investigation. 1969; **48**: 2309-2319

[17] Caumo A, Luzi L. First-phase insulin secretion: does it exist in real life? Considerations on shape and function. American Journal of Physiology. 2004; **287**: E371-385

[18] Grodsky GM. A threshold distribution hypothesis for packet storage of insulin and its mathematical modeling. The Journal of clinical investigation. 1972; **51**: 2047-2059

[19] Cerasi E. Potentiation of insulin release by glucose in man. I. Quantitative analysis of the enhancement of glucose-induced insulin secretion by pretreatment with glucose in normal subjects. Acta Endocrinologica. 1975; **79**: 483-501

[20] Mitrakou A, Kelley D, Mokan M*, et al.* Role of reduced suppression of glucose production and diminished early insulin release in impaired glucose tolerance. The New England Journal of Medicine. 1992; **326**: 22-29

[21] Mitrakou A, Kelley D, Veneman T*, et al.* Contribution of abnormal muscle and liver glucose metabolism to postprandial hyperglycemia in NIDDM. Diabetes. 1990; **39**: 1381-1390

[22] Shah P, Basu A, Basu R, Rizza R. Impact of lack of suppression of glucagon on glucose tolerance in humans. The AmericanJournal of Physiology. 1999; **277**: E283-290

[23] Ganda OP, Srikanta S, Brink SJ*, et al.* Differential sensitivity to beta-cell secretagogues in "early," type I diabetes mellitus. Diabetes. 1984; **33**: 516-521

[24] Garvey WT, Revers RR, Kolterman OG, Rubenstein AH, Olefsky JM. Modulation of insulin secretion by insulin and glucose in type II diabetes mellitus. The Journal of Clinical Endocrinology and Metabolism. 1985; **60**: 559-568

[25] Luzi L, DeFronzo RA. Effect of loss of first-phase insulin secretion on hepatic glucose production and tissue glucose disposal in humans. The American Journal of Physiology. 1989; **257**: E241-246

[26] Del Prato S, Marchetti P, Bonadonna RC. Phasic insulin release and metabolic regulation in type 2 diabetes. Diabetes. 2002; **51 Suppl 1**: S109-116

[27] Luzio SD, Owens DR, Vora J, Dolben J, Smith H. Intravenous insulin simulates early insulin peak and reduces post-prandial hyperglycaemia/hyperinsulinaemia in type 2 (non-insulin-dependent) diabetes mellitus. Diabetes Research (Edinburgh, Scotland). 1991; **16**: 63-67

[28] Steiner KE, Mouton SM, Williams PE, Lacy WW, Cherrington AD. Relative importance of first- and second-phase insulin secretion in glucose homeostasis in conscious dog. II. Effects on gluconeogenesis. Diabetes. 1986; **35**: 776-784

[29] Guerci B, Sauvanet JP. Subcutaneous insulin: pharmacokinetic variability and glycemic variability. Diabetes & Metabolism. 2005; **31**: 4S7-4S24

[30] Gualandi-Signorini AM, Giorgi G. Insulin formulations--a review. European Review for Medical and Pharmacological Sciences. 2001; **5**: 73-83

[31] Hoffman A, Ziv E. Pharmacokinetic considerations of new insulin formulations and routes of administration. Clinical Pharmacokinetics. 1997; **33**: 285-301

[32] Bonora E, Muggeo M. Postprandial blood glucose as a risk factor for cardiovascular disease in Type II diabetes: the epidemiological evidence. Diabetologia. 2001; **44**: 2107-2114

[33] Monnier L, Lapinski H, Colette C. Contributions of fasting and postprandial plasma glucose increments to the overall diurnal hyperglycemia of type 2 diabetic patients: variations with increasing levels of HbA(1c). Diabetes Care. 2003; **26**: 881-885

[34] Dimitriadis GD, Gerich JE. Importance of timing of preprandial subcutaneous insulin administration in the management of diabetes mellitus. Diabetes Care. 1983; **6**: 374-377

[35] Lean ME, Ng LL, Tennison BR. Interval between insulin injection and eating in relation to blood glucose control in adult diabetics. British Medical Journal (Clinical research ed. 1985; **290**: 105-108

[36] Heinemann L. Time-Action Profiles of Insulin Preparations. Mainz, Germany: Kirchheim & Co GmbH, 2004.

[37] Heinemann L, Woodworth, J. Pharmacokinetics and Glucodynamics of Insulin Lispro. Drugs of Today: Prous Science, 1998:23-36

[38] Actrapid 100 IU/mL, Solutino for Injection in a Vial, Summary of Product Characteristics. Novo Nordisk Limited, 2007

[39] Hirsch IB. Insulin analogues. The New England journal of medicine. 2005; **352**: 174-183

[40] Brange J, Owens DR, Kang S, Volund A. Monomeric insulins and their experimental and clinical implications. Diabetes Care. 1990; **13**: 923-954

[41] Brange J, Ribel U, Hansen JF, *et al.* Monomeric insulins obtained by protein engineering and their medical implications. Nature. 1988; **333**: 679-682

[42] Joslin EP, Kahn CR. Joslin's diabetes mellitus. 14th edn. Philadelphia: Lippincott Williams & Willkins, 2005.

[43] Mitri J, Pittas AG. Inhaled insulin--what went wrong. Nature Clinical Practice. 2009; **5**: 24-25

[44] Pfizer Inc. Exubera Prescribing Information. 2006

[45] Heinemann L, Heise,Tim Review: Current status of the development of inhaled insulin The British Journal of Diabetes & Vascular Disease. 2004; **4**: 295-301

[46] Boss AH, Yu, Wen, Ellarman, Karen. Prandial Insulin: Is Inhaled Enough? Drug Development Research. 2008; **69**: 138-142

[47] DeFronzo RA, Binder C, Wahren J, Felig P, Ferrannini E, Faber OK. Sensitivity of insulin secretion to feedback inhibition by hyperinsulinaemia. Acta Endocrinologica. 1981; **98**: 81-86

[48] Koivisto VA, DeFronzo R, Hendler R, Felig P. The difference in insulin sensitivity and metabolic response to acute exercise in trained and sedentary subjects. Current Problems in Clinical Biochemistry. 1982; **11**: 122-132

[49] DeFronzo RA, Hendler R, Christensen N. Stimulation of counterregulatory hormonal responses in diabetic man by a fall in glucose concentration. Diabetes. 1980; **29**: 125-131

[50] Heinemann L, Linkeschova R, Rave K, Hompesch B, Sedlak M, Heise T. Time-action profile of the long-acting insulin analog insulin glargine (HOE901) in comparison with those of NPH insulin and placebo. Diabetes Care. 2000; **23**: 644-649

[51] Heise T, Heinemann L. Rapid and long-acting analogues as an approach to improve insulin therapy: an evidence-based medicine assessment. Current Pharmaceutical Design. 2001; **7**: 1303-1325

[52] Heise T, Weyer C, Serwas A*, et al.* Time-action profiles of novel premixed preparations of insulin lispro and NPL insulin. Diabetes Care. 1998; **21**: 800-803

[53] Howey DC, Bowsher RR, Brunelle RL, Woodworth JR. [Lys(B28), Pro(B29)]-human insulin. A rapidly absorbed analogue of human insulin. Diabetes. 1994; **43**: 396-402

[54] Yalow RS, Berson SA. Immunoassay of endogenous plasma insulin in man. The Journal of Clinical Investigation. 1960; **39**: 1157-1175

[55] Hooper SA. Peptides, Peptoids, and Proteins. Cinncinnati, OH: Harvery Whitney Books, 1991.

[56] Gopalakrishnan M, Suarez S, Hickey AJ, Gobburu JV. Population pharmacokinetic-pharmacodynamic modeling of subcutaneous and pulmonary insulin in rats. Journal of Pharmacokinetics and Pharmacodynamics. 2005; **32**: 485-500

[57] Landsdorfer C. PK/PD Modeling of Glucose Clamp Effects of Inhaled Insulin. Tucson, AZ: American Conference on Pharmacometrics, March 9-12, 2008

[58] Osterberg O, Erichsen L, Ingwersen SH, Plum A, Poulsen HE, Vicini P. Pharmacokinetic and pharmacodynamic properties of insulin aspart and human insulin. Journal of Pharmacokinetics and Pharmacodynamics. 2003; **30**: 221-235

[59] Tornoe CW, Jacobsen JL, Madsen H. Grey-box pharmacokinetic/pharmacodynamic modelling of a euglycaemic clamp study. Journal of Mathematical Biology. 2004; **48**: 591-604

[60] Woodworth JR, Howey DC, Bowsher RR. Establishment of time-action profiles for regular and NPH insulin using pharmacodynamic modeling. Diabetes Care. 1994; **17**: 64-69

[61] Woodworth JR, Howey DC, Bowsher RR, Brunelle RL. Relating glucose clamp profiles to reduction of blood glucose after insulin administration. Diabetes Technology & Therapeutics. 2004; **6**: 147-153

[62] Sakagami M. Insulin disposition in the lung following oral inhalation in humans : a meta-analysis of its pharmacokinetics. Clinical Pharmacokinetics. 2004; **43**: 539-552

[63] Duckworth WC, Bennett RG, Hamel FG. Insulin degradation: progress and potential. Endocrine Reviews. 1998; **19**: 608-624

[64] Duckworth WC, Hamel FG, Peavy DE. Hepatic metabolism of insulin. The American Journal of Medicine. 1988; **85**: 71-76

[65] Rabkin R, Ryan MP, Duckworth WC. The renal metabolism of insulin. Diabetologia. 1984; **27**: 351-357

[66] Levy J, Olefsky JM. The effect of insulin concentration on retroendocytosis in isolated rat adipocytes. Endocrinology. 1987; **120**: 450-456

[67] Hovorka R, Powrie JK, Smith GD, Sonksen PH, Carson ER, Jones RH. Five-compartment model of insulin kinetics and its use to investigate action of chloroquine in NIDDM. The American Journal of Physiology. 1993; **265**: E162-175

[68] Meibohm B, Derendorf H. Basic concepts of pharmacokinetic/pharmacodynamic (PK/PD) modelling. International Journal of Clinical Pharmacology and Therapeutics. 1997; **35**: 401-413

[69] Rave K, Potocka, E., Heinemann, L., Heise, T., Boss, A., Marino, M., Costello, D., Chen, R. Pharmacokinetics and linear exposure of AFRESA™ compared with the subcutaneous injection of regular human insulin. Diabetes, Obesity and Metabolism. 2009:

[70] Sheiner LB, Stanski DR, Vozeh S, Miller RD, Ham J. Simultaneous modeling of pharmacokinetics and pharmacodynamics: application to d-tubocurarine. Clinical Pharmacology and Therapeutics. 1979; **25**: 358-371

[71] Landersdorfer C. Modeling Diverse Anti-Diabetic Drug Effects Using Indirect Response Models: Review. Population Approach Group in Europe. Dunedin, New Zealand: Abstracts of the Annual Meeting 2008

[72] Lin S, Chien YW. Pharmacokinetic-pharmacodynamic modelling of insulin: comparison of indirect pharmacodynamic response with effect-compartment link models. The Journal of Pharmacy and Pharmacology. 2002; **54**: 791-800

[73] Tolic IM, Mosekilde E, Sturis J. Modeling the insulin-glucose feedback system: the significance of pulsatile insulin secretion. Journal of Theoretical Biology. 2000; **207**: 361-375

[74] Berger M, Rodbard D. Computer simulation of plasma insulin and glucose dynamics after subcutaneous insulin injection. Diabetes Care. 1989; **12**: 725-736

[75] Thomaseth K, Pavan A, Berria R, Glass L, DeFronzo R, Gastaldelli A. Model-based assessment of insulin sensitivity of glucose disposal and endogenous glucose production from double-tracer oral glucose tolerance test. Computer Methods and Programs in Biomedicine. 2008; **89**: 132-140

[76] Landersdorfer CB, Jusko WJ. Pharmacokinetic/pharmacodynamic modelling in diabetes mellitus. Clinical Pharmacokinetics. 2008; **47**: 417-448

[77] Landersdorfer C. PK/PD Modeling of Glucose Clamp Effects of Inhaled Insulin. American Conference on Pharmacometrics Tucson, AZ, 2008

[78] Rave KM, Nosek L, de la Pena A*, et al.* Dose response of inhaled dry-powder insulin and dose equivalence to subcutaneous insulin lispro. Diabetes Care. 2005; **28**: 2400-2405

[79] Owens DR. Human insulin. Intermediate-acting insulin preparations 'initial ratio' method. In: Owens DR, ed. Clinical Pharmacological Study in Normal Man: MTD Press Limited, 1986:138

[80] Muir KT GR. Non-compartmental analysis. In: Bonate P HD, ed. Pharmacokinetics in Drug Development: Clinical Study Design and Analysis. Arlington, VA: American Association of Pharmaceutical Scientists, 2004:235-266

[81] Puckett WR, Lightfoot EN. A model for multiple subcutaneous insulin injections developed from individual diabetic patient data. The American Journal of Physiology. 1995; **269**: E1115-1124

[82] Jonsson EN, Karlsson MO. Xpose--an S-PLUS based population pharmacokinetic/pharmacodynamic model building aid for NONMEM. Computer Methods and Programs in Biomedicine. 1999; **58**: 51-64

[83] Steiner S, Pfutzner A, Wilson BR, Harzer O, Heinemann L, Rave K. Technosphere/Insulin--proof of concept study with a new insulin formulation for pulmonary delivery. Exp Clin Endocrinol Diabetes. 2002; **110**: 17-21

[84] Humalog® Insulin Lispro Injection, USP (rDNA origin), 100 units per mL (U-100). Prescribing Information: Eli Lilly and Company, 2009

[85] Nucci G, Cobelli C. Models of subcutaneous insulin kinetics. A critical review. Computer Methods and Programs in Biomedicine. 2000; **62**: 249-257

[86] Richardson PC, Boss AH. Technosphere insulin technology. Diabetes Technology & Therapeutics. 2007; **9 Suppl 1**: S65-72

[87] Leone-Bay A. Technosphere®/Insulin: mimicking endogenous insulin release. In: Rathbone M HJ, Roberts M, Lane M, Eds, ed. Modified Release Drug Delivery Technology. 2 edn. New York, NY: Informa Healthcare USA, Inc., 2008

[88] Brain JD. Inhalation, deposition, and fate of insulin and other therapeutic proteins. Diabetes Technology & Therapeutics. 2007; **9 Suppl 1**: S4-S15

[89] Gad SC. Drug safety evaluation. New York: J. Wiley, 2002:xi, 1007

[90] Sindelka G, Heinemann L, Berger M, Frenck W, Chantelau E. Effect of insulin concentration, subcutaneous fat thickness and skin temperature on subcutaneous insulin absorption in healthy subjects. Diabetologia. 1994; **37**: 377-380

[91] Cassidy J, BAughman, R, Richardson, P. AFRESA™ (Technosphere® Insulin) Dosage Strengths Are Interchangeable. American Diabetes Association Annual Meeting, New Orleans, LA: American Diabetes Association, 2009

[92] Bonate PL. Pharmacokinetic-Pharmacodynamic Modeling and Simulation. S.l.: Springer Science+Business Media, 2006.

[93] Parke J, Holford NH, Charles BG. A procedure for generating bootstrap samples for the validation of nonlinear mixed-effects population models. Computer Methods and Programs in Biomedicine. 1999; **59**: 19-29

[94] Potocka E, Baughman, R., Derendorf, H. Population Pharmacokinetic Model of Regular Human Insulin Following Different Routes of Administration. 2009 AAPS National Biotechnology Conference, Seattle, WA: American Association of Pharmaceutical Scientists, June, 2009

[95] Bavenholm PN, Pigon J, Ostenson CG, Efendic S. Insulin sensitivity of suppression of endogenous glucose production is the single most important determinant of glucose tolerance. Diabetes. 2001; **50**: 1449-1454

[96] Rizza RA, Mandarino LJ, Gerich JE. Mechanism and significance of insulin resistance in non-insulin-dependent diabetes mellitus. Diabetes. 1981; **30**: 990-995

BIOGRAPHICAL SKETCH

Elizabeth Potocka received her Bachelor of Science degree in mathematics at Fairfield University in 1994. After graduation, Elizabeth joined Boehringer Ingelheim Pharmaceuticals, Inc, in Ridgefield, CT, in 1997, where she worked in the Department of Drug Metabolism and Pharmacokinetics. Her responsibilities primarily included interpretation of pharmacokinetic and pharmacodynamic data from the clinical program, as well as population modeling and simulation work in support of drug development. She joined the University of Florida doctoral program under the supervision of Dr. Hartmut Derendorf in the Department of Pharmaceutics, College of Pharmacy, in August 2004. In 2007, Elizabeth joined MannKind Corporation as a Pharmacokineticist in the Experimental Pharmacology Department, where her responsibilities encompassed the design and interpretation of clinical studies for pharmacokinetics and pharmacodynamics as well as pharmacokinetic and pharmacodynamic modeling of insulin. She is a contributing author to a number of peer-reviewed presentations and publications, as well as a contributing author to the Technosphere® Insulin New Drug Application. She received her Ph.D. in pharmaceutical sciences from the University of Florida in August 2009, where her primary research focus included population pharmacokinetics and pharmacodynamics of insulin.